Aalto University
School of Chemical
Engineering

Department of Chemical and Metallurgical Engineering

Shahid Sarfraz

PHASE EQUILIBRIA AND MODELLING OF POLYMER SYSTEMS

Master's thesis for the degree of Master of Science in Technology submitted for inspection, Espoo, 22-11-2018.

Supervisor Professor **Ville Alopaeus**

Instructor **D.Sc.(Tech.) Petri Uusi-Kyyny**
Mohammad Al-haj Ali, PhD

Aalto University
School of Chemical
Technology

Aalto University, P.O. BOX 11000, 00076
AALTO
www.aalto.fi
Abstract of master's thesis

Author Shahid Sarfraz

Title of thesis Phase Equilibria and Modelling of Polymer Systems

Department Department of Chemical and Metallurgical Engineering

Professorship Processes and products **Code of professorship** Kem-42

Thesis supervisor Professor Ville Alopaeus

Thesis advisor(s) / Thesis examiner(s) Petri Uusi-Kyyny, Mohammad Al-haj Ali

Date 07.05.2018 **Number of pages 87+19** **Language** English

Abstract

Polymer solutions can form homogenous mixtures or they can undergo phase separation. With linear low density polyethylene (LLDPE) production using solution polymerization process, better understanding of phase equilibrium and phase separation is important to design such desired process.

The goal of this work is to determine liquid–liquid phase boundaries during the phase separation. For binary and multicomponent systems, liquid-liquid phase boundaries are determined by measuring liquid-liquid phase separation points also known as cloud points. These cloud point measurements are conducted at a temperature range of 130 ℃ to 250 ℃ and pressures up to 100 bar for systems in 15-29 mass percentage (m-%) polymer concentration. For binary systems consisting of polyethylene and n-hexane, as well as for multicomponent systems containing polyethylene, ethylene monomer, 1-butane or 1-octene comonomer, butane or Iso-octane, and a hexane solvent, cloud point values were measured for six different types of polymers. And these experiments were done in a pressure and temperature controlled variable volume cell.

Lower critical solution temperature (LCST) behavior was observed in the investigated temperature range. With increasing polymer concentration (increasing solubility of polymers), cloud points are observed at lower pressure values. On the other hand, with an increase in size and density difference between the polymer and solvent, a decrease in polymer solubility is observed. Hence this causes the cloud point values shift to higher pressures.

Keywords Linear low density polyethylene, solution polymerization, cloud point, Lower critical solution temperature, liquid-liquid split, bubble point, modelling, Polyethylene process, variable volume cell.

Preface

First of all I would like to thank my advisor D. Sc. (Tech) Petri Uusi-Kyyny and PhD Mohammad Al-Haj Ali for their vital help and guidance throughout the experiments and writing work. Specially Petri Uusi-Kyyny, who helped me a great deal in tackling all problems during this work. I also wish to thank my supervisor Prof. Ville Alopaeus for his helpful guidance and comments during the group meetings. In addition to this, I wish to thank all those people in workshop for helping me during troubleshooting and maintaining the experimental apparatus in top condition.

I would also like to express my deepest gratitude towards my family specially my mother, friends and colleagues for their support throughout this work. Finally, I wish to thank Borealis Polymers for the resources and funding, which made this thesis possible.

Table of Contents

Abbreviations

Symbol	Description	Dimension
HPS	High pressure separator	
LPS	Low pressure separator	
EOS	Equation of state	
HDPE	High-density polyethylene	
LCSP	Lower critical solution pressure	$[M\ L^{-1}\ T^{-2}]$
LCST	Lower critical solution temperature	[K]
LDPE	Low-density polyethylene	
LLDPE	Linear low-density polyethylene	
LL	Liquid-liquid	
LLV	Liquid-liquid-vapor	
LST	Lower solution temperature	[K]
MM	Molar mass	[M]
MMD	Molar mass distribution	$[MLT^{-2}]$
MW	Molecular weight	
MWD	Molecular weight distribution	
SAFT	Statistical associating fluid theory	
PE	Polyethylene	
SAFT	Statistical associating fluid theory	
UCEP	Upper critical end point	
UCSP	Upper critical solution pressure	$[M\ L^{-1}\ T^{-2}]$
UCST	Upper critical solution temperature	[K]
UST	Upper solution temperature	
MI	Melt index	[K]
MFI	Melt flow index	
VLE	Vapor-liquid equilibrium	
MIR	Melt index ratio	
LCEP	Lower critical end point	$[L^3]$
VE	Excess volume of mixing	
SEC	Size exclusion chromatography	
GPC	Gel permeation chromatography	
SEC	Site expansion and conservation	
SL	Solid-liquid	
M_n	Number average molecular weight	
M_W	Weight average molecular weight	

1. Introduction

In polymer solutions, understanding of phase equilibria is vital for the design of polymerization processes. Many polymer products consist of binary or multicomponent systems of polymers. The Multicomponent polymer system consists of mixtures of different polymers or mixtures of polymers and other compounds such as solvents, monomers and comonomers. In most cases, mixtures of polymers are not miscible, that is, only very few pairs of polymers are known to be miscible and then only in a narrow temperature and concentration range. The main factors that determine the phase behavior are average molecular weight and distribution of molecular weights, structure and chemical composition of the polymers and other compounds in a mixture, polymer concentration or polymer volume fraction in the blend and temperature and pressure values. (Malpass, 2010)

Polymer solutions can form either homogenous mixtures or they can undergo phase separation. Phase separation conditions of polymer systems are of special importance in polymer processing. Information about liquid-liquid equilibria (LLE) is specifically important for polymerization processes where production of polymer is done in more than one liquid phase. Unreacted monomers, comonomers and solvents are then separated from such polymer solutions. The formation of a two liquid phases is usually induced by a change in temperature or molecular weight of polymer. Whether two polymers are mutually miscible or whether a polymer is soluble in a solvent depends on the free energy curve shape and the composition. To better understand the phase behavior of polymer solutions, we have to understand how the shape of the free energy curve of mixing effects the stability of the system. For any phase the free energy, G, is dependent on the temperature, pressure and composition. For polymer solutions, free energy is discussed in details in the next chapter. (Robenson, 2007)

Polyethylene is the most commonly used polymer with variable crystalline structure and large number of applications depending upon certain type. This classification of PE is based on density and branching difference, most commonly are linear low-density polyethylene (LLDPE), low-density polyethylene (LDPE) and high-density polyethylene (HDPE). This work focuses on LLDPE, a significantly linear polymer with prominent numbers of short branches, usually prepared by copolymerization of ethylene with long-chain olefins. (Siow, 1972)

The goal of this study is to examine the phase equilibria of LLDPE in different polymer – solvent systems. For these LLDPE-solvent systems, liquid-liquid separation temperatures and pressures are measured. Literature part of this thesis covers general information on manufacturing processes, phase behavior and factors affecting the liquid-liquid phase separation. Finally, the experiments conducted with the different LLDPE – solvent systems along with measurement results will be presented.

Literature Part

2. Polyethylene processes and Phase behavior phenomena

In order to identify the significance of the cloud points in polymer solutions, it is first important to understand the current industrial processes and phenomenon involved in these processes. Therefore, this chapter presents a general overview of current industrial PE processes and discusses the phase behavior of polymer solutions involved in these processes. These industrial polymerization processes are based on different physical state of media and reactor conditions. In binary polymer systems, in order to understand phase behavior, a sound knowledge of molecular thermodynamics of polymer solution is very important. Therefore, this part of literature briefly explains not only molecular thermodynamics, but also phase diagrams and phase separation mechanism of polymer solution.

2.1. Industrial polymerization processes

PE a polymer of ethylene ($CH_2=CH_2$) having the formula $(–CH_2CH_2–)_n$, is one of the most used plastic. Its production can be done at high temperatures (350-570 K) and pressures (10-3000 bar) in the presence of different catalysts, depending upon the end user product. Depending upon those procedures used for the synthesis of PE, different structures may be present, i.e. long and short-branched PE. It is the most consumed polymer in the world and the main reason for that is the versatility of the material, which provides high performance as compared to other materials and can be used as alternative for materials such as glass, paper or metal. These versatile ranges of products of PE is obtained by utilizing different and complex PE manufacturing processes. (Vasile et al., 2005)

The polymerization processes are categorized with respect to the physical state of medium and on the basis of reactor type used in manufacturing processes. These polymerization processes are,

1. solution polymerization
2. suspension polymerization
3. gaseous phase polymerization
4. bulk polymerization

Pressure range is also an important part in classifying these processes. For example, a coordination mechanism is used in first three processes and a free radical mechanism

is utilized in the last mentioned polymerization process. Range of pressure for first three processes is approximately 10MPa and for last process it is approximately 100 MPa. New catalyst technology and a wider range of reactor designs has enabled the possibility to produce these polymers with improved performance of end-use products. Borstar of Borealis is one of such new concept of manufacturing PE, which combine different processes to increase the product versatility.

The polymer mechanical properties, chain length and degree of crystallinity can be controlled by adjusting polymerization reaction conditions and reactant amount. LLDPE, which are copolymers of ethylene and α-olefin (butene, hexene, octene etc.) with a wide range of short-chain branched molecular structures provide better crystallinity and mechanical properties.

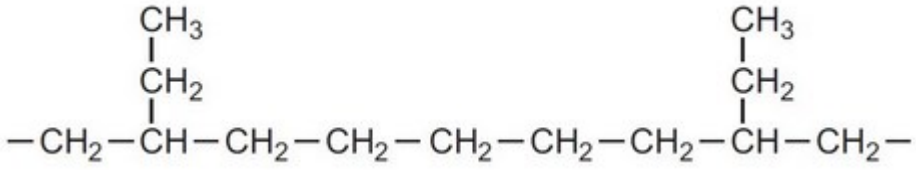

Figure 1. But-1-ene, ethylene polymer structure with side chains. (Vasile et al., 2005)

For example, with but-1-ene, ethylene polymer structure exhibits short chain branching also known as pendant groups as shown in Figure 1. Such structure provides better resilience, tear strength and flexibility in polymer without any plasticizers. (Vasile et al., 2005)

In solution polymerization polymer molecules form more homogenous resins and this process also provide a better ability to incorporate higher α-Olefin co-monomers.

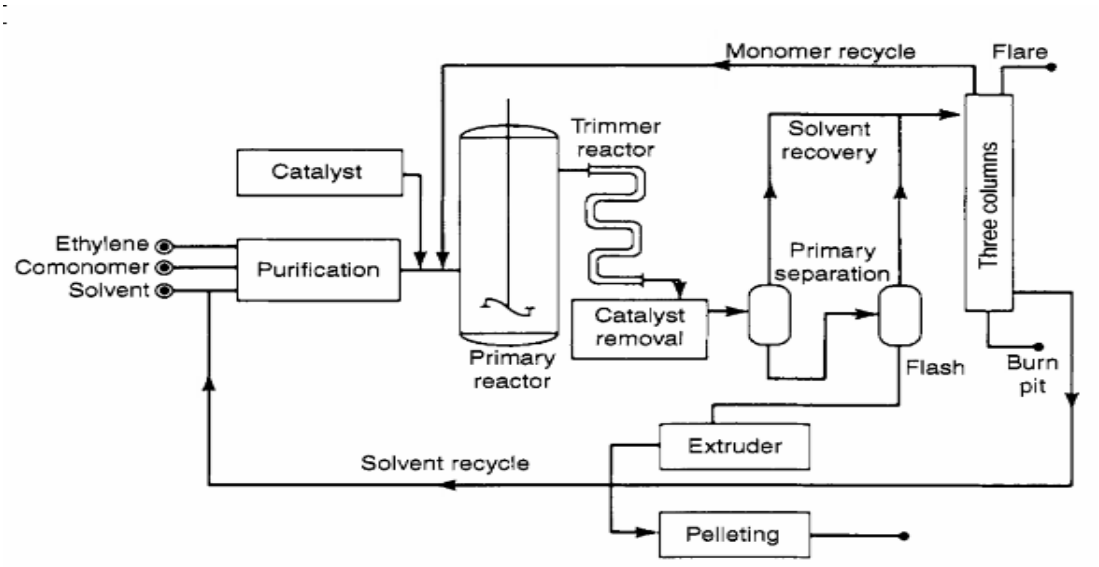

Figure 2. Schematic process flow diagram for the solution process for production of polyethylene.(Kirk-Othmer, 2006)

Figure 2 shows a schematic diagram of the Solution process, which mostly utilizes Ziegler-Natta catalysts at 160-220 ℃ temperature and 34-344 bar pressure. The polymer is dissolved in a solvent, normally cyclohexane C8 aliphatic hydrocarbons and this polymerization process is homogeneous, which occurs at temperatures well above the melting range of polyethylene. Polymerization takes place in a solution and the catalyst residence time is short in this process. Catalyst and co-catalysts exhibits reasonably good high temperature stability in the solution polymerization process. Catalyst morphology and particle size distribution are less important and a wide range of co-monomers can be used. (Malpass, 2010)

The suspension or slurry-phase process shown in Figure 3 can also be used to produce LLDPE. In the presence of solvent an organometallic compound with a metal alkyl react in a temperature range of 100-130 ℃ and at a pressure of 20 bars to produce LLDPE. PE is produced because of reacting ethylene in gas phase with an active site of catalyst. This suspension solution is then passed over a catalyst decomposition bed to deactivate the remaining catalyst, which is not utilized completely during the polymerization process. (Cheremisinoff, 1989)

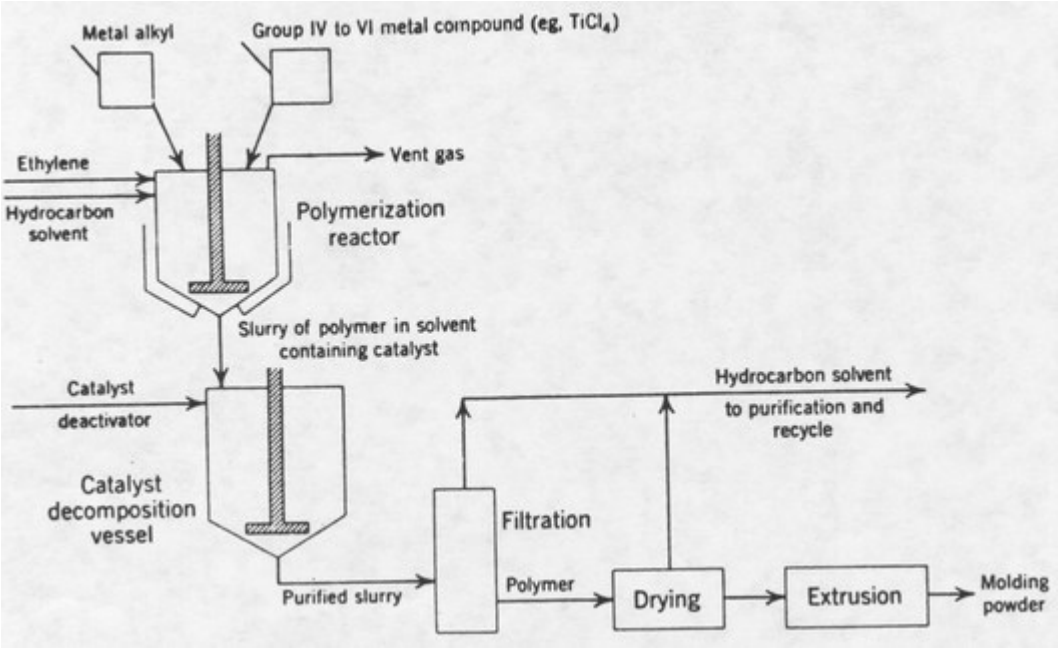

Figure 3. Suspension polymerization (Ziegler-Natta) process. (Rodriguez, 2003)

Solution polymerization produces polyethylene with a broad range of densities and limited range of molecular weights. The suspension polymerization process produces polyethylene with a broad range of melt index and a small range of densities. This difference makes solution polymerization more suitable for the production of polyethylene. (Rodriguez, 2003)

LLDPE and HDPE are commonly produced by gas phase polymerization process shown in Figure 4. HDPE is produced at 80-100 ℃ temperature and 30-35 bar pressure in a fluidized bed reactor by reacting α-Olefin with an active chromium based catalyst. Because of narrow differences between the melting point and polymerization temperature, LLDPE is more difficult to produce with gas phase than HDPE. LLDPE produced as a result of gas phase polymerization exhibits strong

intermolecular bonds, making material denser and more rigid.

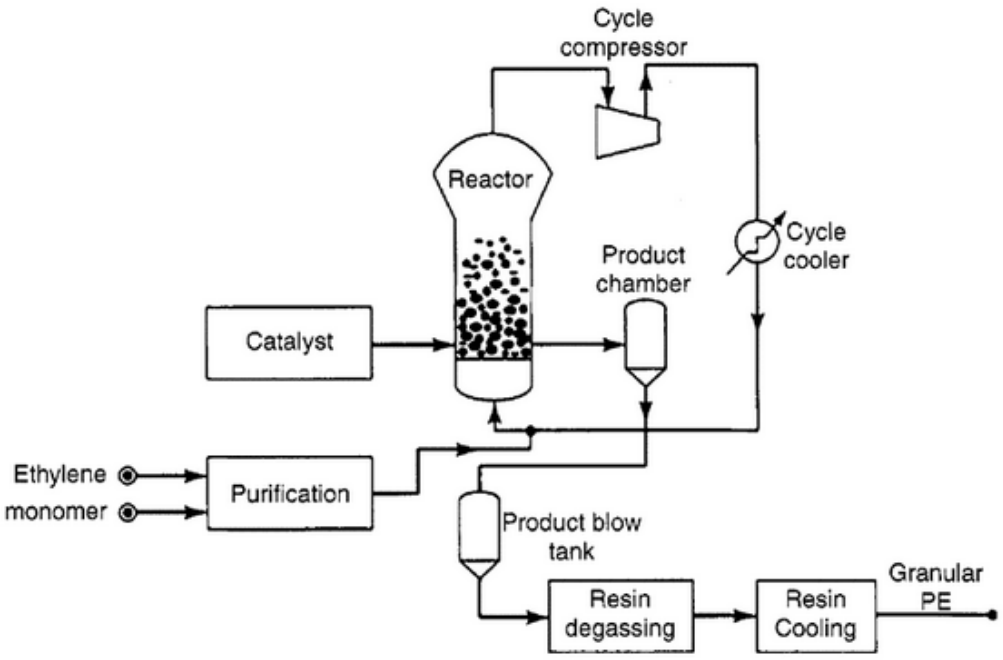

Figure 4. Gas phase ethylene polymerization process. (Kirk-Othmer, 2006)

With each combination of polymerization conditions, reactor systems use catalysts or initiators in a polymerization process and produce a different molecular structure. (Xie et al., 1994)

2.2. Molecular Thermodynamics of polymer-solvent solution

Molecular thermodynamics explains the relationship between physicochemical properties and classical thermodynamics of components in a solution. To get the condition in which polymer dissolves in a solvent, a molecular thermodynamic approach is utilized along with a series of experimental work where solvent and its properties are varied consistently in order to clarify the basic features of the components of that solvent. This kind of molecular approach provides useful information to design processes to produce polymers and copolymers at low pressure conditions that are miscible in solvents. Therefore, Gibbs free energy must be a minimum and negative in order to form a stable polymer-solvent solution at given temperature and pressure. (Prausnitz et al., 1986)

The Gibbs free energy of mixing is

$$\Delta G_{mix} = \Delta H_{mix} - T\Delta S_{mix} \quad (1)$$

ΔH_{mix} = Change of enthalpy of mixing

ΔS_{mix} = Change of entropy of mixing

T = Absolute temperature

ΔG_{mix} = Gibbs free energy of mixing

Enthalpic interactions are largely affected by polymer segment-segment, polymer segment-solvent, solvent-solvent interaction and by Solution density. ΔS_{mix} , depends on the combinatorial and non-combinatorial entropy of mixing which are related to the volume change of mixing, also called the equation of state effect. (Patterson, 1982)

It is reasonable to assume that the combinational entropy of mixing for a polymer-solvent solution should not change largely as long as the density of the solvent does not drastically change in the solution. Pressure and temperature values are close to dissolving conditions of polymer in solvent for such assumptions. The combinatorial entropy encourages the blending of a polymer with the solvent. Even though it is impossible to strictly separate the influence of entropic and energetic contributions on the ΔG_{mix}, it is convenient to conduct phase behavior experiments that can enhance the impact of energetic contributions compared to entropic contributions. In such circumstances, the polymer-solvent mixture phase behavior is governed by the molecular thermodynamic principles, which provides with resources to calculate the interactions that can significantly affect the phase behavior of the mixture. ΔH_{mix} , expected to be equal to change in internal energy (ΔU_{mix}) when the polymer-solvent solution is dense. Assuming pairwise additivity of solution energetics with density, is shown by the following expression (Equation 2) of internal energy of such isotropic homogeneous mixture compared to an ideal gas mixture: (Lee, 1988) (Blanks et al., 1964)

$$\Delta U_{mix} \approx \frac{2\pi\rho(P,T)}{kT} \sum_{i,j} x_i x_j \int \Gamma_{ij}(r,T)\, g_{ij}(r,\rho,T) r^2 dr \quad (2)$$

ΔU_{mix} = Internal energy of mixing

$x_i x_j$ = Mole fractions of component i and j

$g_{ij}(r,\rho,T)$ = Radial distribution function

$\Gamma_{ij}(r,T)$ = Intermolecular pair potential energy of the polymer segments and the solvent

$\rho(P,T)$ = solution density

r = Distance between molecules

k = Boltzmann constant

Solution energetics or energetics of solution formation is defined in two steps. First, the solute molecule units are pulled apart with help of energy (endothermic step) and second that solute molecule introduced in solvent. If solute is A and solvent is B two possibilities can observed. (Wohlfarth, 2005)

1. Exothermic if A-B attractions are stronger than A-A plus B-B.
2. Endothermic if A-B attractions are weaker than A-A plus B-B.

Spatial positioning of molecules with respect to one another is described by a function called as radial distribution function. Radial distribution function defines how density varies as a function of distance from a reference particle. The solubility of the polymer is likely to increase with the increasing pressure of the system or by using a denser solvent. In this way, internal energy of the mixture is approximately proportional to its density. Such general information can be extracted from the above given approach. However, the only feasible condition to dissolve the polymer is when the energetics of polymer segment-solvent interaction dominate the polymer segment-segment and solvent-solvent interactions. (Danner et al., 1993)

$$\Gamma_{ij}(r,T) = -\left[C_1\left(\frac{\alpha_i\alpha_j}{r^6}\right) + C_2\left(\frac{\mu_i^2\mu_j^2}{r^6KT}\right) + C_3\left(\frac{\mu_i^2Q_j^2}{r^8KT}\right) + C_4\left(\frac{Q_i^2\mu_j^2}{r^8KT}\right) + C_5\left(\frac{Q_i^2Q_j^2}{r^{10}KT}\right) + complex\ formation\right] \quad 3$$

$\Gamma_{ij}(r,T)$ = Intermolecular pair potential energy of the polymer segments and the solvent

α = Polarizability,

μ= Dipole moment,

Q = Quadrupole moment,

$C_{1\text{-}5}$ = Constants,

r = Distance between molecules,

k = Boltzmann constant,

Intermolecular interaction effects on phase behavior of polymer-solvent solution is described by $\Gamma_{ij}(r,T)$. The induction interactions effect on the potential energy in comparison to dispersion and polar interactions is much smaller that is why they are not shown in Equation 3. Since chain connectivity controls the segmental motion, interactions between polymer segments or with solvents are less effective. First term in equation 3, $C_1\left(\frac{\alpha_i\alpha_j}{r^6}\right)$ known as nonpolar dispersion interactions, depend only on the components polarizability in the solution and not on temperature conditions. Therefore, with the increase in polarizability of the solvent, pressure needed to dissolve non-polar polymer into non-polar solvent should decrease. The solvents containing heteroatoms have bond dipoles, difference in electron affinity of these heteroatoms cause such dipoles that results in a dipole or a quadrupole moment i.e. higher order polar moments. Dipole moment measure distribution of poles along an axis whereas quadrupole moment measures distribution in a plane. $\left(\frac{\alpha_i\alpha_j}{r^6}\right)$ and $\left(\frac{Q_i^2Q_j^2}{r^{10}KT}\right)$ are terms for the potential energy of the dipole and quadrupole interactions is inversely proportional to temperature. (Buckingham et al., 1968) (Kirby et al., 1999)

At elevated temperatures, solvent molecules behave as non-polar. Reason for such behavior is the disturbance in the configurational alignment of the polar moments of these molecules. There are a few possibilities to dissolve such non-polar polymer in a polar solvent. For example, dimethyl ether, a polar solvent can dissolve a non-polar polymer if temperature is high enough to break the ether-ether polar interactions which are reasonably strong at low temperature conditions. To achieve a single phase in a solution, pressure is applied to that solution in the presence of a solvent with suitable density. Hydrogen bonding or complex formations can also contribute to the potential energy of attractive pair of polymer-solvent molecule. Similarly, directional interaction strengths are also very sensitive to temperature changes. Equations 1- 3 describe how pressure and temperature can affect the solvent quality. (Kirby et al., 1999)

With the increase in solvent molecule size, polarizability within given chemicals (e.g. ethylene, hexane) can also increase, which is shown in Table 1. Polarizability in these chemicals is due to polar molecules. Polar molecules are those in which electric charge is distributed asymmetrically. Though the critical properties of alkanes and alkenes do not vary considerably from each other, but the double bond present in alkenes can

cause quadrupole moment, which can provide a potential site for complex formation. (Buckingham et al., 1968)

Table 1. Supercritical fluid solvents with their physical properties. (McHugh et al., 1994)

solvent	T_c (°C)	P_c (bar)	$\alpha \times 10^{25}$ (cm^3)	μ (D)
ethane	32.3	48.8	45.0	0.0
propane	96.7	42.5	62.9	0.1
butane	152.1	38.0	81.4	0.0
hexane	234.1	29.7	118.3	0.0
ethylene	9.2	50.4	42.3	0.0
propylene	91.9	46.2	62.6	0.4
1-butene	146.5	39.7	82.4	0.3
2-*trans*-butene	155.5	39.9	84.9	0.0
dimethyl ether	126.9	52.4	51.6	1.3
tetrafluoromethane	−45.6	37.4	28.6	0.0
hexafluoroethane	19.7	29.8	47.6	0.0
octafluoropropane	71.9	26.8	66.7	0.0
hexafluoropropylene	94.0	29.0	60.4	0.4
difluoromethane	78.5	53.4	24.8	2.0
trifluoromethane	26.2	48.6	26.5	1.6
chlorotrifluoromethane	28.8	38.7	45.8	0.5
chlorodifluoromethane	96.2	49.7	44.4	1.4
difluoroethane	113.1	45.2	41.5	2.3
tetrafluoroethane	101.1	40.6	43.8	2.1
pentafluoroethane	66.3	36.3	45.6	?
sulfur hexafluoride	45.4	37.6	54.6	0.0
carbon dioxide	31.0	73.8	27.6	0.0

T_c = Critical temperature in ℃

P_c = Critical pressure in bar

α = Polarizability in cm^3

μ = Dipole moment in Debyes, D

The effects of solvent physical properties on the phase behavior of polymer solutions can be described by comparing the solubility characteristics of a single polymer or copolymer in a series of solvents. Configurational interactions such as dipolar and quadrupole moments behave in a different way with respect to volume. The strength of dipolar interactions is $\mu_i^* = \frac{\mu_i}{v_i^{1/2}}$ i.e. inversely proportional to square root of molar volume and the strength of quadrupole interactions $Q_i^* = \frac{Q_i}{v_i^{5/6}}$ i.e. inversely proportional to 5/6 power of molar volume. Changing strengths of these configurational interaction with volume can affect the phase behavior of polymer-solvent solution as they directly related to intermolecular interaction shown in equation 3. While interpreting solubility

data of polymer dissolved in given solvent, this dipole and quadrupole interaction scaling becomes very important. (Kirby et al., 1999)

2.3. General phase Diagrams of Binary Mixtures

Binary phase diagrams are shown from Figure 5-8, where C1 and C2 represents critical points of components of 1 and 2 respectively. The dashed curves are critical mixture curves for binary mixtures and open triangles are critical end points. Three different cases are discussed in this study. (McHugh et al., 1994)

Due to specific pressure and temperature, the liquid phase separate into two liquid phases as shown in Figure 5. The phase separation results in a liquid-liquid-vapor (LLV) line. A three dimensional P-T-X diagram of LLV surface is shown in Figure 5.

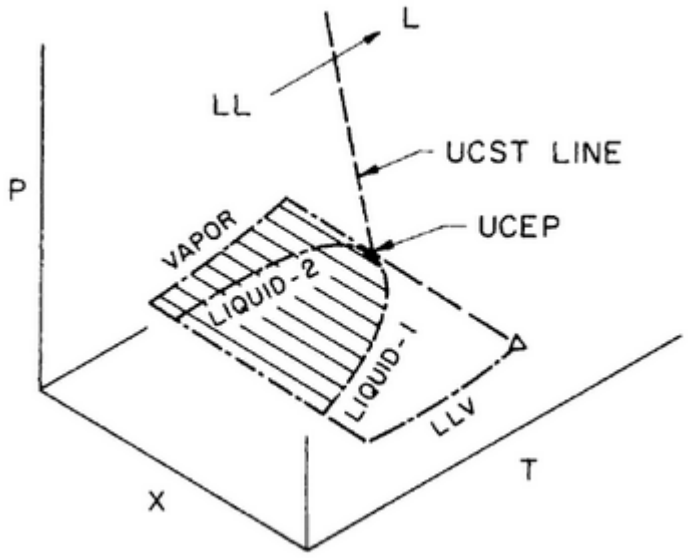

Figure 5. Pressure (P)-Temperature (T) -Composition (x) diagram for the three-phase LLV region of a binary mixture. UCST (upper critical solution temperature), UCEP (upper critical end point), LL (liquid-liquid line), LLV (Liquid-liquid-vapor line) (McHugh et al., 1994)

Notice that in the presence of gas phase, two liquids become critically identical (having identical critical points) at upper critical end point (UCEP). Only L-L equilibria exist at pressures above the ruled surface representing equilibrium of the three phases shown in Figure 5. (Streett, 2009)

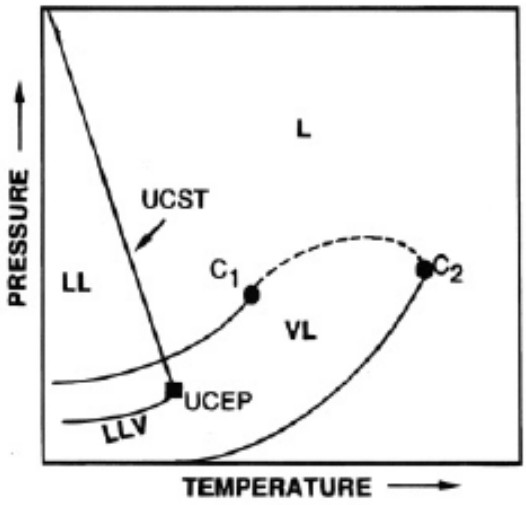

Figure 6. Binary phase diagram case 1. (McHugh et al., 1994)

The P-T locus of L-L critical points also termed as upper critical solution temperature (UCST). The location of critical points is relatively insensitive to pressure as indicated by the steepness of the UCST line in Figure 6. Location of UCST curve is governed by enthalpic interactions between the two components in a solution. Enthalpic interactions between mixture components primarily determine the state of miscibility and many of the physical properties of the mixture. (Prausnitz et al., 1986)

The UCST curve basically describe the transition of LL phase to L phase when temperature is increased isobarically. It is not unexpected to see that the UCST curve is comparatively unaffected by pressure since the temperature is quite low because the phases under consideration are dense liquids. (Kirby et al., 1999)

As critical properties (pressure, temperature and density) of substances are a function of intermolecular forces between the molecules of different structures and molecular weights, given phase behavior in Figure 7 is observed due to differences in these critical properties of two mixture components. These two pure component critical points are C1 and C2 shown in Figure 7, where C1 is more volatile component and C2, is the less volatile component. This phase behavior occurrence is due to the location of LLV region which is very close to the critical point of the more volatile component.

Critical mixture curve branch that starts from the critical point of the first component of mixture with the higher critical temperature intersects the LLV line at the low-temperature end called a lower critical solution temperature (LCST). The other branch

of the critical mixture curve, which starts at the critical point of the second component of lower critical temperature intersects the LLV line at the high-temperature end sometimes called a UCEP. A similar LLV behavior is observed in figure 6 as temperature go below the LCST. (McHugh et al., 1994)

From dashed curve of critical mixture from C2 to C1 in Figure 7, pressure dependency of vapor-liquid (VL) to liquid transition with decrease in temperature isobarically represents the characteristic of the LCST curve. (Kirby et al., 1999)

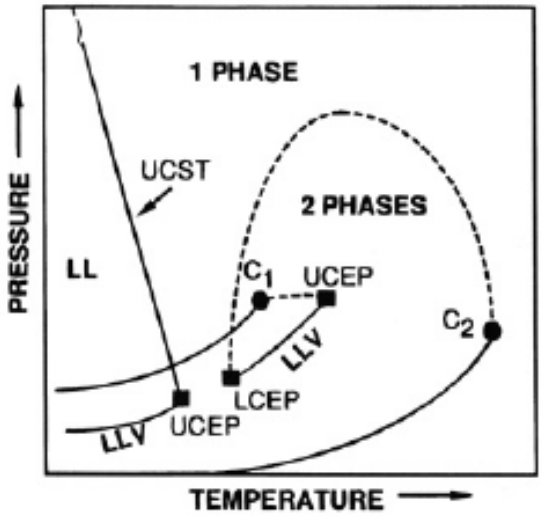

Figure 7. Binary phase diagram case 2. (Kirby et al., 1999)

As dissimilarities of critical properties increases between mixture constituents, two-phase regions (liquid-liquid and vapor-liquid) of diagram expand over a wider range of temperature and pressure. (McHugh et al., 1994)

In this P-T diagram 8, as the difference between intermolecular force strength, size and structure of mixture constituents becomes much larger, the UCST curve at higher temperature shifted and critical mixture curve branch that intersect with the LLV line at LCST shift to lower temperatures (UCST curve moves to higher temperatures and combines with the LCST curve) as shown in Figure 8. Now branch from a critical point of less volatile component will not intersect with LLV region, but rather it exhibits a pressure decrease and then displays a steep negative slope indicator of the UCST curve. (Kirby et al., 1999)

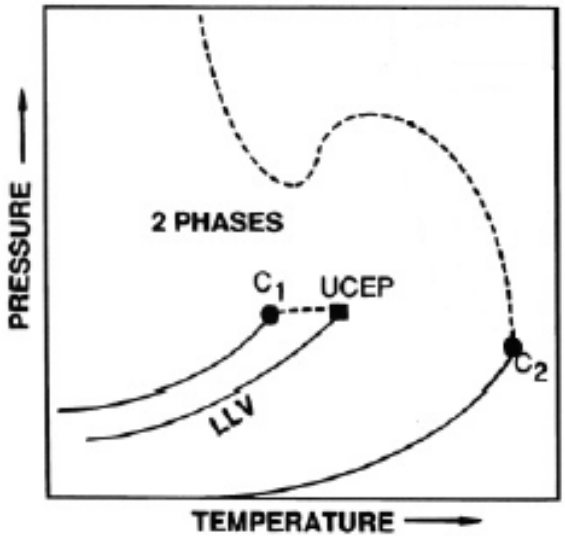

Figure 8. Binary phase diagram case 3. (McHugh et al., 1994)

2.4. Phase Separation mechanisms

Phase separation is one of the important aspects in designing efficient process equipment, especially for the development of continuous separation processes. In polymer-solvent systems, vapor liquid equilibrium (VLE) phase separation is achieved by two main mechanisms.

1. Dew point-type transition
2. Bubble point-type transition

A bubble point type transition features formation of a minor phase of lower density than the original single phase mixture. On the other hand, dew point type transition is described by the growth of a minor phase of a higher density than the original single phase mixture. These mechanisms are analogical to phase transitions in VLE systems. In VLE system, at bubble point a low density vapor phase starts to appear in liquid phase and at dew point a high density liquid phase starts to appear in vapor phase. These dew and bubble point-type transitions upon lowering pressure at constant temperature (shaded area represents polymer rich phase) are shown in figure 9. (Cameron, 2016) (Voorn, 1959)

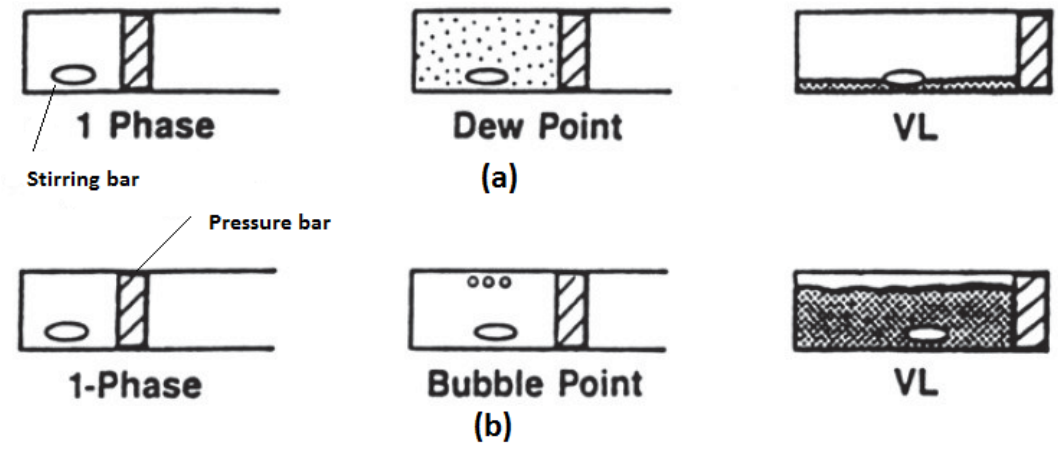

Figure 9. Dew and bubble point-type transitions. (Cameron, 2016)

As shown in Figure 9 (a), an increase in high density phase (liquid) occur upon lowering the pressure. Similarly in Figure 9 (b), an increase in low density phase (vapor) occur upon lowering the pressure.

As shown in Figure 10 (a), Bubble point type transition is achieved when initial polymer concentration (X_i) is larger than critical polymer concentration (X_{crt}) and in Figure 10 (b), Dew point type transition is achieved when X_i is smaller than X_{crt}. So X_i and X_{crt} play vital roles in describing such phase separation mechanism. Since molecular weight of polymers are in inverse relation with the X_{crt}, that means with increase in X_{crt}, MW of the polymer will decrease as shown in Figure 10. Therefore high MW polymer solutions tends to be separated under bubble point type mechanism and diluted polymer solution will follow the dew point type mechanism for separation. (Folie et al., 1996)

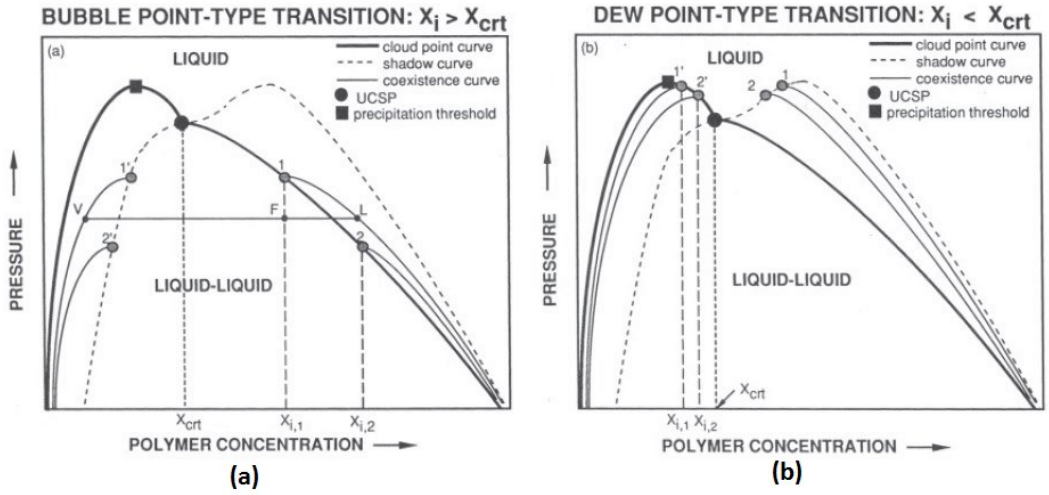

Figure 10. P-x diagrams for polydisperse polymer-solvent systems presenting UCSP behavior. (Folie et al., 1996)

Bubble and dew point-type transitions occur at the cloud point depending on the critical polymer concentration of the system and the initial concentration of the polymer. (Folie et al., 1996)

2.5. Phase behavior of polymer solutions

Shape and curvature of Gibbs free energy on mixing (ΔG_{mix}) as a function of concentration of polymer at a given T and P helps to understand the phase state of polymer-solvent solution and phase separation mechanism of that solution.

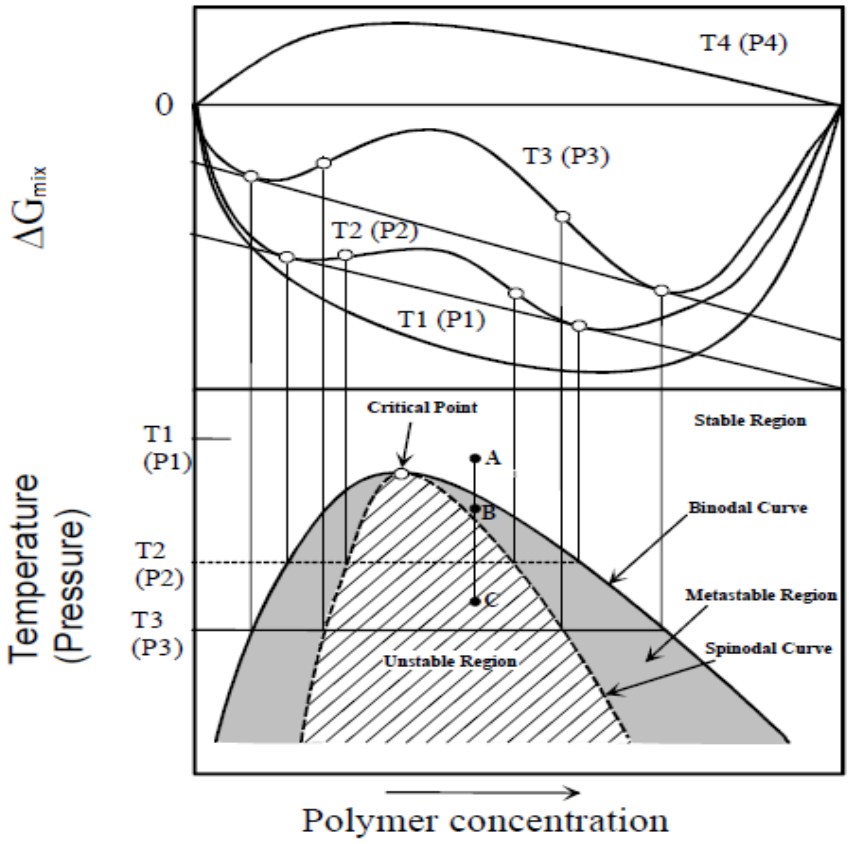

Figure 11. A diagram representing relationship between ΔG_{mix} and polymer concentration at different pressure or temperature in the upper portion. Lower portion represents a phase diagram of pressure or temperature and polymer concentration. (Utracki, 1994)

In Figure 11, at T1 over the polymer concentration range, ΔG_{mix} exhibits only one minimum, which shows that in the phase diagram over a whole range of polymer concentration, system is completely miscible. Further, at T2 and T3, the system shows only partial miscibility over a range of polymer concentration even though ΔG_{mix} is still lower than zero. In order to have ΔG_{mix} for the overall system to be minimized, ΔG_{mix} show two local minima that will separate the system into two phases. A concentration of these two phases is determined by ΔG_{mix} curve. (Zhang, 2005)

$$\left[\frac{\partial(\Delta G_{mix})}{\partial x}\right]_1 = \left[\frac{\partial(\Delta G_{mix})}{\partial x}\right]_2 \qquad 4$$

These two points on ΔG_{mix} called as binodal points and binodal curve is formed by connecting binodal points at different temperations. From the $\Delta G_{mix} - x$ curve, variation

points $\partial^2\left(\frac{\Delta G_{\mathrm{mix}}}{\partial x^2}\right)=0$ are spinodal points and curve is spinodal curve. Both curves meet at the critical point given as

$$\partial^2\left(\frac{\Delta G_{mix}}{\partial x^2}\right)=\partial^3\left(\frac{\Delta G_{mix}}{\partial x^3}\right)=0 \qquad 5$$

A stable region above the binodal curve is shown in Figure 11 and because of the stability, a homogenous solution can be formed in that region. The term $\partial^2(\frac{\Delta G_{\mathrm{mix}}}{\partial x^2})<0$, corresponds to an unstable region inside the spinodal curve. In this region, a spontaneous phase separation occurs that splits the system into two co-continuous phases. Similarly, term $\partial^2(\frac{\Delta G_{\mathrm{mix}}}{\partial x^2})>0$ represents a region between spinodal and binodal curves called as metastable region. In this region, system may have one unstable phase. T4 shows fully immiscible region over the entire range of polymer concentration, as ΔG_{mix} is larger than zero. (Zhang, 2005)

In lower part of Figure 11 shows a typical UCST behavior in a system. By increasing temperature from C to A, such systems exhibits the one phase region. On the other hand, if increasing temperature can shift the system from miscible to immiscible region, such system exhibits LCST behavior. (Zhang, 2005)

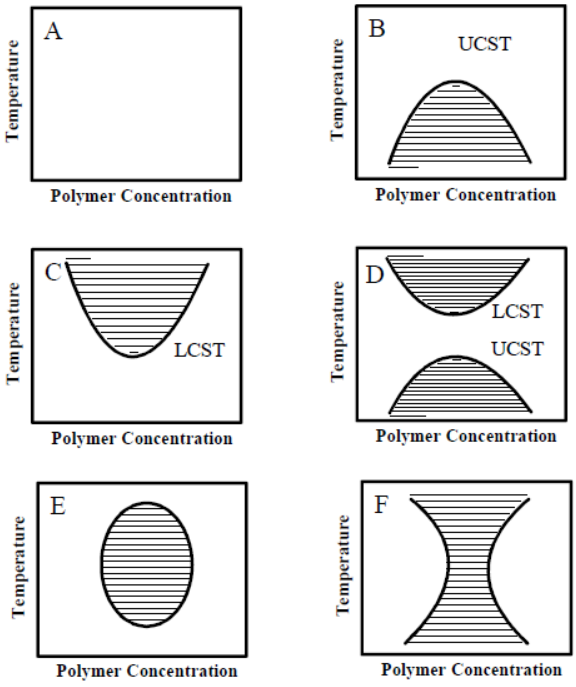

Figure 12. Different combinations of UCST and LCST types of phase behaviors. (Olabisi et al., 1979)

Figure 12 illustrates different patterns of these two phase behaviors. In Figure 12, only B and C display pure UCST and LCST behavior respectively. D and E shows an island of immiscibility. A phase diagram of hourglass shape can be observed in Diagram F where LCST and UCST branches merge with each other. Experimentally, polystyrene solutions in acetone exhibits such behavior. In the beginning two branches at higher pressures move into each other and later by lowering the pressure these two branches merge with each other. Phase diagrams shown in Figure 12 cannot explain the complexity of LL phase behavior. (Luszczyk et al., 1995)

Solid-fluid transition is another important phase transition in polymer solutions. If the polymers (linear polyethylene, polypropylene) have a regular chain structure, they can exist in crystalline state. The melting and crystallization temperature can be highly reduced in the presence of solvent. When the temperature decreases below the crystallization temperature range, solid-liquid phase behavior is involved in solution of semi-crystalline polymer. For a binary system, Equation 6 gives the solid-liquid phase separation temperature T. (Koningsveld et al., 2001)

$$T = \frac{\frac{\Delta H^0_{mi}}{R} + gT(1-x_i)^2}{\frac{\Delta H^0_{mi}}{RT^0_{mi}} - lnx_i} \qquad 6$$

T = phase separation temperature

T^0_{mi} = Melting temperature of pure components

ΔH^0_{mi} = Enthalpy of melting of pure component

g = Interaction function

x_i = Composition of component i

R = General gas constant

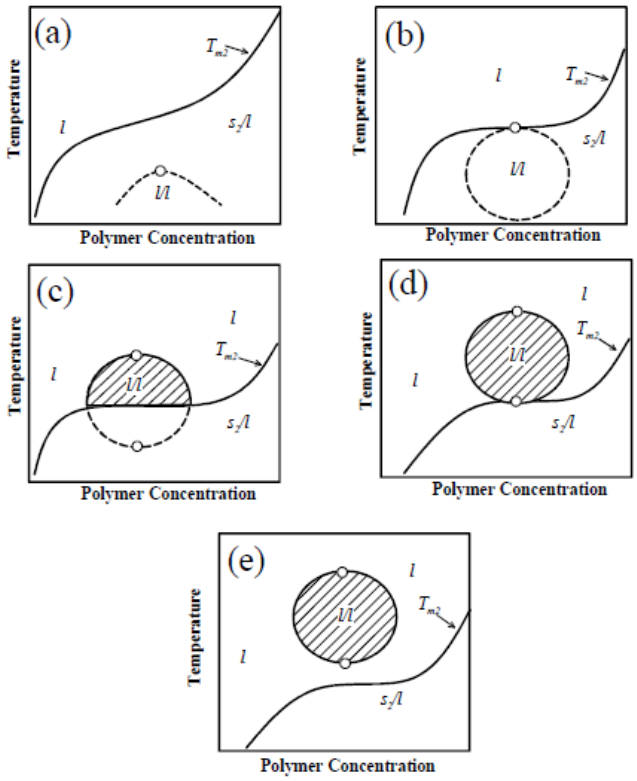

Figure 13. T-x phase diagram of a semi crystalline polymer in solution with a liquid-liquid phase boundary. (Koningsveld et al., 2001)

In Figure 13, **(a)** shows a LL phase boundary of the crystalline polymer solution submerged under the solid-fluid (S-L) phase boundary. As shown in an open circle of **(b)**, with the decrease in melting temperature of the polymer, the LL critical point meets the solid-fluid line. With further decrease in temperature, a UCST type of phase diagram appear in **(c)**, where the LL phase boundary is more exposed to the solid-liquid line. In **(d)** and **(e)**, UCST and LCST types of boundaries appear respectively. According to experimental data from Zhang, melting temperature increases with pressure. So pressure can control the L-L phase boundary location. (Zhang, 2005)

2.6. Summary

The phase state of reaction mixture controls the polymerization kinetics of the mixture. These polymerization kinetics define the polymer structure and end-use properties. So, this chapter generally explained the principles of molecular thermodynamics, which helps to understand about the conditions in which a polymer dissolve in the solvent. As a result of this literature review, it is appears that the ΔG_{mix} must be a minimum and

negative for a stable polymer-solvent solution. A diagram of ΔG_{mix} as a function of polymer concentration at different pressures or temperature conditions showed different combinations of UCST and LCST phase behaviors. Similarly, phase separation kinetics are also very important in order to minimize the separator volume and polymer residence time inside the separator.

3. Factors effecting the cloud point

When considering only a PE + ethylene system at high pressures, ethylene is soluble to the PE phase and only one phase appears. If either the pressure is decreased or the temperature is increased at this point the polymer mixture might become cloudy and this pressure-temperature-composition point is called as the cloud point. This chapter mainly focuses on the importance of cloud point measurements for polymer solutions and different parameters that can affect the measurement values in polymer solutions. Effect of solvent quality is one major parameter that can impact the cloud point values. Along with that temperature, pressure, molecular weight and polydispersity of the polymer are also discussed.

3.1. Cloud point measurement

The cloud point data is important for the reactor operation to ensure that polymerization occurs in a desired phase. (Liu et al., 1980)

de Loos et al. investigated these LLDPE + solvent phase equilibria for different types of LLDPE and solvents. They showed that the cloud point temperature increased in isobaric conditions when the alkane chain length increased. Similarly, cloud point temperature increase with increasing weight fraction of the polymer when polymer solution is at isobaric conditions. For the higher density polymers, the cloud point temperature is lower than that for low density polymers. (de Loos et al., 1983)

The binary polymer-solvent diagram in Figure 7 in actual represents the multicomponent phase behavior of polymer-solvent system. Cloud Point, a multicomponent analogue of binodal point, represents the transition of a clear single phase to two cloudy phases at either UCST or LCST points. This transition from a single phase into two phases can be achieved by decreasing the temperature isobarically i.e. crossing the UCST curve or by crossing LCST curve, which is attained by increasing the temperature. Since the polymer do not have critical points, during the transition at high temperature values LCST curve cannot achieve a discrete end point. So, for polymer solvent solution the LLV lines can superpose onto the vapor pressure curve of the solvent. (Kirby et al., 1999)

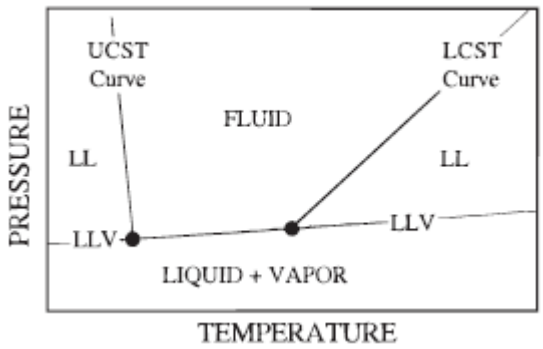

Figure 14. Temperature-pressure phase diagram for binary mixtures of low MW solvent with a higher MW polymer. (McHugh et al., 1994)

Figure 14 represents phase behavior for small molecules inferred to polymer-solvent mixture. It is observed that the LCST curve becomes more sensitive to the pressure changes when temperature at the point is quite close to the critical temperature of the solvent, where this solvent is highly compressible. Therefore, molar volume of the solvent is decreased with increased pressure that can help to reduce the free volume difference between the polymer and the solvent. (Freeman et al., 1960)

It is important to be aware that the binary polymer-solvent diagram in Figure 14 actually represents multicomponent phase behavior since all polymers have a molecular weight polydispersity fixed by the synthesis technique used to make the polymer. For polymer-solvent mixtures term cloud point is defined as transition of a transparent single phase to an opaque two-phase system occur either at LCST or UCST. This is the multicomponent analogue of a bimodal point. Isothermal maximum P-x curve, which is measured as a cloud point, does not correspond with critical point of the mixture. Binary mixture of monodisperse components does behave opposite to that. So, critical point for such mixture shifted to higher overall polymer concentration and a lower pressure than the maximum of p-x curve. For polydisperse systems, a horizontal line does not define the composition of the two simultaneously existing phases at each pressure of the P-x curve. This trend might be true for a binary mixtures as each of coexisting phase contains different molecular weights of participating oligomers that leads to partial fractionation of the parent polymer. A shadow curve is observed by measuring the composition of the phase that participates at the cloud point. Interaction of shadow and cloud point curves, which also occur at the interaction of spinodal and binodal curves, represents the true critical point of polydisperse polymer solvent mixture. (Rowlinson et al., 1982) (de Loos et al., 1983)

Another difference between small molecule and polymer-solvent behavior shown in Figure 7 and 14 respectively, is that the curves in the small molecule diagram are the curves of points for mixtures with differing compositions. Whereas the curves in polymer-solvent diagram are at essentially one fixed composition. (Kirby et al., 1999)

For a mixture of monodisperse components, it is observed that over a pressure interval greater than that of observed pressure, a transition of cloud point can occur. Usually for a polymer having molecular weight polydispersity of less than ~3.0 and having a higher molecular weight, the transition of cloud point is measured between a pressure range of 5-7 bar. If the molecular weight polydispersity of the polymer is large, the LLV signifies the higher pressure at which three phases exist also shown in figure X. (Lee et al., 1997)

In figure 15 illustrates the effect of higher pressure values on UCST and LCST curves to get general understanding on phase behavior for polymer of range 3-15 weight %. In this temperature-composition diagram of polymer-solvent solution, temperature maximum or minimum is unresponsive to composition. Similarly, for pressure-composition diagram, pressure and composition behave the same way. This means cloud point curve with composition between 3-15 weight %, essentially superpose. It can be seen from the Figure 15, curves are comparatively flat that the UCST and LCST points between the range of 3-15 weight percent of polymer. (Irani et al., 1986)

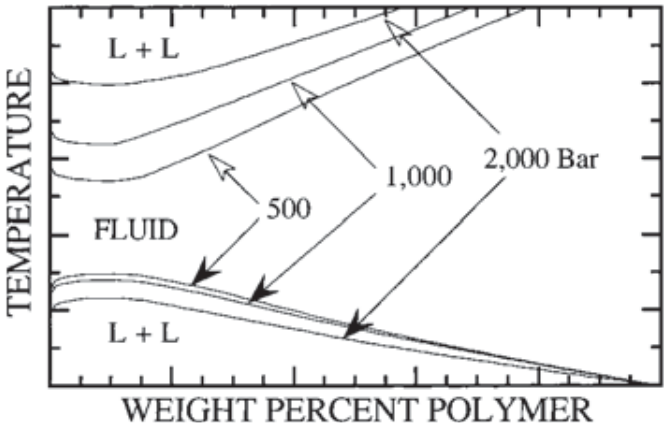

Figure 15. A diagram to represent the effect of pressure on the maximum (UCST) and minimum (LCST) for a polymer-solvent mixture. (Kirby et al., 1999)

For high molecular weight and for molecular polydispersity higher than ~3.0, pressure maximum of P-x curve move to lower polymer concentration values. At that point, at a fixed polymer concentration between 3-15 weight %, cloud point curve may not

represent maximum pressure required to sustain single phase at all concentrations. So for a polymer of molecular weight greater than ~100 000 g/mol, a weakening effect of polymer molecular weight in a liquid solvent can be observed on UCST curve, as shown in Figure 16. Similar kind of behavior is predictable if the pressure axis is exchanged with the temperature axis. (de Loos et al., 1983)

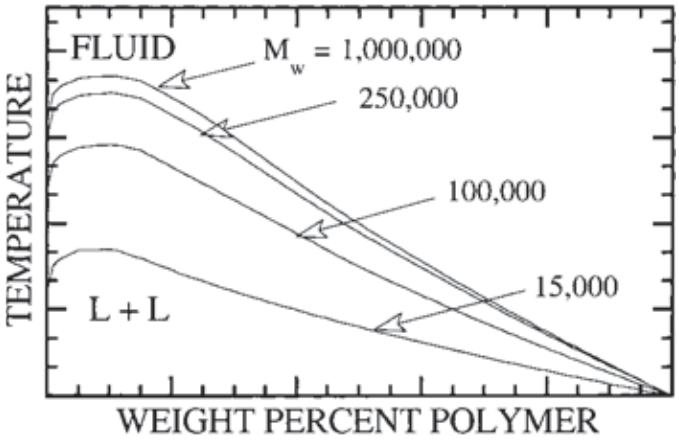

Figure 16. Effect of polymer molecular weight on the phase behavior of a polymer-solvent solution at random pressure values. (Kirby et al., 1999)

As already discussed in Figure 7, when two components in solution differ considerably with respect to their intermolecular potential or molecular size, the UCST curve shifts to higher temperatures and merges with the LSCT curve. Figure 17 illustrates similar behavior in polymer-solvent mixture, when one of the two components is non-polar and others are polar. For polymer-solvent system, at higher temperatures the cloud point curve is comparatively constant and show a sudden increase with a decrease in temperature. (Kirby et al., 1999)

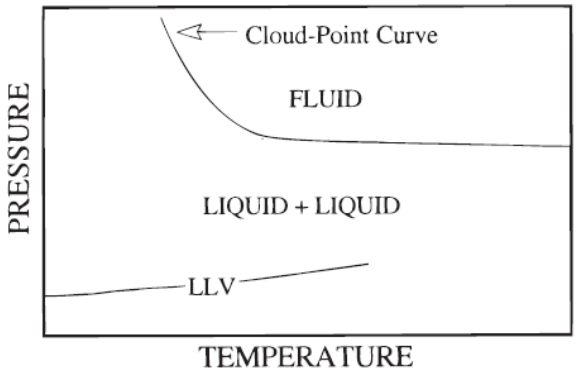

Figure 17. T-P phase diagram for binary mixtures of low MW solvent with a higher MW polymer. (Kirby et al., 1999)

Figure 18 represents fluid-phase behavior. This behavior is observed when polymer in mixture is semi-crystalline. For all practical purposes the solubility is so low at temperatures below the solidification boundary that polymer fractionation or extraction processes would not be operated in this regime. Generally, regardless of the system pressure, solution of polymer remains very dark (clouded) at temperature below solidification temperature. (Kirby et al., 1999)

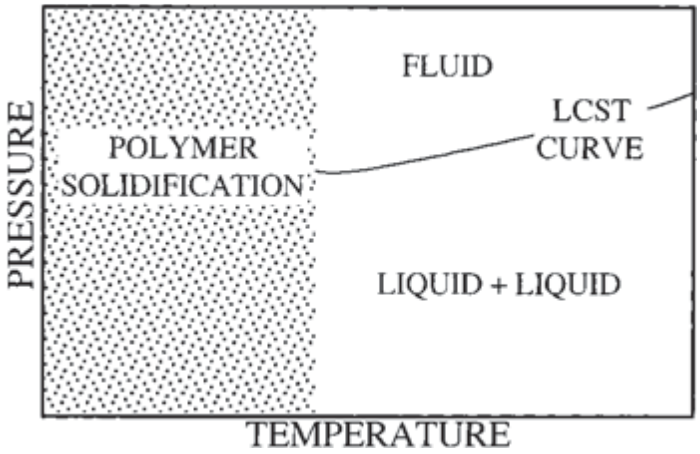

Figure 18. Polymer solidification effects on the phase behavior of polymer-solvent mixtures. (Kirby et al., 1999)

The temperature is increased at constant pressure to find out whether this region represents liquid-fluid or solid-fluid equilibria. A liquid-fluid region exists at a lower temperature if solution becomes clear with the increase in temperature of about one – to-two ℃. However, if solution becomes clear after 10-20 ℃ increase, solid-fluid region exists at lower temperature. (Kirby et al., 1999)

3.2. Effect of solvent molar mass

With increasing molecular size of solvent, the pressure required to achieve a single-phase decreases. Figure 19 shows the phase behavior of polyethylene in a verity of different solvents. For example, starting from ethylene, 1600 bars pressure is required to obtain a single-phase at 393K. In case of propylene, cloud point pressure reduces from 1000 bar to ~600 bar and a decrease of 400 bar to ~200 bar occur with two different butenes (1-butene and 2-trans-butene) to achieve a single phase. In the case of n-hexane, single phase is obtained up to a pressure of 140 bars. (Nagy et al., 2007)

The properties of polymers in solution are determined by the balance between effective monomer–monomer attractions and excluded volume repulsions. These two terms explains the solvent quality in a polymer-solvent mixture. The excluded volume of a molecule in solution is the effective volume that is inaccessible to other molecules in the solution due to the presence of the first molecule. In good solvents dominance of excluded volume effects cause the better mixing of polymers in solvent molecules. (Hansen et al., 2005)

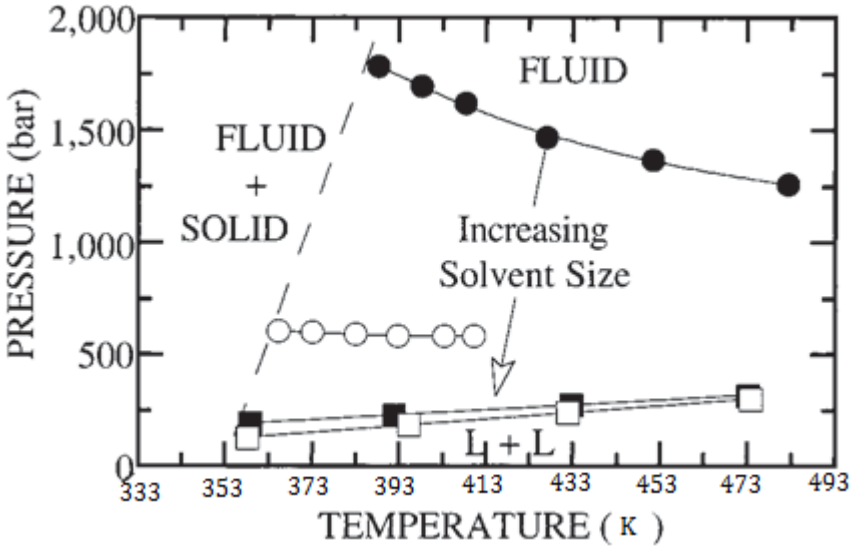

Figure 19. Effect of solvent quality on PE of MW 108 000 (g/mol), Polydispersity (Mw/Mn) 3.0, Melting temperature (Tm) 386 K solubility at 5 weight percentage in normal alkenes (closed circles, ethylene; open circles, propylene; closed squares, 1-butene; open squares, 2- butene). (Kirby et al., 1999)

Figure 19 also gives an idea about the strength of double bonds in polymer-alkene mixtures. (Ehrlich et al., 1963) showed that the polyethylene-alkane mixtures exhibit very similar trends to those found with the alkene solvents. PE-propene and PE-butene curves superpose onto propane and butane curves respectively. Only PE-ethylene curve is more than 400 bars higher than ethane curve. Reason for such behavior is strong quadrupole solvent characteristic of ethylene due to presence of a double bond. These quadrupole interactions favor ethylene-ethylene bond rather than non-polar PE-ethylene bond. With the increase in system temperature, quadrupole ethylene-ethylene bond strength decrease which results in pressure drop in PE-ethylene cloud point curve, as described in Equation 3. The location of the ethane and ethylene curves is intimately related to the balance of polymer segment-solvent energetic interactions since these two solvents have similar densities at their respective cloud point

conditions. The double bond, quadrupolar effect is decrease in propylene and butane because the quadrupole moment is spread over much larger volume in comparison to ethylene case, which weakens the quadrupole effectiveness by a factor of molar volume ($v_i^{-\frac{5}{6}}$) (Ehrlich et al., 1963) (Lee et al., 1994).

Similarly, propylene curve is ~30 bar higher in pressure than the propane curve. Similarly, polar butene-butene bond cause a minor effect on phase behavior of PE in 1-butene and 2-trans-butene. At temperature around 353 K, PE-1-butene curve is ~50 bars greater in pressures than the 2-trans-butene curve. This difference is due to those polar butene-butene interactions as 2-trans-butene is less polar than 1-butene. That difference is notable at low temperatures, because difference between components intermolecular potential energy in a solution makes interchangeable energy very sensitive that can cause non-polarity in PE. Generally, in a solution consisting of one polar and other non-polar component, with decreasing value of temperature, cloud point curve of that system will exhibit a negative slope. That means even with decreasing value of temperature (x-axis), pressure values increase (y-axis). (Whaley et al., 1997)

For other systems showing LCST behavior, effect of solvent on cloud point temperature is presented below in Figure 20.

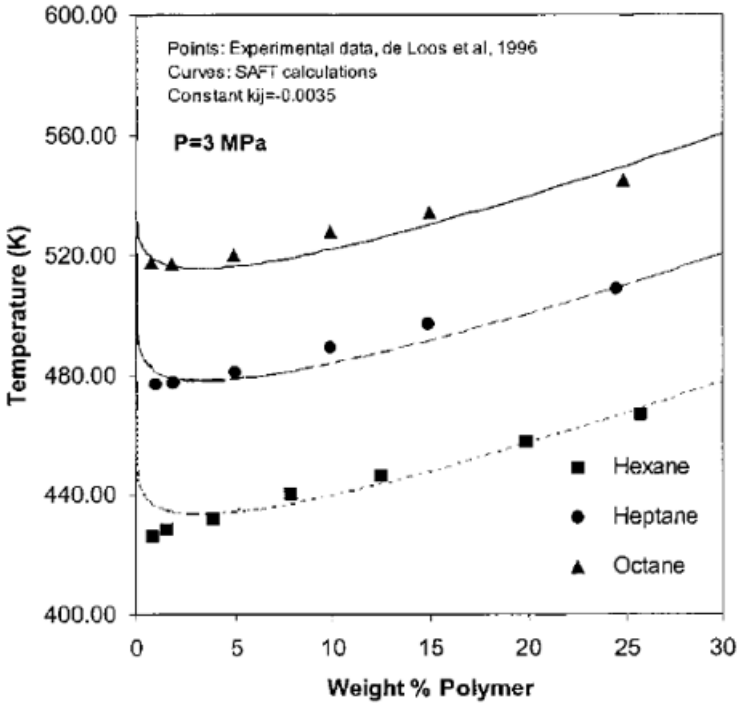

Figure 20. Effect of different solvents (hexane, heptane, and octane) on the cloud-point temperatures of poly-(ethylene-octene) (Mn) 33 000 (g/mol) and (Mw) 124 000 (g/mol) at a constant pressure of 30 bars. (Jog et al., 1996)

It can be seen in figure 20 that all of these systems show lower critical solution temperature (LCST) behavior. In systems showing LCST behavior, the solution splits into two phases at higher temperatures and becomes one phase at lower temperatures. A higher LST means a smaller region of L-L immiscibility. So a solvent with a higher LST with LLDPE is a better solvent for LLDPE. According to (de Loos et al., 1996), with every addition of CH2-group, there is an increase in LST by ±43 K. This explains how increasing molar mass influence the LST. Figure 20 gives comprehensive information that with increasing molar mass of solvent, solubility of polymer in solvents increase, which reduces the density difference and tends to lower the cloud point pressure values. Another comparison with different solvents is presented in chapter 3.6.

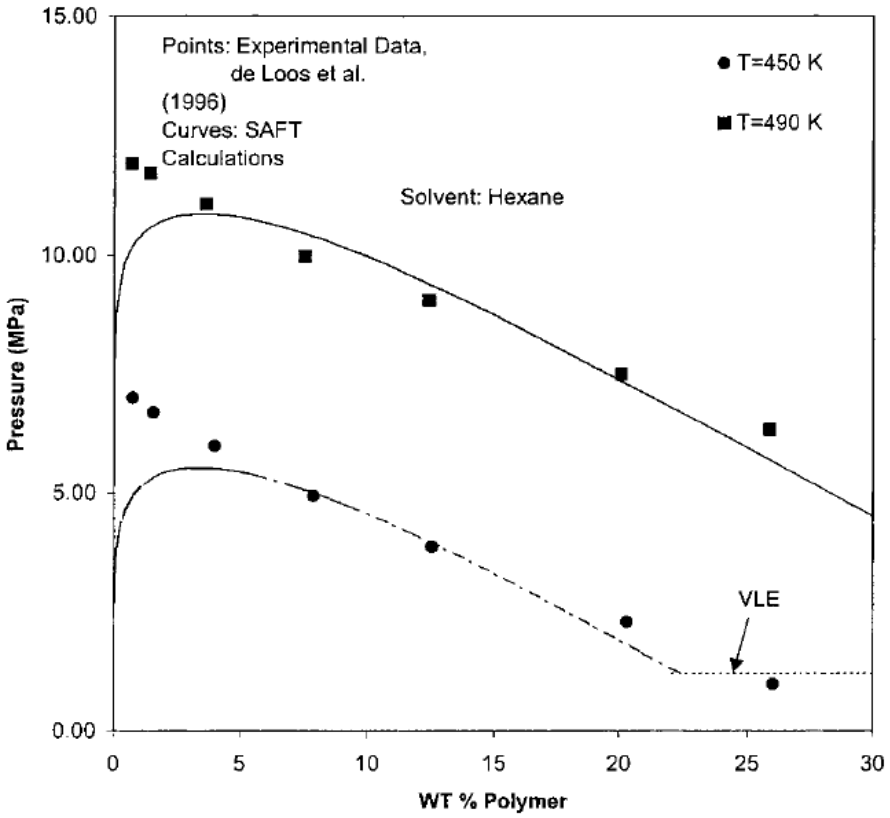

Figure 21. PE-hexane system with cloud point data at constant pressure (isobaric) from SAFT and experimental points. (Jog et al., 2002)

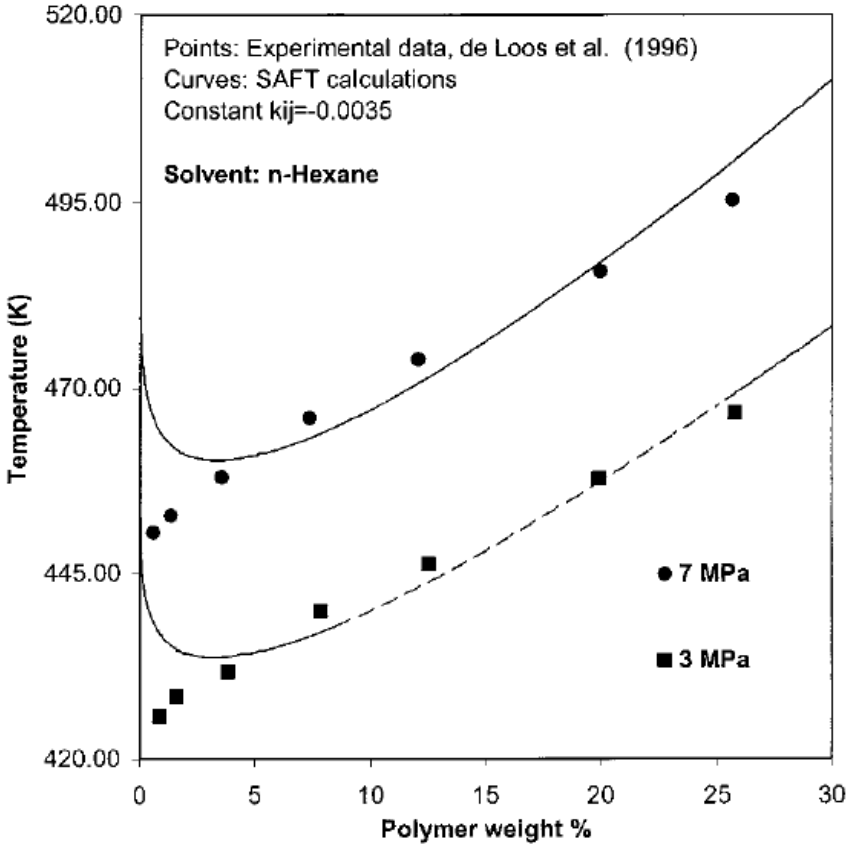

Figure 22. PE-hexane system with cloud point data at constant temperature (isothermal) from SAFT and experimental points. (Jog et al., 2002)

Similarly, Figure 21 and 22 shows cloud point curves at constant pressure and temperature for LLDPE + n-hexane system.

3.3. Effect of Molecular Weight distribution

3.3.1 Effect on cloud point pressure

Effect of molecular weight on cloud point pressure in polymer-solvent system is presented in figure 25. Figure 25 shows a polyisobutylene-butane system.

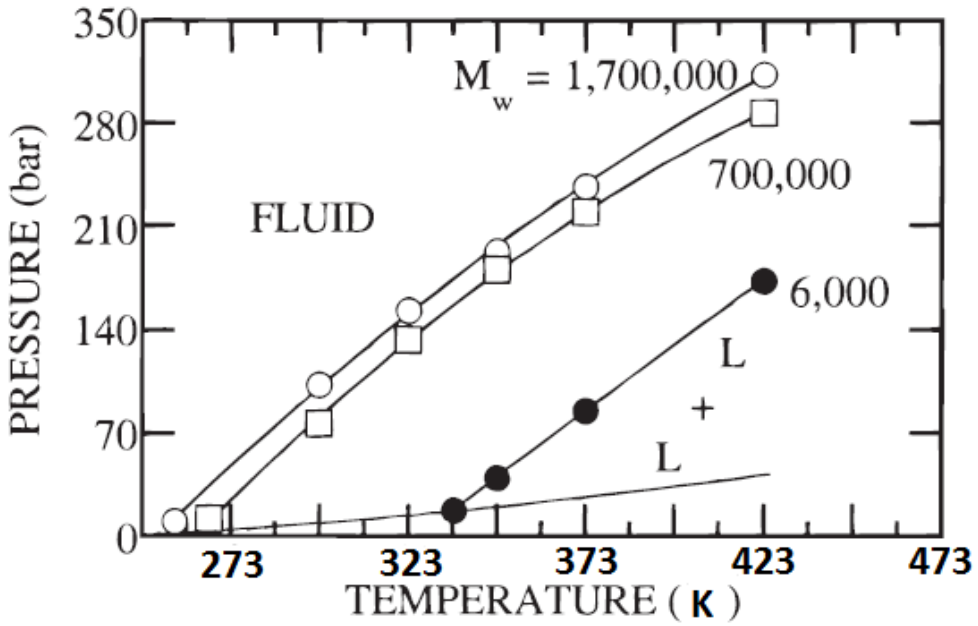

Figure 23. Molecular weight average (M_W) effect on cloud point for polyisobutylene-butane system. The polymer concentration is ~5 wt % in each case. (zeman et al., 1972)

The LCST curve becomes less sensitive to MW when MW of the polymer exceed a few hundred thousand and this MW value vary differently for different polymer-solvent systems. For example in Figure 23, at 423 K the cloud point pressure increase by ~100 bar as MW increases from 6000 (g/mol) to 700,000(g/mol); it increases again by ~30 bar as the MW increases from 700,000(g/mol) to 1,700,000(g/mol). This will help to understand how after some specific MW value, LCST curve becomes less sensitive to MW of the polymer in polymer-solvent system. (Zeman et al., 1972)

Similar is the case for the PE-ethylene system when MW exceeds 100,000, change in LCST curve becomes far less noticeable. At 423 K the cloud point value increases by 300 bar with increase in MW from 3700(g/mol) to 9200(g/mol). And when MW increase from 9200(g/mol) to 55000(g/mol) cloud point increases by 300 bar again. A contradiction comes when MW increases from 55000 to 118000. During this increase in MW, cloud point pressure increases only by 100 bar. (de Loos et al., 1983)

3.3.2 Effect on cloud point temperature

Cloud point temperature is also effected by MW of the polymer. Figure 24 shows poly(ethylene-octene) (M_n 33000 (g/mol) and M_w 124000 (g/mol)) and heptane system at fixed pressure 50 bar.

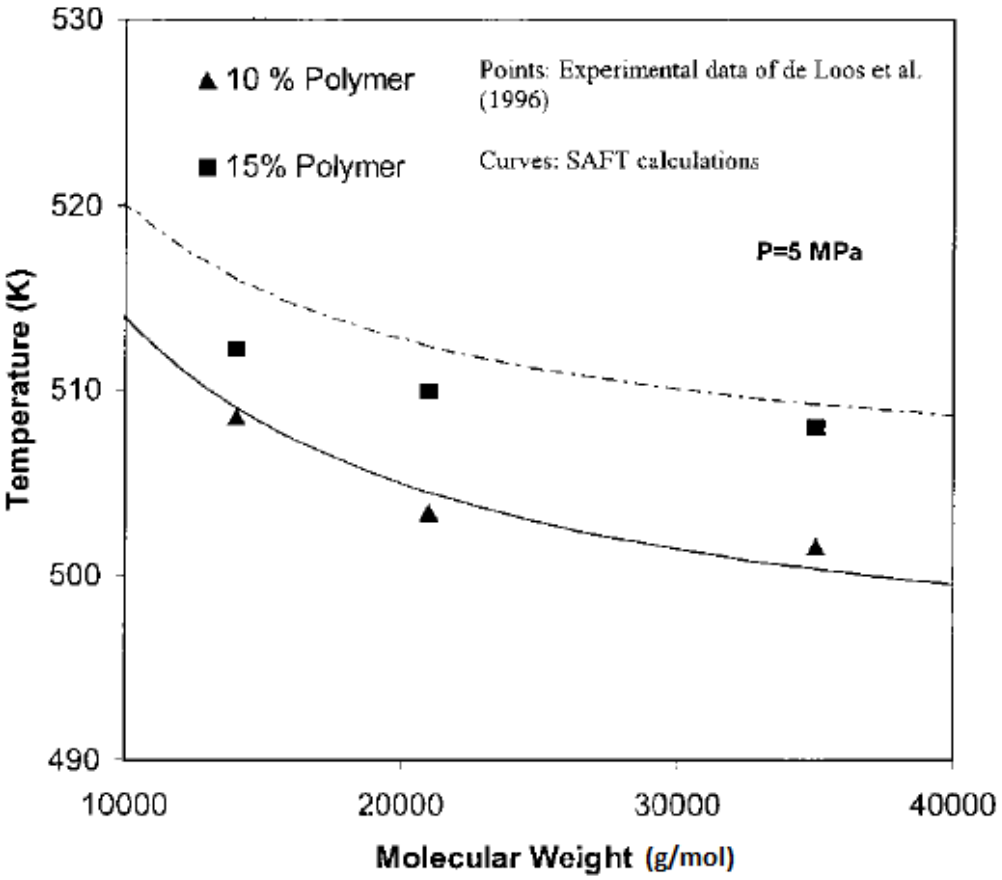

Figure 24. Effect of molecular weight at constant polymer concentration on the cloud-point temperature of the poly(ethyleneoctene) (Mn= 33 000 g/mol) and (Mw= 124 000 g/mol) + heptane system at P= 5 MPa from experiment points and SAFT (Jog et al., 2002)

The SAFT (statistical associating fluid theory) results shows in Figure 24 that the cloud point temperature is decreased with increasing MW until it reaches a level of high enough MW. In SAFT calculations, a monodispersed polymer is used with different values of MW, where as in experimental calculations polydispersed samples are utilized and a polydispersity index (PDI) is obtained at different data points. So polydispersity is partly responsible for difference in SAFT and experimental points. (Jog et al., 2002)

PE-pentane system shows a decrease in temperature with increase in MW. When MW is increased from 34900(g/mol) to 97200(g/mol), the LSCT of PE-pentane systems decreases from 433 K to 422 K. Similarly when MW increased further to 204900(g/mol), this time temperature is decreased to 418 K and it only decrease to 414 K with further increase in MW up to 442100(g/mol). So this explains how temperature is effected by different ranges of MW. (Hamada et al., 1973)

3.4. Effect of polydispersity

The ratio $\frac{\text{Weight average molecular weight } (Mw)}{\text{Number average molecular weight (Mn)}}$ called the polydispersity index (PDI) (also known as heterogeneity index and dispersity index) and is an indication of the broadness of molecular weight distribution. As PDI increases, MWD broadens. For polyethylene produced with transition metal catalysts, largely the catalyst employed dictates MWD shown in Figure 25. Polydispersities typically range from 2-3 for polyethylene made with single site catalysts, 4-6 for polymer produced with Ziegler-Natta catalysts and 8-20 for polyethylene made with supporting chromium catalysts. These distributions are said to be unimodal. (Malpass, 2010)

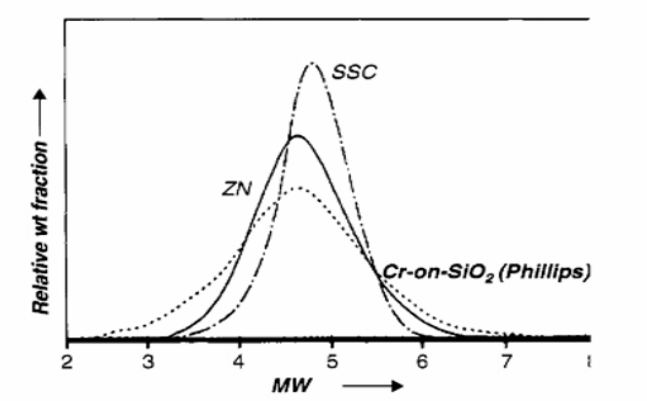

Figure 25. MWD of polyethylene from transition metal catalyst. (Kirk-Othmer, 2006)

According to isothermal cloud point data, with the decrease in concentration, cloud point, pressure increases. But SAFT calculation shows as the polymer concentration decreases below the critical concentration (depends upon MW of polymer), pressure at the intercept of the two-phase equilibrium decreases. A shadow curve represents the monodisperse case. A P-X diagram (Figure 26) shows the result of these calculations. The polydispersity of the polymer explains the behavior of the cloud-point curve at low polymer concentrations. (Jog et al., 2002)

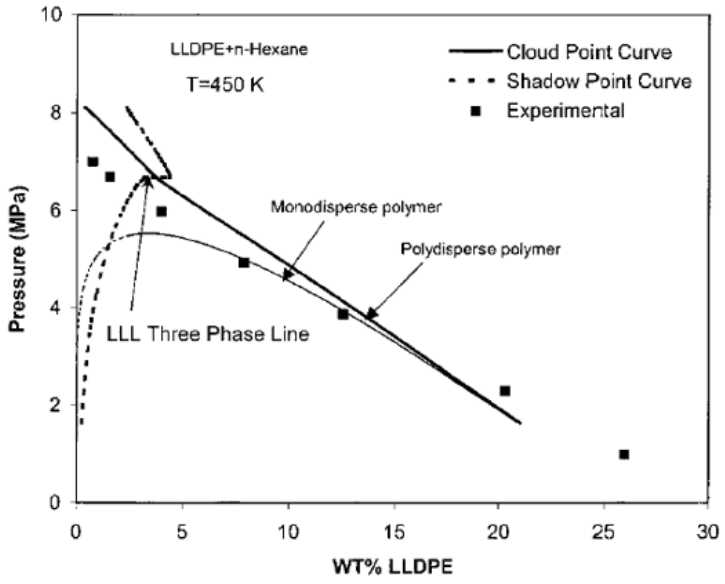

Figure 26. SAFT and experimental points data representing cloud and shadow curves for poly(ethyleneoctene) system at 450 K temperature. (Jog et al., 2002)

Figure 26 shows measured data for monodisperse and polydisperse polymer systems. It can be seen from Figure 26, at cloud point, dotted curve represents the composition of an emerging phase and interestingly at polymer weight fraction of about 3.73 %, a three phase LLL equilibrium point appears. This appearance of three-phase point indicates the inconsistencies in cloud point pressure measurements with increasing or decreasing values of polymer concentration. (Jog et al., 2002)

3.5. Effect of Pressure

Miscibility in liquid mixtures can be affected by pressure applied to the system. This study tries to explain that effect with one of the experimental example available in literature. The pressure effect is directly related to volume change during mixing (excess volume of mixing V^E) at fixed temperature and composition values. Solubility of polymer in solvents at various pressure trends depends upon V^E values. Therefore, with increasing pressure, if V^E value is positive it will cause a decrease in solubility whereas, with increasing pressure, if V^E value becomes negative solubility increases. (Prausnitz et al., 1999)

Difference in intermolecular forces between polymer and solvent is a major reason for UCST phase separation in polymer-solvent mixture. Based on experimental findings, pressure can affect the UCST curve in compliance to positive or negative values of V^E.

The LCST, in comparison to UCST, mainly affected by the free volume differences between the polymer and the solvent. Main concept behind this statement is that the expansion of the solvent in comparison to polymer especially when temperature is quite close to critical temperature of the solvent. As it is common knowledge that the solvent is more compressible than the polymer, therefore, by increasing the pressure the difference in free volume can decrease and decrease the possibility of achieving partial miscibility at constant temperature i.e. rise in the LCST curve. (Zeman et al., 1972)

One experimental case study is discussed here, involving polystyrene (PS) and acetone system. The systems examined in this study, the type of phase separation they exhibit, and the temperature range of the available experimental data are listed in Table 2.

Table 2. Polystyrene/acetone system LLE experimental data. (Pappa et al., 2001*)*

System	M_w/M_n	Pressure(bar)	LLE type	T range (K)	Data used for
PS/acetone	<1.06	1	hourglass	284.2-413.3	Correlation
		20	UCST,LCST	288.1-407.7	Prediction
		50	UCST,LCST	283.4-427.8	Prediction
		100	UCST,LCST	276.1-455.0	Prediction

It can be seen from experimental data available from Table 2; an hourglass behavior can be observed for such partially miscible system for all temperatures at atmospheric pressure value, shown in Figure 27. Now by increasing the pressure a complete miscible region is obtained in such system at intermediate values of temperatures. Such behavior is UCST and LCST behavior. The equation of states (EoS) model is utilized to measure the difference in free volume in solvents. This model yields negative V^E and try to predict the increasing miscibility with pressure. Results are presented in Figure 27 with remarkably accurate predictions of pressure effect where deviation for UCST and LCST is less than 5K temperature at highest pressure of 100 bars. (Pappa et al., 2001)

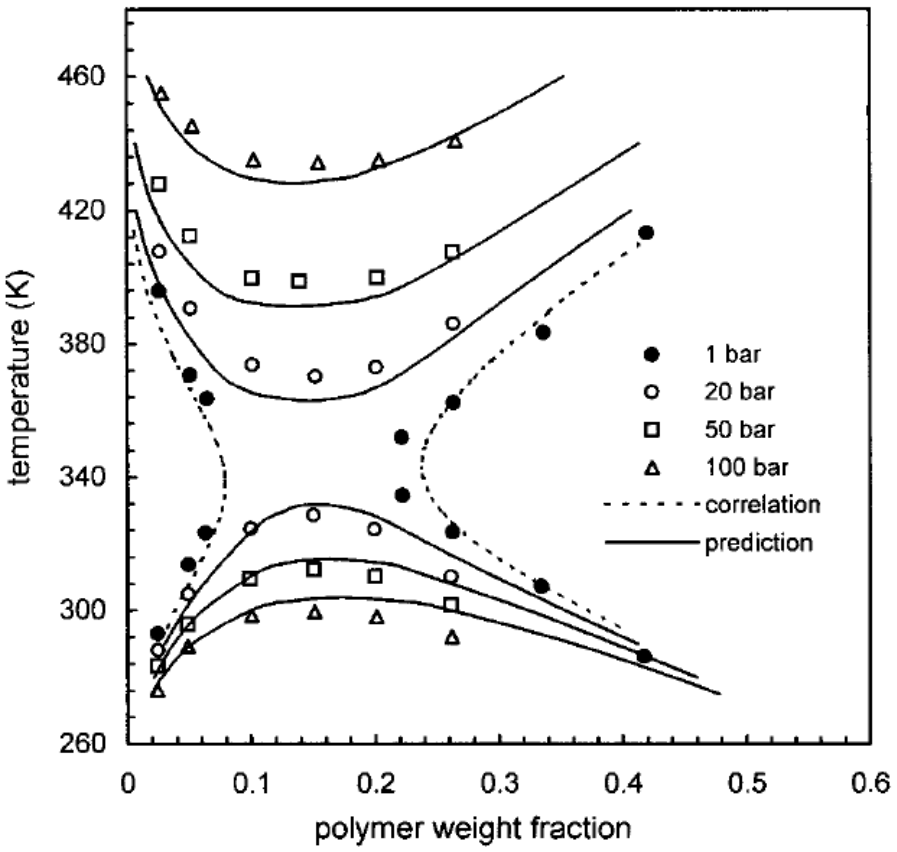

Figure 27. For PS/acetone system, experimental results of pressure effect on LLE. (Pappa et al., 2001)

As experiments show, the pressure effect is more noticeable on the LCST than on the UCST. (Patterson, 1969)

3.6. Effect of components weight fractions

The effect of component weight fraction changes to the cloud and bubble point lines was studied for polymers. When the polymer, monomer and co-monomer weight fractions increase, the cloud point lines shifts to higher temperatures and lower pressures (Lönnqvist, 2016). First, we will discuss the effect of 1-butene and 1-hexene as solvent on cloud point pressure values. Figure 28, represents the cloud point pressure values for propylene, 1-butene and 1-hexene.

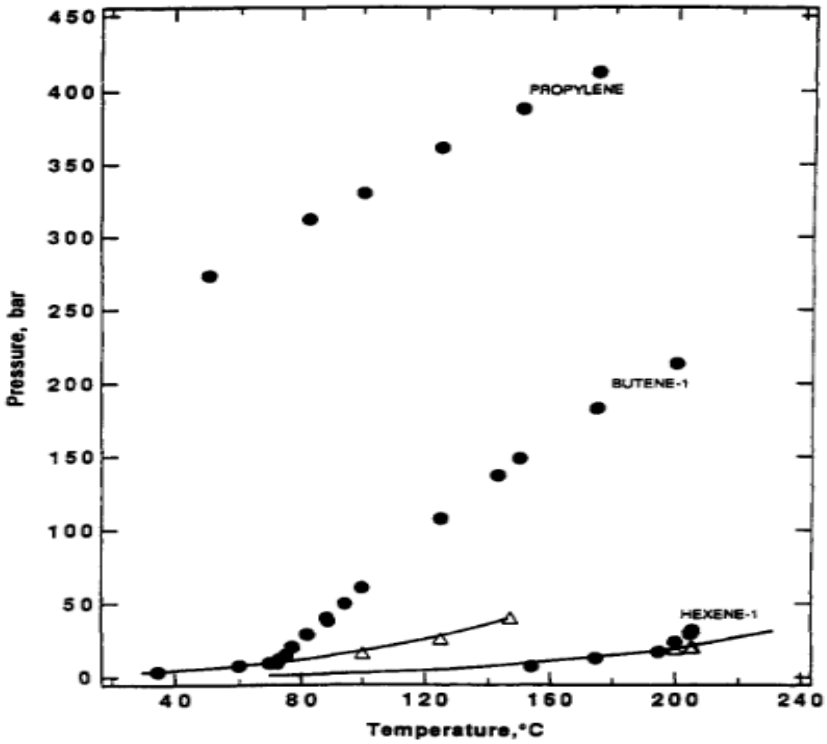

Figure 28. Pressure-temperature cloud-point curves for poly (ethylene-propylene) 26K (PEP26K) in propylene (W2=15.1 wt. %), in 1-butene (W2=16.0 wt. %), and in 1-hexene (W2=15.0 wt. %). Open circles indicate a dew-point-like phase boundary while filled circles indicate a bubble-point-like phase boundary and triangles indicate a two-to-three phase boundary. The heavy lines are the vapor pressure curves of the solvents (Chen & Radosz, 1992).

It can be seen in figure 28, in binary systems like this, different solvents shift the cloud point values depending upon their molar mass. As the molar mass of propylene is lower than 1-butene and 1-hexene, it tends to exhibits highest cloud point pressure values. Experimental data obtained from (Chen & Radosz. 1992) in case of 1-butene and 1-hexene as solvent is presented in table 3 and 4. Data comparison presented in figure 2 helps to understand the effect of the molar mass of the solvents.

Table 3. Measurement results for poly (ethylene-propylene) 26K (PEP26K) 16 wt % + 1-butene 84 wt % (Chen & Radosz, 1992).

T (°C)	p. cloud (bar)
150	149
175.2	183
200.2	213.4

Table 4. Measurement results for poly (ethylene-propylene) 26K (PEP26K) 16 wt % + 1-hexene 84 wt % (Chen & Radosz, 1992).

T (°C)	p. cloud (bar)
200	23.5
204.8	29.4
205.5	31.6

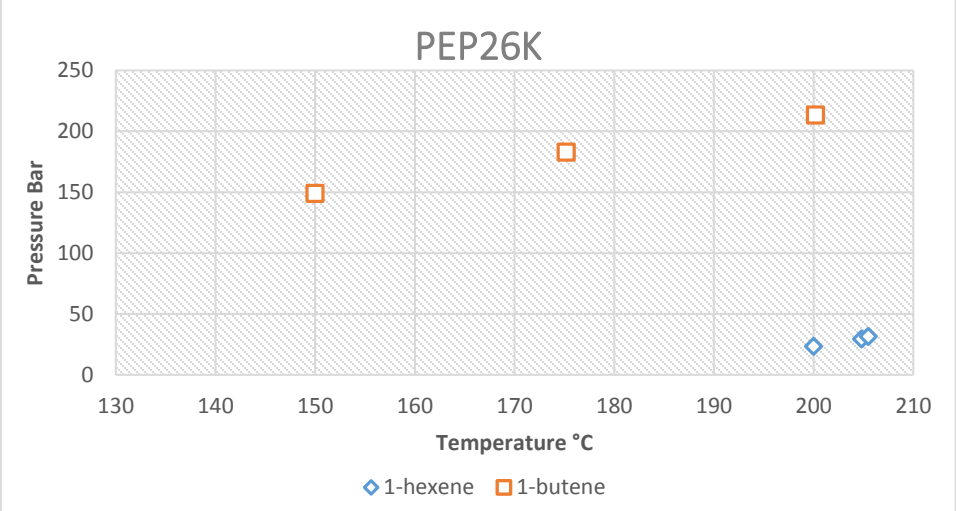

Figure 29. Cloud point curves for PEP26K (16 wt %) in 1-butene and 1-hexene (Chen & Radosz, 1992).

In figure 29, at 200 °C, cloud point values for both cases shows a large difference of approximately 190 bars. So we can conclude from this discussion that 1-butene having lower molar mass shift the cloud point pressure to higher values in comparison to 1-hexene which has lower molar mass. It is also interesting to see how the concentration of solvent effect the phase behavior with the same concentration of polymer in the system. Figure 30 explain such a behavior.

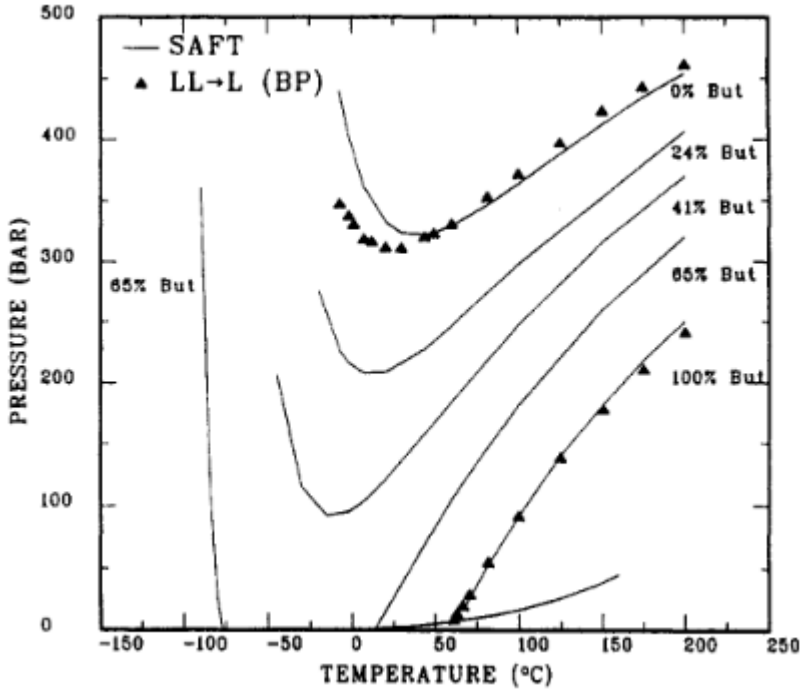

Figure 30. Experimental and theoretical P-T phase boundaries for PEP96K (15 wt %) + propylene + 1-butene (Chen et al., 1992).

From figure 30, in the absence of 1-butene, the UCST and LCST curves merge. As concentration of 1-butene increase, phase boundary shift to lower pressure and higher temperature values. For 65 wt % 1-butene in the system, UCST and LCST curves separate. This kind of behavior is also observed with n-hexane and 1-octene. With the increase of solvent concentrations in the system tends to lower the cloud point pressure values (Chen et al., 1992).

Polymer solution phase behavior strongly depends on both free-volume and energetic contributions of the constituent components. As temperature increases, especially near the solvent critical point, polymer solutions exhibit liquid-liquid immiscibility that is due mainly to large density difference between the polymer molecules and the solvent molecules. Table 5, gives the critical temperature for such constituting components used in experimental work (Chen et al., 1992).

Table 5. Pure component critical temperatures (Chen et al., 1992).

Component	Critical Temperature °C
ethylene	9.1
propylene	91.9
1-butene	146.5
1-hexene	230.9
n-hexane	234.4

1-butene shifts the phase boundary to lower pressure values in comparison to propylene, as density and critical temperature of 1-butene is higher than propylene. Similarly, for 1-hexene and 1-butene case where 1-hexene have higher values for critical temperature and pressure (Chen et al., 1992).

As we know in binary (1-butene + PEP26K), (1-hexene + PEP26K) systems, with increasing concentration of 1-butene or 1-hexene, polymer solubility increases and that tends to shift the cloud point values to lower pressure values and higher temperatures. But in ternary systems where ethylene is also included which acts as powerful antisolvent, causes the phase boundary shifts to higher pressure values. Ethylene, as antisolvent drastically reduce the polymer + solvent density. This leads to the shift of phase boundary to a higher pressure values. As 1-butene is lower molar mass solvent and have lower critical temperature value in comparison to 1-hexene, ethylene effect on 1-butene + polymer system is higher. Figure 31 and 32 shows the effect of ethylene on 1-butene and 1-hexene systems (Chen et al., 1992).

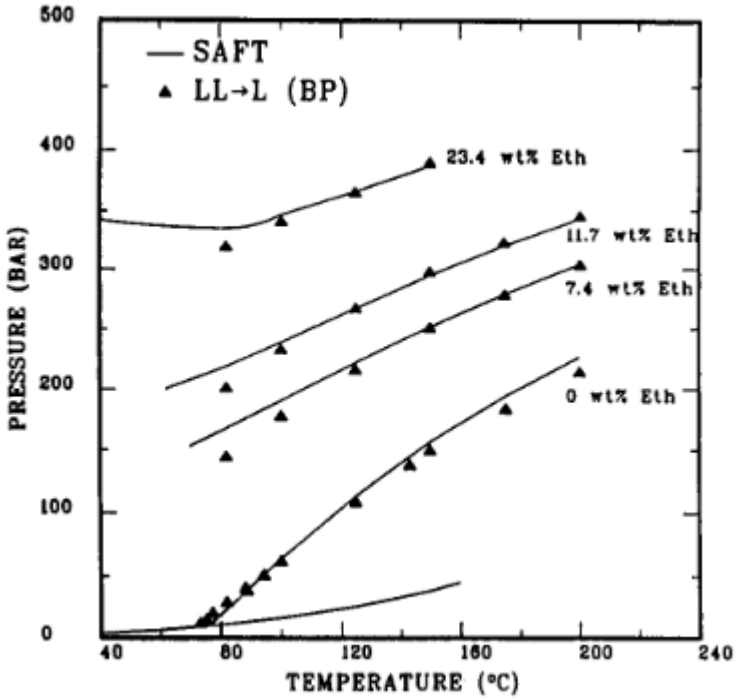

Figure 31. Experimental and SAFT P-T phase boundaries for PEP26K + 1-butene + ethylene at different ethylene concentrations (Chen et al., 1992).

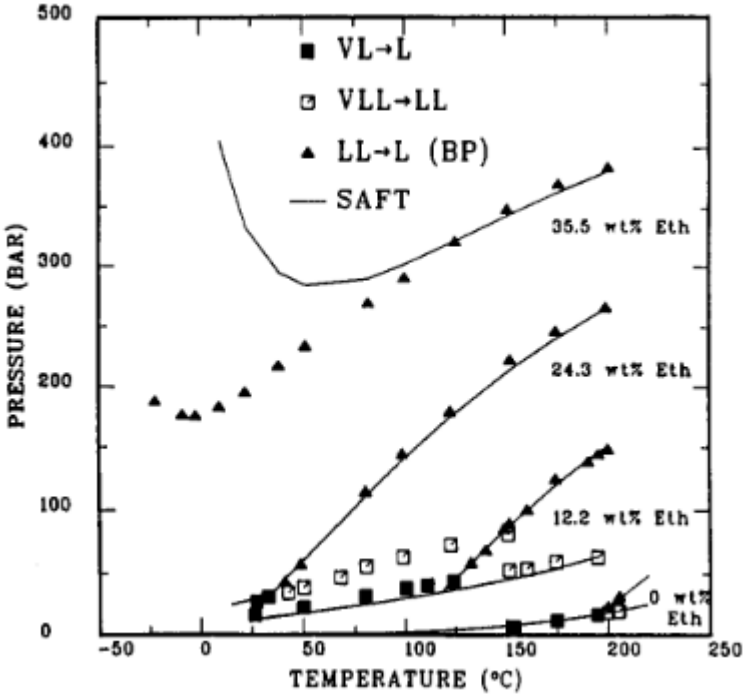

Figure 32. Experimental and SAFT P-T phase boundaries for PEP26K + 1-hexene + ethylene at different ethylene concentrations (Chen et al., 1992).

From figure 31, addition of about 10 wt % of ethylene can increase the cloud point pressure by as much as 100 bars. So for every wt % increase of ethylene in 1-butene + polymer system, can cause an increase of 10 bar in cloud point pressure (Chen et al., 1992). From experimental data in (Chen et al., 1992), a comparison is done to measure the effect of ethylene in two (1-butene & 1-hexene) different systems. Table 6 & 7, represent those temperature and pressure values.

Table 6. Measurement results for poly (ethylene-propylene) 26K (PEP26K) 16.2 wt % + 1-butene 72.1 wt % system containing ethylene 11.7 wt % (Chen et al., 1992).

T (°C)	p. cloud (bar)
82.2	200.4
100.2	232
125.1	266.4
150	296.8
174.8	322
200.3	344.5

Table 7. Measurement results for poly (ethylene-propylene) 26K (PEP26K) 15.8 wt % + 1-butene 72 wt % system containing ethylene 12.2 wt % (Chen et al., 1992).

T (°C)	p. cloud (bar)
132.6	58
140	68
149	85
151.6	89.2
160.3	100
174.5	124
190.5	138
195.4	144
200.2	148

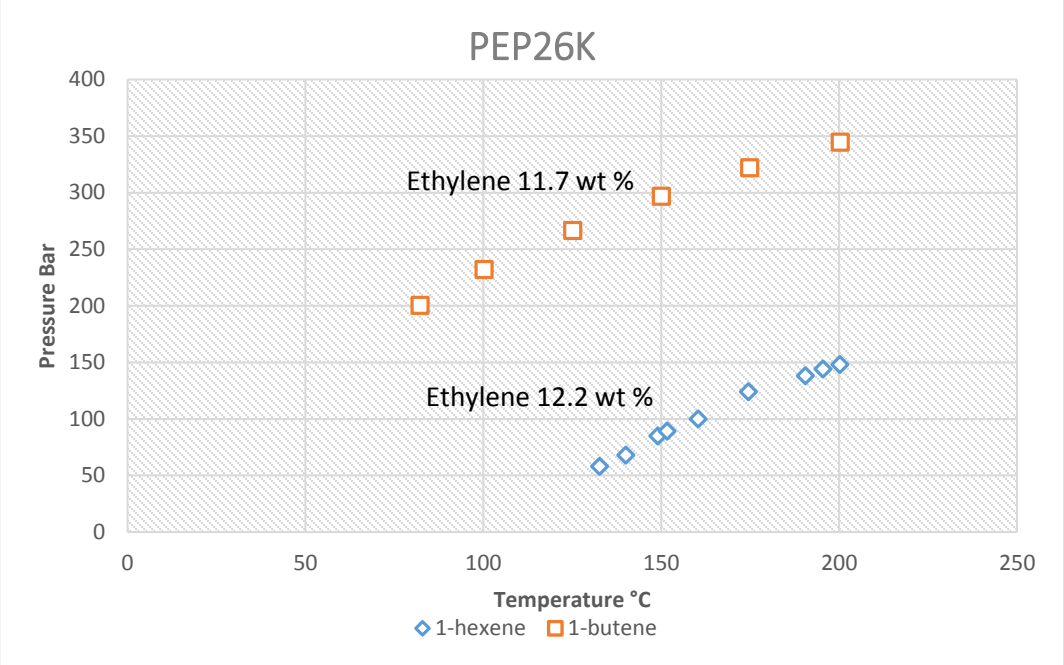

Figure 33. Cloud point curves for PEP26K (16 wt %) in 1-butene and 1-hexene containing ethylene 11.7 and 12.2 wt % respectively (Chen et al., 1992).

In figure 33, as we can see at 200 °C cloud point difference is 196.5 bars, even though the ethylene concentration in 1-hexene system is higher that of 1-butene system. Ethylene tends to shift the cloud point to higher values. But it strongly depends upon the solvents in the system. 1-butene with lower molar mass and critical temperature values, shows drastic reduction in solubility of polymer in comparison to 1-hexene. In a similar way, we have concluded from experimental data available in (Nagy et al., 2006), for LLDPE and n-hexane system, with every wt % of ethylene, cloud point pressure increase approximately 7.5 to 10 bars (Nagy et al., 2006). So cloud point shifts to higher values with lower molar mass solvents and effects of ethylene depends on the solvent used in the system. As 1-butene shows higher cloud point values in comparison to 1-hexene even though the ethylene concentration is lower in 1-butene case.

Similarly, in case of LLDPE and n-alkane systems, phase behavior is characterized by lower solution temperature (LST) and upper solution pressure. Table 8 represents experimental data for n-butane, n-hexane and n-octane and figure 34 represents isobaric cloud point curves for n-alkanes + LLDPE system.

Table 8. Temperature values at different weight fraction of n-alkanes in LLDPE. This data is obtained from (de Loos et al., 1996).

n-butane		n-hexane		n-octane	
polymer wt-%	T °C	polymer wt-%	T °C	polymer wt-%	T °C
1	66	1	152	1	238
2	68	2	154	2	240
4	70	4	156	4	242
8	80	8	166	8	252
12	86	12	172	12	258
20	95	20	181	20	267
25	107	25	193	25	279

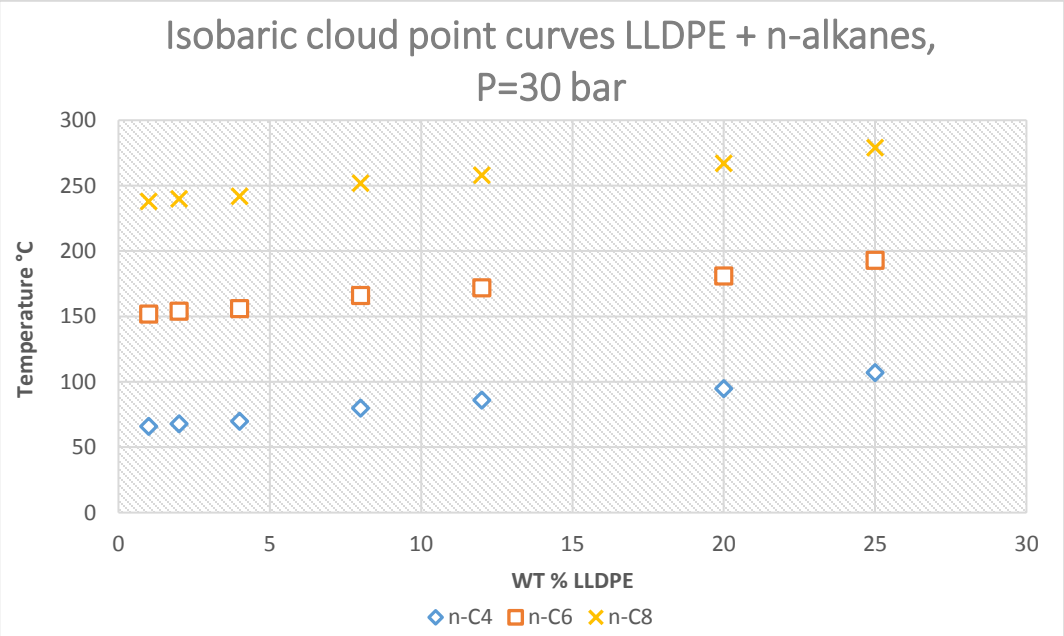

Figure 34. Isobaric cloud point curves for LLDPE + n-alkanes at approximately P= 30 bar (de Loos et al., 1996).

Figure 34 shows with increasing solvent molar mass, LST increases. A higher LST means a smaller region of L-L immiscibility. So a solvent with a higher LST with LLDPE is a better solvent for LLDPE. According to (de Loos et al., 1996), with every addition of CH2-group, there is an increase in LST by ±43 K. This explains how increasing molar mass influence the LST. Figure 34 gives comprehensive information that with

increasing molar mass of solvent, solubility of polymer in solvents increase, which reduces the density difference and tends to lower the cloud point pressure values.

In Cameron (2016), he also shows the effect of components on cloud point values. According to Cameron (2016), increasing polymer concentration was found to increase the solubility of the polymer. And also with increasing differences between the polymer and solvent in properties such as molar mass and density was found to decrease polymer solubility, for example, increasing the concentration of lower molar mass components such as ethylene and 1-butene. One of such example is mentioned below to have a better understanding how the concentration of solvent and comonomer affect the cloud point values.

Two experiments are done for a same polymer grade with multicomponent systems containing n-hexane cut, ethylene and C4 comonomer.

Table 9. Measurement results for PE + multicomponent system containing 17.7 m-% polymer and 2.3 m-% ethylene (Cameron, 2016).

T (°C)	p. cloud (bar)
170.8	49.39
180.7	64.32
190.6	78.08
200.6	91.68

Table 10. Measurement results for PE + multicomponent system containing 17.4 m-% polymer and 3.5 m-% ethylene (Cameron, 2016).

T (°C)	p. cloud (bar)
130.4	46.80
140.3	60.35
150.4	71.11
160.6	81.19
170.5	94.51

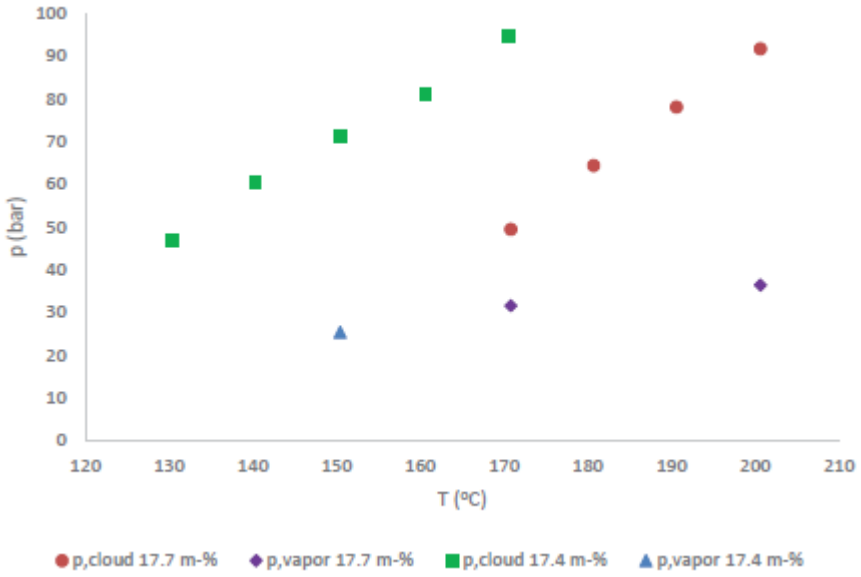

Figure 35. Measured vapor pressures and cloud points for the 17.7 m-% and 17.4 m-% PE and multicomponent systems. Green squares represents system with 2.3 m-% of ethylene and higher 1-butene and butane concentration. Red circles represents the system with 3.5 m-% ethylene and lower 1-butene and butane concentration (Cameron, 2016)

In figure 35, measurement results clearly show a considerable difference in cloud point pressures between the measurements, even though the difference between the polymer concentrations in both systems is 0.3 m-%. The difference between ethylene weight fractions in 2 experiments is only 1 wt %, the cloud point pressure difference is almost 45 bars. This is likely caused by the difference in the overall composition of the systems, as system the 17.4 m-% system has a larger concentration of 1-butene, butane and ethylene. This results in an increased difference in size and density between the polymer and solvent mixture, and reduces the solubility of the polymer shifting cloud points to higher pressures and lower temperatures.

3.7. Summary

This chapter discuss the cloud point in general and how different factors can affect the cloud point temperature and pressure.

Section 3.1 explained that the cloud point temperature increased in isobaric conditions when the alkane/alkene chain length increased or when the weight fraction of the

polymer in the solution increased. For the higher density polymers, the cloud point temperature is lower than that for low density polymers.

In section 3.2, polymer solubility and effect of solvent quality is discussed. In the sub-critical pressure, solubility increases with increasing temperature and decreasing pressure. In the super-critical pressure range, solubility always increases with increasing pressure.

Section 3.3 explained the effects of molecular weight on cloud point temperature and pressure. With increase in MW of the polymer, polymer solubility increase in polymer solutions. Therefore, the polymer MW have directly proportional effect on UCST and inversely proportional effect on LCST by decreasing overall temperature of limited miscibility region.

Section 3.4 discuss the polydispersity of the polymer and it explains the behavior of the cloud-point curve at low polymer concentrations. At higher polymer concentrations, cloud point values decrease for both monodisperse and polydisperse polymer system. At lower polymer concentration, a three phase LLL equilibrium point appears. This appearance of three-phase point indicates the inconsistencies in cloud point pressure measurements with increasing or decreasing values of polymer concentration.

Section 3.5 briefly discuss how miscibility in liquid mixtures can be affected by the pressure. The pressure effect is directly related to volume change during mixing (excess volume of mixing V^E) at fixed temperature and composition values. Solubility of polymer in solvents at various pressure trends depends upon V^E values. Therefore, with increasing pressure, if V^E value is positive it will cause a decrease in solubility whereas, with increasing pressure, if V^E value becomes negative solubility increases.

Section 3.6 explained shift in cloud point pressure and temperature measurements with increasing or decreasing values of different components (Ethylene, butane, 1-butene, iso-octane and 1-octene). And also with increasing differences between the polymer and solvent in properties such as molar mass and density was found to decrease polymer solubility, for example, increasing the concentration of lower molar mass components such as ethylene and 1-butene. Effect of ethylene as antisolvent in with different comonomer (1-butene and 1-octene) is also discussed.

Experimental part

4. Experimental material and apparatus

Goal of this experimental work is to determine cloud and bubble points for LLDPE in different solvent systems. Apparatus used in these experiments previously used by Tom Cameron (Cameron, 2016).

Table 11. Chemical components utilized during the experimental work.

Component	Purity	Supplier
n-hexane	≥99%	Sigma-Aldrich
2-methyl-pentane	≥99%	Sigma-Aldrich
3-methyl-pentane	≥99%	Sigma-Aldrich
Methyl-cyclo-pentane	97 %	Sigma-Aldrich
1-octene	98 %	Sigma-Aldrich
Iso-octane	99.8%	Sigma-Aldrich
n-butane	99.95 %	AGA AB
1-butene	99.4%	AGA AB
Ethylene	99.95 %	AGA AB
Nitrogen		AGA AB

Two types of systems are observed in these experiments based on these chemicals. PE and n-hexane solvent (called as hexane-cut or C6) system with ethylene and 1-butene+ 1-butane mixture (C4 mixture) whereas second system composed of PE and C6 with ethylene, C4 and 1-octene/iso-octane (called as C8).

Figure 36 shows the variable volume cell, which is utilized in these experiments to determine cloud and bubble points.

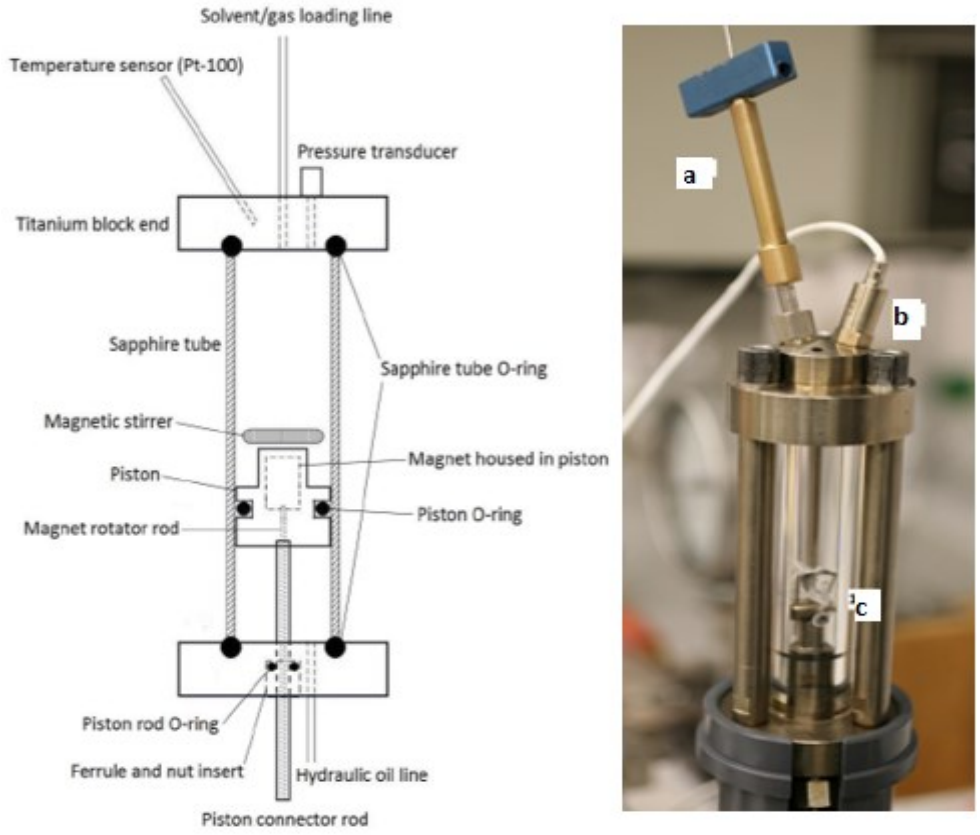

Figure 36. Variable volume cell (Cameron, 2016)

a: Variable volume cell valve

b: Pressure transducer

c: Magnetic mixer

This cylindrical shaped sapphire glass tube is covered with titanium caps (supported with 3 titanium rods) and the whole structure is sealed with graphite seals. Pressure in the cell is controlled with hydraulic oil which is pumped into the cell with the help of a positive displacement pump. That hydraulic oil moves the sealed piston in the cell and the sealing also prevent the mixing of experimental mixture and the hydraulic oil. Mixing of solution in cell is done with a small magnetic mixer.

Gas chromatograph oven (5890 series II plus) is used to heat up the cell. Temperature values are measured by F200 Tempcontrol. Temperature is measured from the top cap of volume cell. Kulite Semiconductor XTEH pressure transducer measures the pressure inside the cell and Omrom K3GN-PDC-FLK DC24V digital panel meter display those values. Figure 37 shows apparatus used in this experiment.

Figure 37. Experimental Apparatus

1: Variable volume cell

2: Gas chromatograph oven

3: Magnetic mixer

4: Positive displacement pump

5: Pressure regulator (Manual)

6: Temperature measuring knob

7: Motor for mixer

8: Safety valve

9: Hydraulic oil reservoir

5. Calibration

Temperature and pressure measuring instruments are calibrated before the experiments and for the system, calibration is done with the help of these instruments. For temperature, model CTR-2000-024 is used which is calibrated at Mikes. Temperature calibration equation is developed to measure corrected temperature value for pressure tests and actual tests.

$$T_{Cali.Func} = 2.00E\text{-}06T_{Display}^{2} + 0.9996T_{Display} + 0.0246 \quad (7)$$

Temperature sensor calibration results are presented in Appendix 1. Using calibration function in Equation 7, any calibrated temperature value can be obtained at any temperature.

The calibration pressure sensor was manufactured by Beamex (external pressure module and MC2-PE output indicator) and had a range of 0 to 600 bars with maximum pressure 900 bar. The calibration in this work was conducted up to a pressure of 100 bar (opening pressure of the safety valve) at several temperatures. The temperature was raised from room temperature to around 50 °C and with 50 °C increment each time overall temperature is raised to 250 °C. The pressure was first set to near 100 bar and then gradually lowered about 10 bars at the time to near atmospheric pressure. Nitrogen gas was used as a pressure calibration gas.

The results of the pressure calibration are presented also in Appendix 1. A slope and intercept were calculated at each calibrated temperature. From display pressure value of system and pressure value of the calibration meter, different values of slope and intercept are obtained. With calibrated temperature values and set of slope, intercept values equations are obtained which will be used to calculate slope and intercept value at any temperature and pressure values. The temperature dependence of the slope and the intercept are presented in Equations 8 and 9. By utilizing these values a pressure calibration line could be generated and this pressure calibration equation is shown in Equation 10:

$$a_{slope} = 1E-06T_{Cali.}^{2} - 0.0005T_{Cali.} + 1.0442 \quad (8)$$

$$b_{Intercept} = 9E-07T_{Cali.}^{3} - 0.0003T_{Cali.}^{2} + 0.025T_{Cali.} + 2.1477 \quad (9)$$

$$P_{Calibrated} = a_{Slope}P_{Display} - b_{Intercept} \quad (10)$$

$P_{Calibrated}$ = Calibrated pressure value (bar)

$P_{Display}$ = Display pressure value of system (bar)

$b_{Intercept}$ = Intercept value temperature dependence curve

a_{Slope}= Slope value temperature dependence curve

$T_{Cali.}$ = Calibrated temperature value ℃

Because of some experimental challenges a few more round of calibrations were done. Challenges are discussed in chapter 7 in this work. Temperature and pressure calibration functions are developed in similar way. Those values are also presented in Appendix 1. Deviation in calibrated and experimental pressure and temperature values are also discussed in chapter 8.

6. Experimental procedure

These experiments are done with specified mass fractions of the polymer and other components based on that polymer amount are calculated with respect to specific mass fractions to achieve a certain composition. After calculating the desired mass fractions of each component, polymer pellets are inserted into the cell. Other liquid components e.g. solvent and C8 mixture is first degassed as shown in Figure 38.

Figure 38 Degassing unit

Degassing removes dissolved air in liquid components, which can affect the cloud point pressure and temperature. Liquid composition is analyzed by using gas chromatography. Cell with polymer pellets is weighted before addition of any other component and then evacuated with a vacuum pump to remove any air from the system. This vacuum also helps to feed in the liquid mixtures from top valve of the cell. An appropriate amount of the liquid solvent mixture was weighed into the cell to achieve the desired overall composition. Lastly, calculated amounts of gas components, if included in the system to be investigated, were weighed into the cell through the top valve.

Cell is inserted into the oven and heated to desired temperature value under mixing for about 30 minutes to achieve thermodynamic equilibrium in the system. System mixing time is suggested in Cameron (2016) and it is sufficient to achieve thermodynamic equilibrium in system.

The cell was heated to the desired temperature under mixing, and left for at least 30 minutes to achieve thermodynamic equilibrium. Bubble point vapor pressure was usually recorded at this point, and all vapor pressures measured for the mixtures in this work are bubble point pressures. As some settling time (~ 30 minutes) was required for achieving thermodynamic equilibrium at each measurement, vapor pressures were not recorded at all of the measurement points due to time constraints, and the system was desired to be kept in a liquid or liquid-liquid state throughout most of the measurements. After the initial vapor pressure measurement, the mixture was observed visually through a window in the oven.

When mixture becomes visually a little clouded, implying a second liquid phase at that point, pressure is increased to achieve a homogenous clear solution inside the cell. Then this mixture is again left for about 30 minutes to achieve equilibrium. After almost 30 minutes, pressure is then lowered slowly and mixture again start to become slightly turbid. This is the indication of second phase and the point at which such turbidity appeared for the first time recorded as cloud point. To confirm the behavior pressure is lowered more until solution become fully clouded. A new temperature value is set and this procedure is repeated again to get another cloud point value. All observations in this experiment is done on visual bases.

Complete mixing of the system was determined to be imperative for achieving equilibrium in the system, as especially with higher polymer concentrations the mixture was quite viscous. To assure complete mixing the amount of sample was matched with the stirrer height. The height of the sample in the cell was calculated beforehand for every experiment from the overall system composition and component masses using approximate component densities and volume of the cell. The amount of sample was adjusted to match or just slightly exceed the height of the stirrer at the lowest temperature of the measurement range.

7. Challenges in experimental work

Several challenges were encountered while conducting the experiments. Proper sealing of the cell during measurements proved to be a considerable issue, as pressure leakage due to O-ring failure was experienced several times during the experiments. Similarly sealing of piston rod was another major challenge. Due to movement and high temperature pressure conditions these small rings can easily rupture and had to be changed during the experiments.

Another challenge during experiments was experienced with mixing. Proper mixing was considered essential for achieving thermodynamic equilibrium, and increasing viscosity in the systems caused the mixing to become less effective resulting in possible concentration gradients inside the cell. If the system was not completely mixed, a lower viscosity phase could start forming at the top of the cell, and this phase would be very hard to mix into the lower phase, as mass transfer at the phase interface was presumably very slow. Several experiments are conducted with beforehand calculated amounts of sample to roughly match the height of the stirrer at the lowest measurement temperature, in order to assure complete mixing of the system.

The biggest challenge in experimental work was failure of pressure value display unit. This problem consumed a great amount of time. In last, observation accuracy of the cloud points was source of uncertainty as observations were done purely visually. As visual observations can depend on the volume and shape of the vessel, the background color behind this vessel, and room illumination, along with human errors made by the operator. The observation window and lighting of the cell were adjusted, as best seen fit under the circumstances of these experiments, and were kept the same throughout the experiments in order to keep measurement results coherent.

8. Experimental results

Measurements were conducted with six different types of industrial LLDPE, designated PE-1, PE-2, PE-3, PE-4, PE-5, and PE-6 in this work. Measurements were conducted in simple multicomponent systems and more complex multicomponent systems. Experiments with PE-1 were conducted in multicomponent mixtures with the hexane-cut solvent, ethylene monomer, 1-butene comonomer, and butane. More complex multicomponent also included 1-octene comonomer, and Iso-octane. PE-2, PE-3, PE-4, PE-5, and PE-6 were investigated in multicomponent mixtures with the hexane-cut solvent, ethylene monomer, 1-butene comonomer, and butane.

Uncertainty in the experiments comes from mass measurements when loading the cell, temperature and pressure measurements, and visual observation accuracy of the cloud points. The accuracy of the scale used when loading the cell is 0.0001 g, but with such accuracy the scale measurements took some time to stabilize, and the final digit would often change slightly back and forth over a range of approximately 0.0005 – 0.0010 g. The uncertainty for the mass measurements could thus be evaluated as ± 0.001 g. Mass fraction uncertainty is presumably larger in the complex multicomponent systems, as more mass measurements needed to be made for these systems. Mass fraction uncertainty for a single experiment can be calculated by multiplying the mass measurement uncertainty (0.001 g) by the number of components (number of mass measurements), and then dividing by the total mass of the system (the sum of masses of the components).

Temperatures were recorded with 0.1 ℃ accuracy. However, the temperature measurement probe is actually situated inside the top titanium end, and not in the cell itself. When warming the cell, temperature inside the cell lagged slightly behind the temperature of the titanium end shown in the measurement. This was another reason to let the cell properly stabilize in the measurement temperature in order to eliminate possible temperature differences between the inside of the cell and the titanium end measured by the sensor. Temperature measurement uncertainty was estimated to be approximately ± 0.5 ℃.

Pressure measurements were recorded at 0.01 bar accuracy. Some uncertainty results from having to apply a correction to the pressure measurement dependent on the measurement temperature. Pressure measurement uncertainty was estimated to be

approximately ± 0.05 bar. The biggest source of uncertainty in the measurements was the observation accuracy of the cloud points. The clarity of cloud point observations varied between experiments, and was usually approximately ± 1.5 – 2 bar. The maximum uncertainty of observations was evaluated to be approximately ± 2.5 bar, and this value was regarded as the uncertainty estimate. All measured values are given with measurement accuracy. Full measurement results with tables and figures for each successful measurement instance are available in a supplementary file Appendix 2.

8.1 Measurements of the multicomponent polymer + hexane system

8.1.1 Measurements with PE-1

Cloud point measurements are done for 18 batches of multicomponent PE-1 + hexane system. PE-1 with different set mass fractions is used with various ratios of n-hexane, ethylene, butane and 1-butene. Results are compared for different PE-1+ hexane systems with different (15-29 m- %) mass fractions of the polymer. The effect of different components in such systems are observed. Two sets of these measurements are presented below in Figure 39 and full measurements are available in Appendix 2.

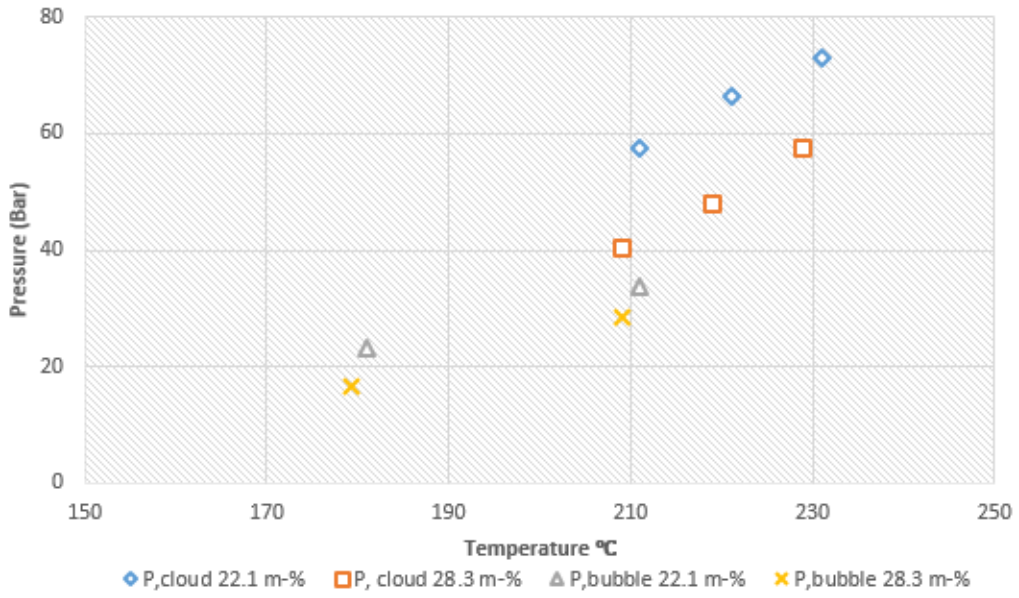

Figure 39 Measured vapor pressures and cloud points for the 22.1 m-% and 28.3 m-% PE-1+n-hexane system.

When the polymer weight fractions increase, the cloud point lines shifts to higher temperatures and lower pressures (Lönnqvist, 2016). Difference in cloud point values is almost 17 bars shown in figure 39. This difference can be explained with ethylene concentration difference between two experiments. Ethylene difference in experiment 1 and 8 is 2 m-%. As we discussed in section 3.6, 2 m-% of ethylene can cause approximately 15 bar in cloud point values. In this comparison, concentration of n-hexane cut and C4 mixture is higher in experiment (22.1 m-%) in comparison to experiment (28.3 m-%). With increasing concentration of solvent and comonomer cloud point shift to lower pressure values (Chen & Radosz, 1992). Ethylene, which acts as powerful antisolvent, drastically reduce the polymer + solvent density. This leads to the shift of phase boundary to a higher pressure values. As 1-butene molar mass is lower and it has a lower critical temperature value in comparison to 1-hexene, so ethylene effect on 1-butene + polymer system is higher. So, a LCST type phase behavior can be observed in this PE-1 + n-hexane system where ethylene and C4 mixture cause a larger cloud point difference than solvent and polymer concentration.

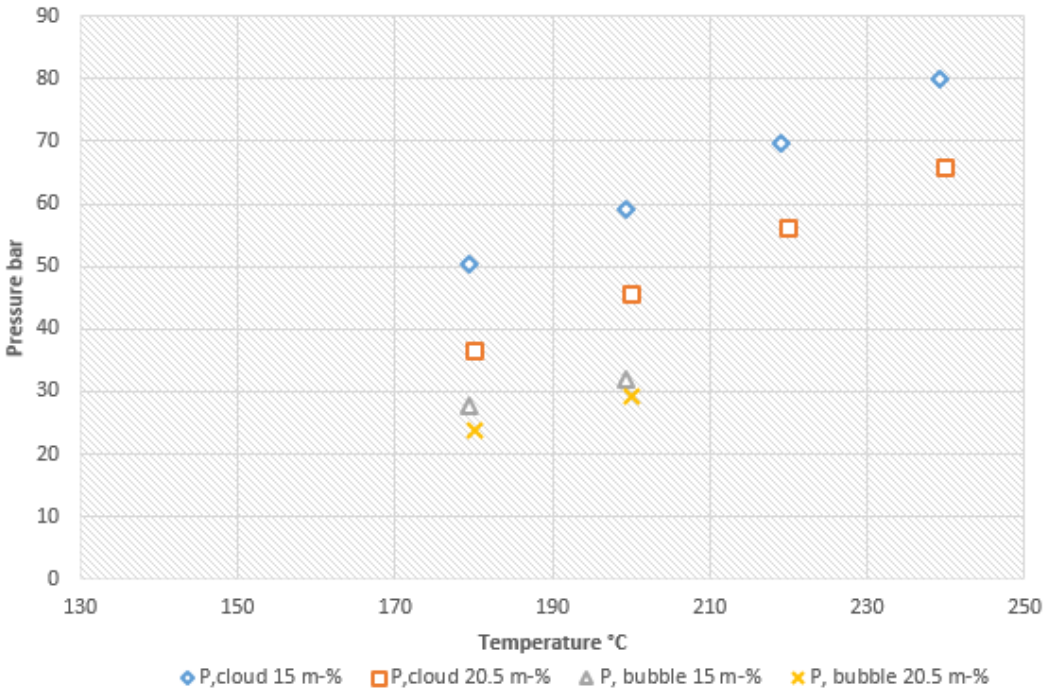

Figure 40 Measured vapor pressures and cloud points for the 15 m-% and 20.5 m-%, PE-1 + hexane system.

The same observations can be made here in Figure 40, where ethylene concentration difference is 2 m-%. The system has LCST type behavior, and experiment (15 m-%) has higher ethylene concentration than experiment (20.5 m-%). In this comparison, concentration of n-hexane cut is higher in experiment (15 m-%) and lower in experiment (20.5 m-%). Similarly, for concentration of C4 mixture (butane+1-butene), which is higher in experiment (20.5 m-%) and lower in experiment (15 m-%). Even with higher concentration of ethylene in experiment (15 m-%), the difference between cloud point values in both experiments is not that large. So, this comparison shows a similar behavior in cloud point pressures, where more m-% of C4 mixture cause higher cloud point shift even with lower ethylene concentration.

Comparison of measurements was also done by gathering results by temperature. Cases for such measurements at approximately 190 °C and 210 °C are presented in Figure 41. The rest of the results can be found in Appendix 2.

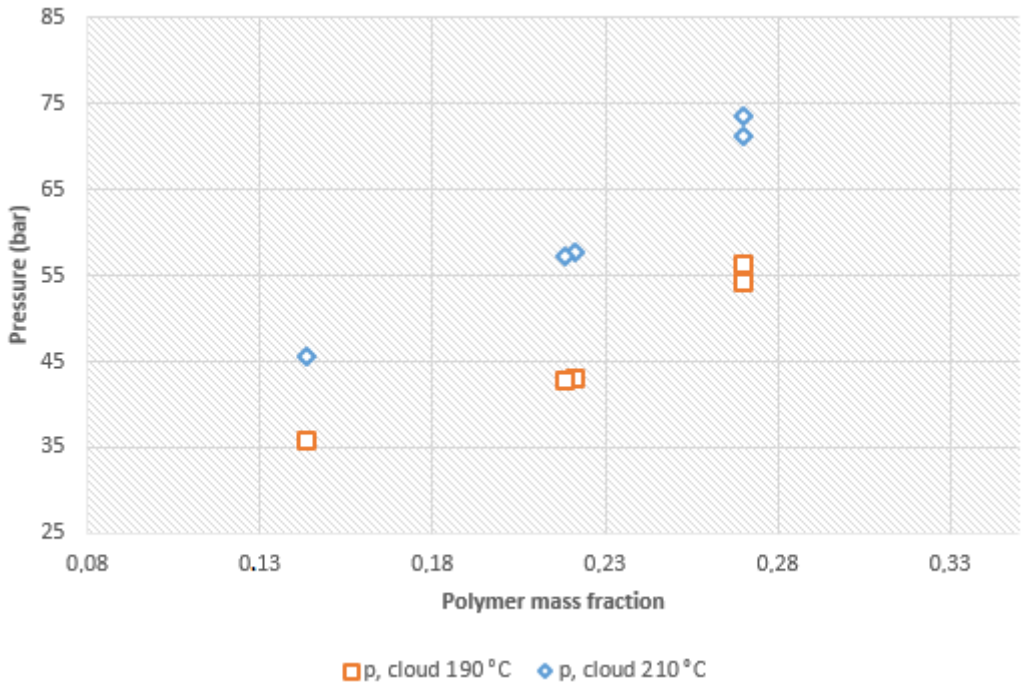

Figure 41 Cloud point measurements for PE-1 + n-hexane systems at approximately 190 °C and 210 °C.

Some variance can be seen in these results. Some of this is caused by slight temperature differences in the measurements, as actual measurement temperatures are not exactly equal. Ethylene quantity in each case is also important. As in Table 8,

ethylene quantity kept increasing with mass fraction of polymer, causing the cloud point values to increase. PE m-% is also increasing which tends to lower the cloud point values even with increasing ethylene concentration. Experiment with 14 m-% of PE contains the highest quantity of n-hexane and lowest quantity of C4 mixture and ethylene.

Figure 42 presented another case where ethylene influenced the cloud point values along with other components. Two measurements were performed for polymer PE-1 in multicomponent systems with approximately 20 m-% polymer concentrations.

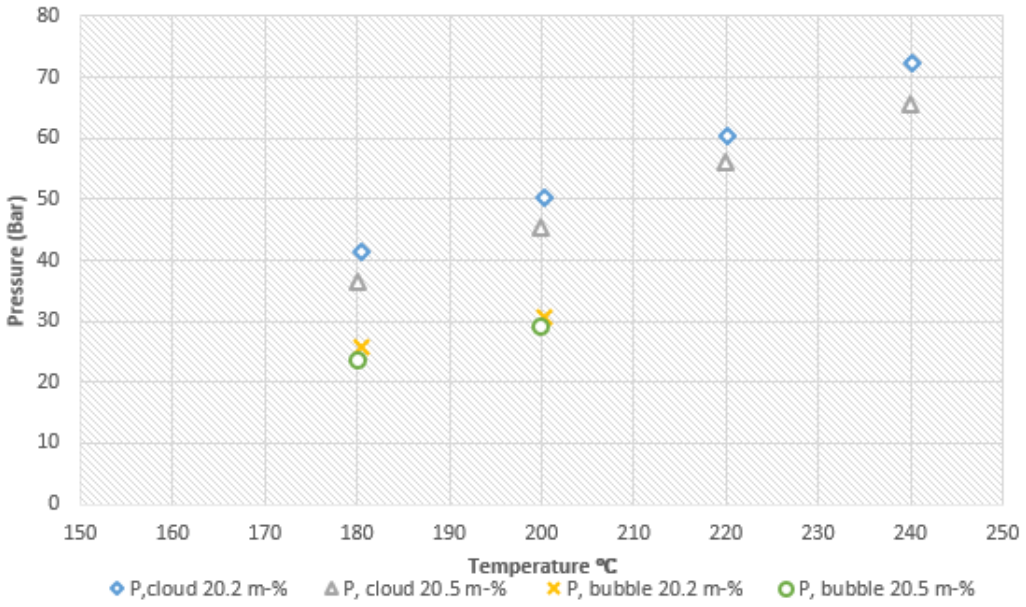

Figure 42 Measured vapor pressures and cloud points for the 20.2 m-% and 20.5 m-% PE-1 multicomponent systems.

In Figure 42 measurement results show a considerably small difference in cloud point pressures, even though the difference in ethylene concentration in both experiments is large. This is due to a difference in the overall composition of the system components, as one of the system (20.5 m- %) has a larger concentration of 1-butene and butane. This results in an increased difference in size and density between the polymer and solvent mixture, and reduces solubility of the polymer shifting cloud points to higher pressures (Cameron, 2016) (de Loos et al., 1996). In experiment (20.5 m-%), the concentration of C4 comonomer is 5 m-% higher than experiment (20.2 m-%). So with higher quantity of comonomer, cloud point shift to higher pressure values even with

small m-% of ethylene in system. Both experiments contains same concentration of n-hexane cut. As we know, ethylene acts as powerful antisolvent and drastically reduce the polymer + solvent density. This leads to the shift of phase boundary to a higher pressure value. So for a system containing more quantity of lighter comonomer (C4), ethylene can shift the cloud point pressure to higher values in comparison to a system containing lower amount of comonomer (C4) (Chen et al., 1992). So this comparison shows such a trend where the higher concentration of C4 mixture in experiment (20.5 m-%) cause a shift of cloud point values to higher pressures.

8.1.2 Measurements with PE-2

A single measurement was performed for polymer PE-2 in the multicomponent system with a polymer concentration of 20.8 m-%. The measurement results for this system are presented in Figure 43.

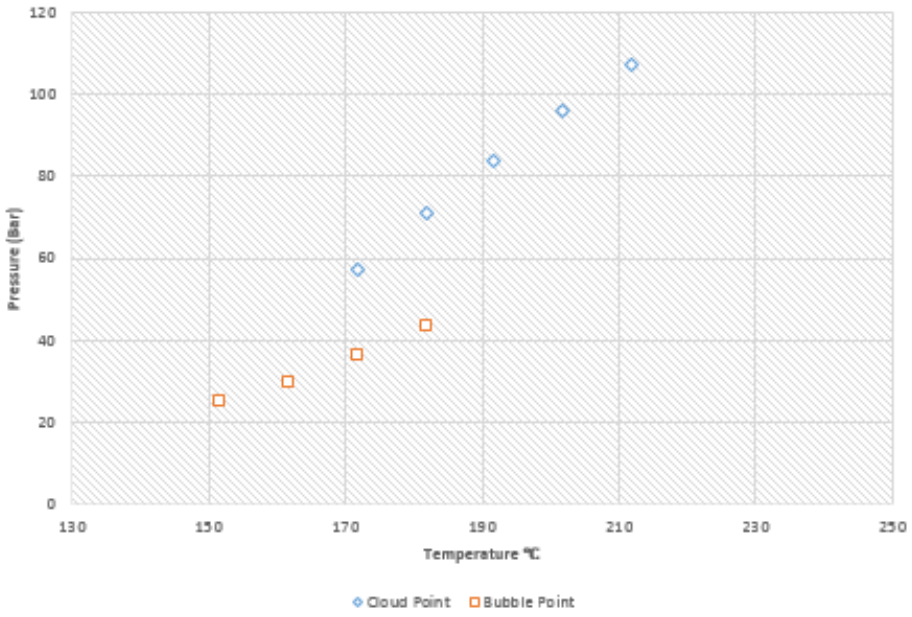

Figure 43 Measured cloud points for the 20.8 m-% PE-2 multicomponent system.

Figure 44 presents the cloud point measurements for experiment (20.8 m-%), compared with (Cameron, 2016) experiment.

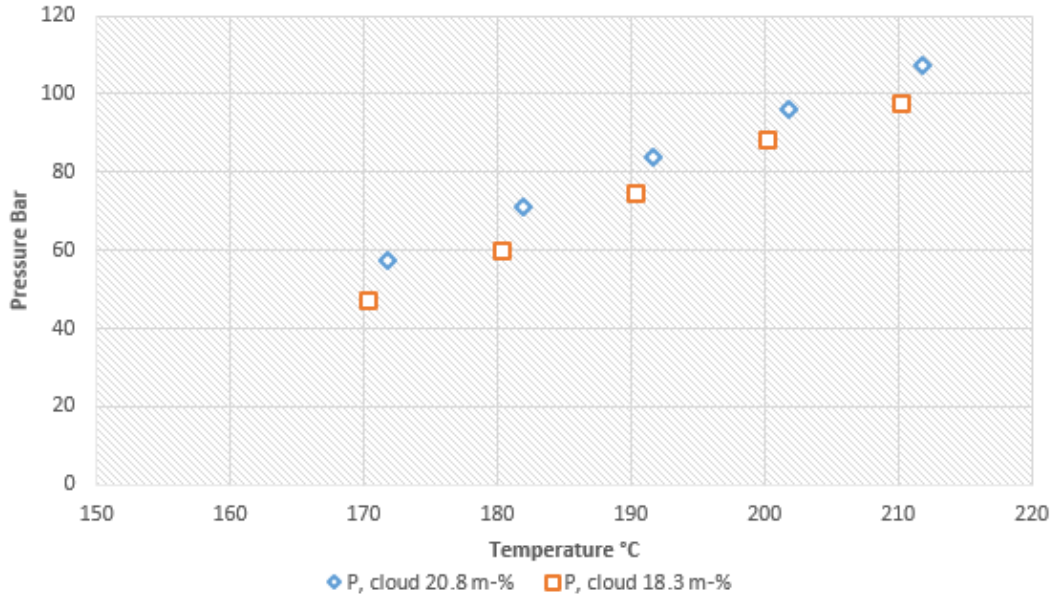

Figure 44 Measured cloud points for the 18.3 m-% and 20.8 m-%, PE-2 multicomponent systems.

Figure 44, shows a small difference in cloud point values even concentration of ethylene is higher in experiment (20.8 m-%). Difference between cloud point values in both experiments is almost 10 bar. In this comparison with ethylene concentration difference of 2 m-%, difference in cloud points is small. The reason for such behavior is the difference in butane and 1-butene m-% in both cases. 1-butene and butane are lighter compounds, and also increase the size and density difference between the polymer and solvent resulting in decreased polymer solubility and higher cloud point pressures (Cameron, 2016) (de Loos et al., 1996). The difference in butane and 1-butene concentrations is 4 m-% and concentration of n-hexane cut is same. But in experiment (18.3 m-%), cloud point shift to higher values with higher concentration of butane and 1-butene even though concentration of ethylene is low in comparison to experiment (20.8 m-%). Such trend in cloud point values is already explained in section 3.6. Polymer mass fraction in experiment (20.8 m-%) is higher, which also tends to lower the overall cloud point value. According to (Lönnqvist, 2016) and (de Loos et al., 1996), when polymer mass fractions increase, the cloud point lines shifts to lower pressures values. So overall concentration difference of different components cause such behavior.

8.1.3 Measurements with PE-3

A single measurement was performed for polymer PE-3 in the multicomponent system with a polymer concentration of 21.2 m-%. The measurement results for this system are presented in Figure 45.

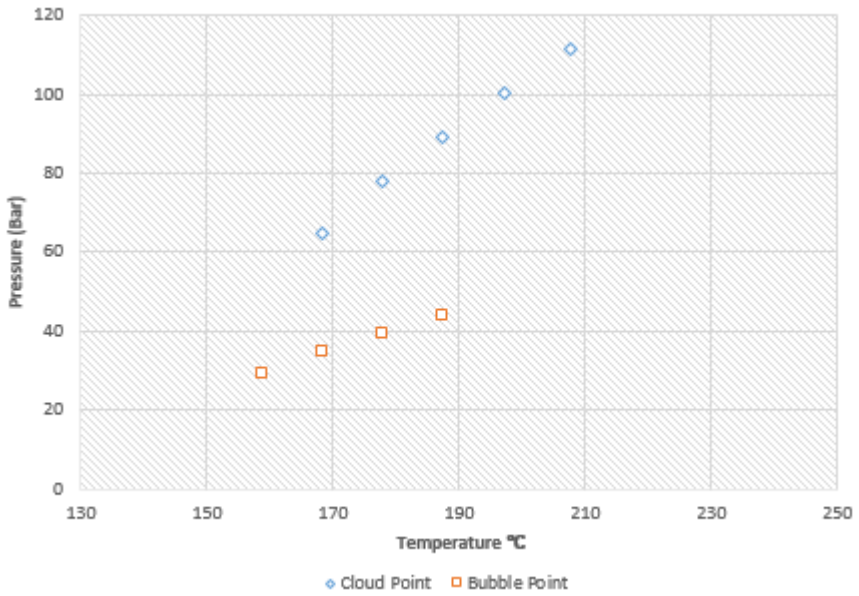

Figure 45 Measured cloud points for the 21.2 m-% PE-3 multicomponent system.

Cloud point measurements presented in figure 46 are compared with (Cameron, 2016) experiment.

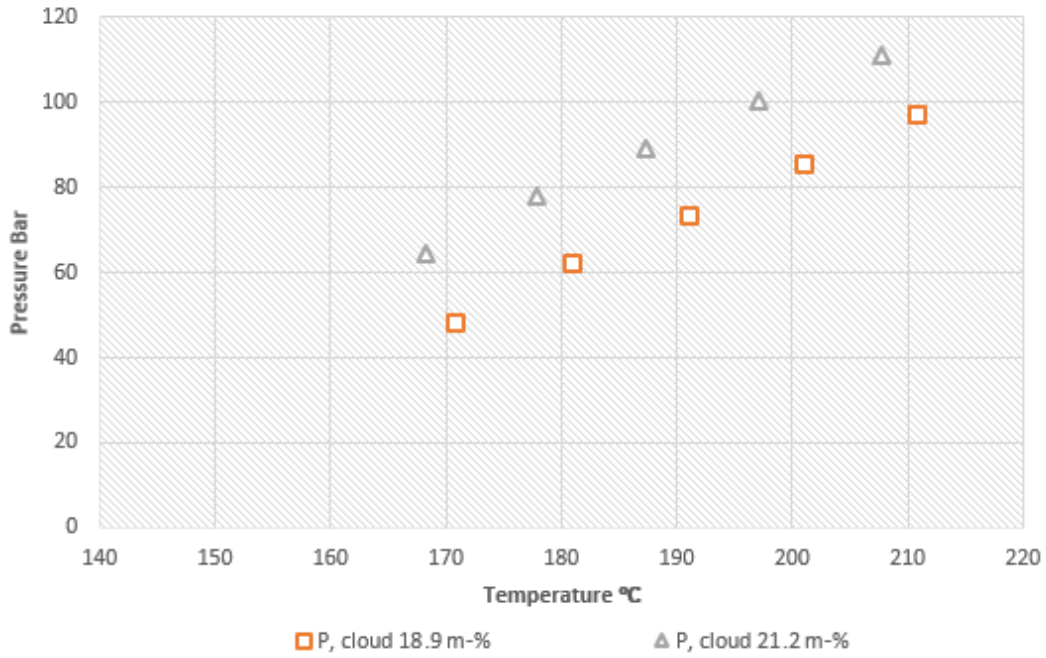

Figure 46 Measured cloud points for the 18.9 m-% and 21.2 m-% PE-3 multicomponent systems.

Figure 46 gives another example where concentration of ethylene shifts the cloud point to higher values. The difference in ethylene concentrations in both cases is 4 m-%. The difference in cloud point values is not as high as (Nagy et al., 2006) predicted and it is only 16 bars. Reason for such behavior is that the experiment (18.9 m-%) contains higher m-% of n-hexane cut and C4 mixture. As discussed in figure 42 & 44, higher m-% C4 mixture in presence of ethylene tends to shift the cloud point to higher values. So, in (18.9 m-%), cloud points are at higher values and difference in cloud points values with experiment (21.2 m-%) reduce to lower values. This comparison shows a similar behavior in cloud point values with difference in overall m-% of different components in multicomponent system.

8.1.4 Measurements with PE-4

A single measurement was performed for polymer PE-4 in the multicomponent system with a polymer concentration of 19 m-%. The measurement results for this system are presented in Figure 47.

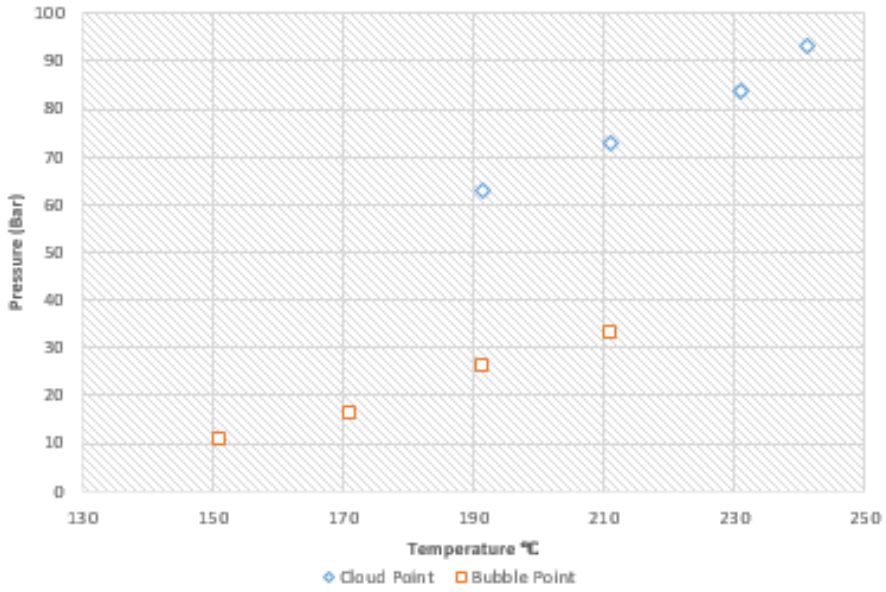

Figure 47 Measured cloud points for the 19 m-% PE-4 multicomponent system.

8.1.5 Measurements with PE-5

A single measurement was performed for polymer PE-5 in the multicomponent system with a polymer concentration of 20 m-%. The measurement results for this system are presented in Figure 48.

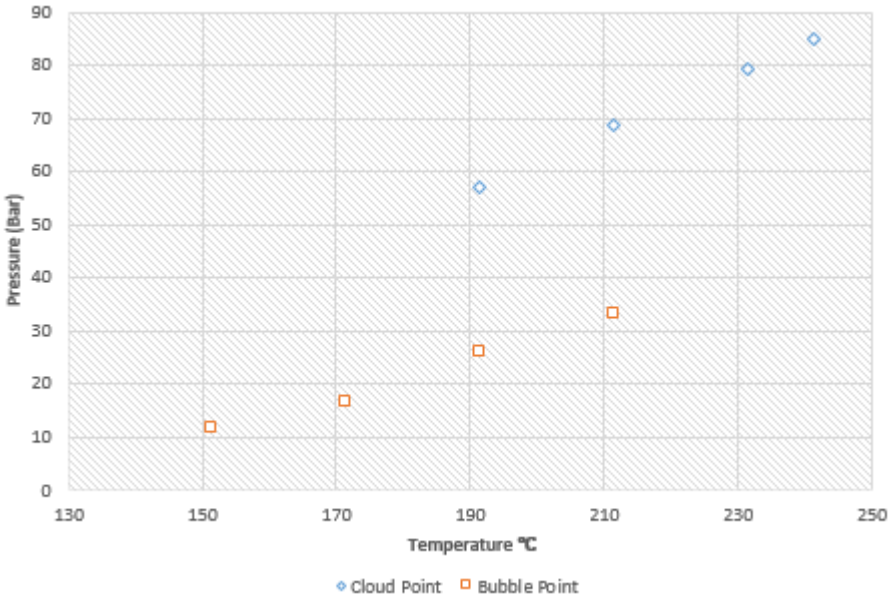

Figure 48 Measured cloud points for the 20 m-% PE-5 multicomponent system.

8.1.6 Measurements with PE-6

A single measurement was performed for polymer PE-6 in the multicomponent system with a polymer concentration of 19 m-%. The measurement results for this system are presented in Figure 49.

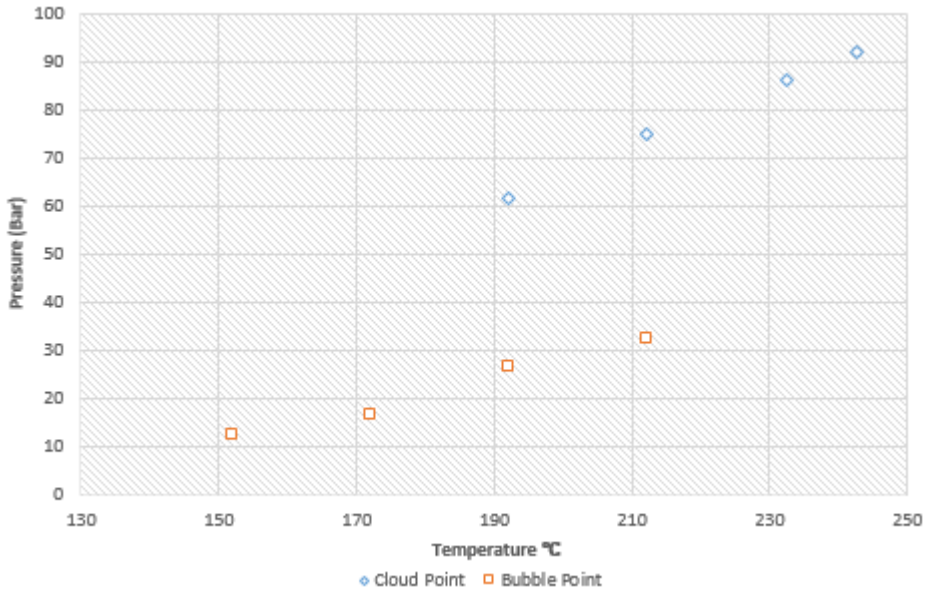

Figure 49 Measured cloud points for the 19 m-% PE-6 multicomponent system.

8.1.7 Comparison of multicomponent system

Since the properties of the polymers used in these experiments are unknown, quantitative comparison to data found in literature cannot be done. Additionally, the mixture used in the multicomponent systems is comprised of many components, and no data on mixtures of this type is readily available. The measured systems to a certain extent are in qualitative agreement with the behavior of such polymer solvent systems presented in literature. The multicomponent systems can, however, be compared with each other.

Measurements with PE-1, PE-2, PE-3, PE-4, PE-5, and PE-6 were all done in a system with the same components, and with polymer concentrations near each other (19-21 m- %). Overall mixture concentrations vary slightly, but are roughly equivalent in all the systems.

Measured cloud points for the systems are presented in Figure 50, and measured bubble points are presented in Figure 51.

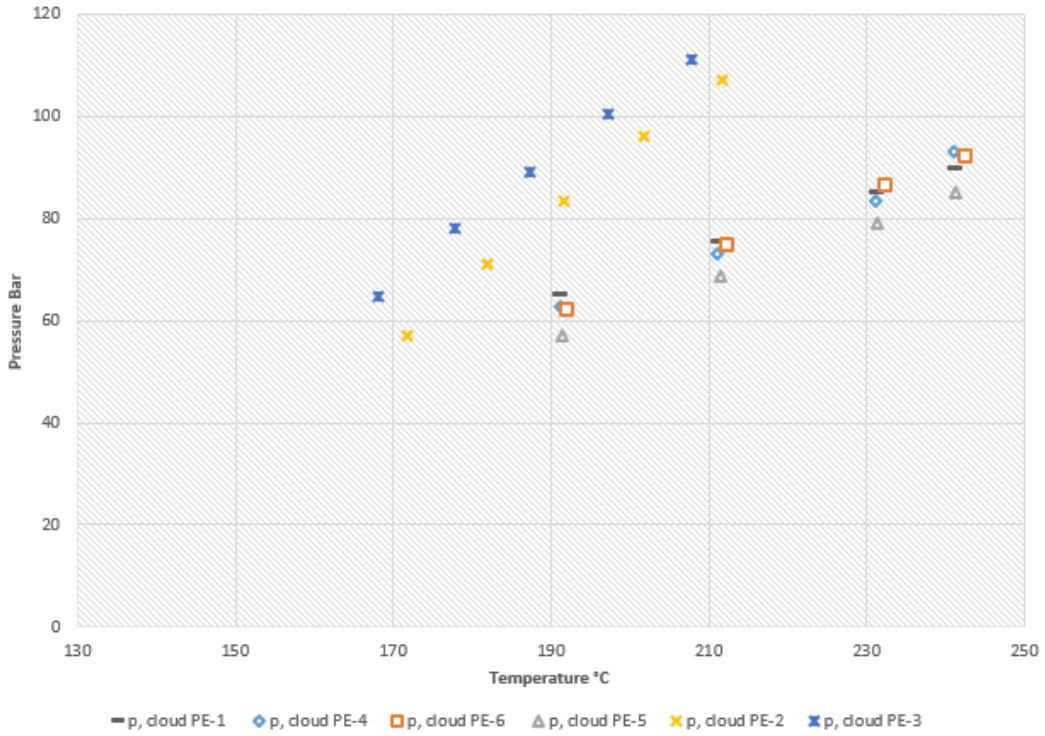

Figure 50 Measured cloud points for the multicomponent systems with 19-21 m-% polymer concentration.

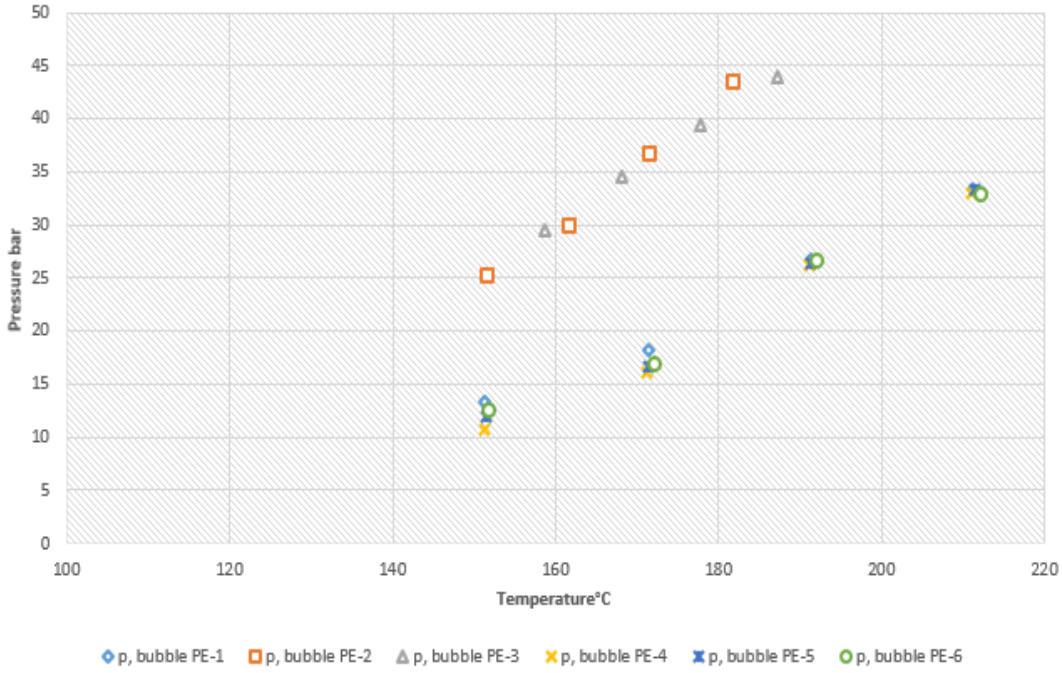

Figure 51 Measured vapor pressures for the multicomponent systems with 19-21 m-% polymer concentration.

As it can be seen from Figure 50 and 51, the PE-3 system has both the highest cloud and vapor point pressures. The reason behind such behavior is overall concentration of ethylene in system. PE-2 and PE-3 show a difference in cloud point as ethylene m-% is different in both cases. The measurements with PE-1, PE-4, PE-5 and PE-6 have quite similar cloud point pressures, with PE-5 having the lowest pressures values. PE-1 system contains highest m-% of butane and 1-butene which cause a shift in cloud point values. PE-4 and PE-5 also show a small gap in cloud point pressures. Even though concentration of ethylene is same in both systems, polymer concentration is bit higher in PE-5 system. Thus cloud point pressure is lower than PE-4 system.
These cloud results shows that the solvent properties in polymer- solvent systems can affect the solubility of the polymer, which can cause changes in cloud point pressures.

8.2 Measurements in multicomponent systems (C8 + C4)

8.2.1 Comparison of measurements with PE-1 + C8

In figure 52, measurements were carried out with the polymer PE-1 in multicomponent systems containing the hexane-cut solvent, ethylene, 1-octene, iso-octane and 1-butene. The mixture was meant to emulate properties of a solution polymerization mixture.
Polymer mass fractions from approximately 19 m-% to 21 m-% were considered. Full measurement results can be found in Appendix 2.

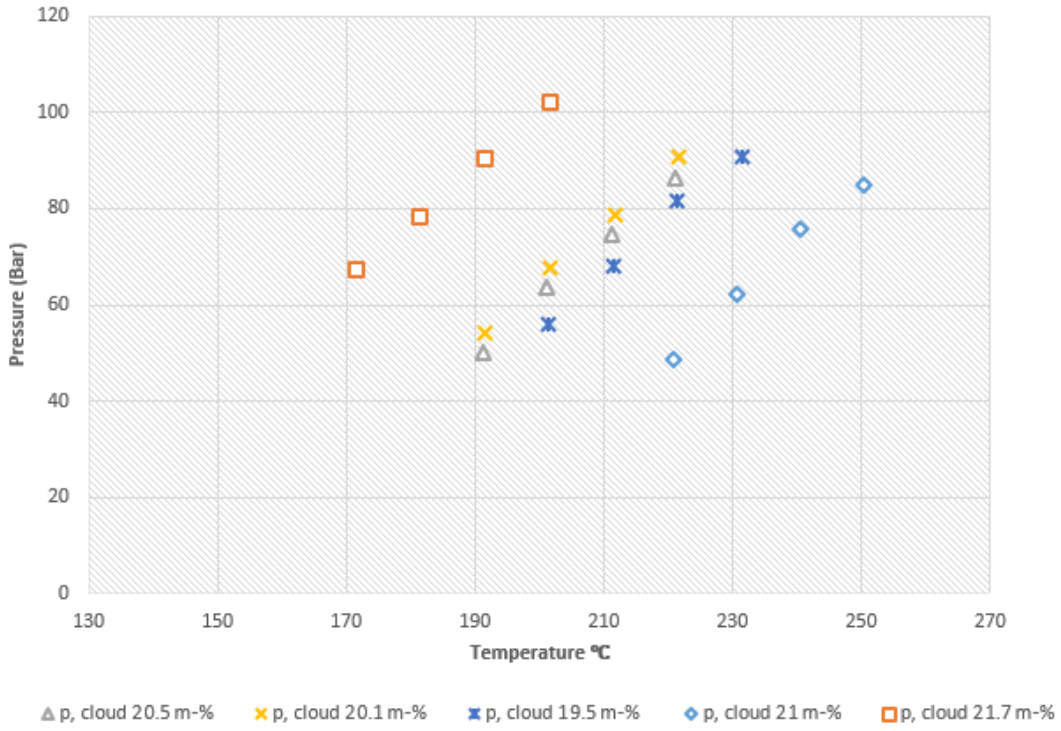

Figure 52 Measured cloud points for the PE-1 multicomponent system containing 19-21 m-% polymer.

This system contains C8 carbon compounds, 1-octene and iso-octane, which are less volatile than C4 compounds. Compared to 1-butene and butane, 1-octene and iso-octane are heavier compounds, and also decrease the size and density difference between the polymer and solvent, resulting in increased polymer solubility and lower cloud point pressure values (Cameron, 2016) (de Loos et al., 1996). Experiment (21.7 m-%) show such behavior where concentration of C8 is 0 m-%. Cloud point is shifted to higher pressure values. As it can be seen in figure 52, with increasing C8 mass fraction cloud point shifts to lower pressure values. In case of experiment (20.5 m-%) and (20.1 m-%), where the cloud point values are higher even with lower concentration of ethylene. Difference in cloud point values is 4-5 bars. For both experiments, having a difference of 3 m-% of ethylene, difference in cloud point values should be higher. Reason for such behavior is m-% of C8. Experiment (20.1 m-%) contains more m-% of C8 in comparison to experiment (20.5 m-%). For other components like n-hexane cut and 1-butene, experiment (20.5 m-%) contains more m-% of both components in comparison to experiment (20.1 m-%). Similarly in case of experiment (21.7 m-%) and

(21 m-%), only difference in cloud point values is m-% of C8. Ethylene concentration is higher in experiment (21 m-%) by 2 m-%. So, even with higher concentration of ethylene, cloud point shift to lower value for experiment (21 m-%). As it can be seen from the results that the concentration of C8 mainly effect the cloud point values.

8.2.2 Comparison of measurements with PE-1

Two measurements were performed for polymer PE-1 in multicomponent systems with approximately 21 m-% and 21.4 m-% polymer concentrations.

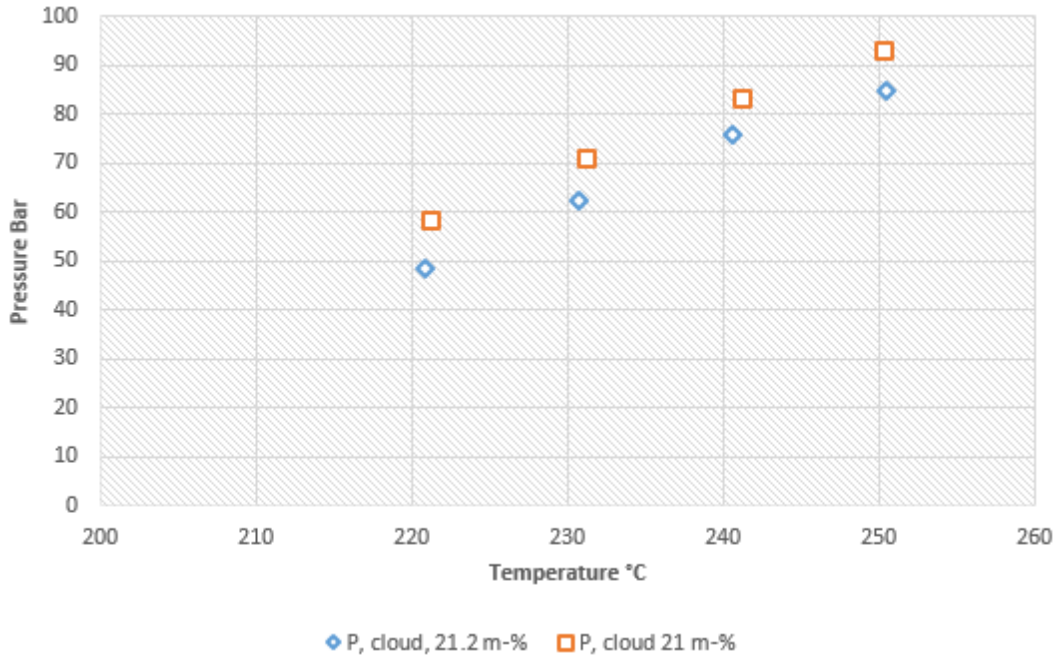

Figure 53 Measured cloud points for the PE-1 multicomponent system containing 21 m-% and 21.4 m-% polymer.

Figure 53 shows a comparison of two PE-1 + multicomponent systems, without any C4 components. The difference in ethylene concentration in both cases is 1 m-% and a cloud point difference of 10 bar. Both experiments contains the same m-% of n-hexane cut and C8 mixture. So cloud point pressure difference is only due to ethylene concentration. We have concluded from experimental data available in (Nagy et al., 2006), for LLDPE and n-hexane system, with every wt % of ethylene, cloud point pressure increase approximately 7.5 to 10 bars. So this comparison shows a similar behavior in cloud point value that can be predicted with such ethylene concentration.

9. Conclusion & suggestions for future work

LCST behavior was observed in the investigated temperature range. In accordance with general findings from other studies, increasing differences between the polymer and solvent in properties such as molar mass and density was found to decrease polymer solubility. That decrease in polymer solubility was achieved by varying the concentrations of some components in the systems, for example increasing the concentration of lower molar mass components such as ethylene. However, phase behavior of polymer – solvent systems also depend on the properties of the polymer, such as molar mass and molar mass distribution, which were unknown in this study. It is important to keep in mind, that even though some generalizations can be made, the actual phase behavior is always specific for each unique system.

The effect of different component (Ethylene, butane, 1-butene, iso-octane and 1-octene) concentrations were also studied in this work. It was detected that the component amount in the system had a clear influence on the cloud point pressures and temperatures. By increasing the component amount in the system the cloud point lines shifted to lower pressures and higher temperatures. However in these studies the bubble points did not shift as much as the cloud points by changing the component amount. Effect of comonomer on cloud point values was very prominent. Butane and 1-butene, as comonomer, have lower molar mass and critical temperature values, which tends to decrease the polymer solvent solubility. So addition of ethylene as an antisolvent, effects the butane and 1-butene system more in comparison to iso-octane and 1-octene system. Section 3.6 discuss such behaviors in details.

The commercial importance of polymers in general will undoubtedly continue to drive the research of polymer manufacturing. Phase equilibria knowledge is of the utmost importance when developing, improving, and implementing various techniques and processes for polymer manufacturing. For the experimental polymer systems in this work more experiments could be systematically conducted to obtain phase boundaries for a larger range of system compositions (e.g. polymer concentration) in the studied temperature and pressure range. The addition of ethylene and/or other components could also be systematically investigated for their impact on the phase boundary behavior. Modeling of the obtained data could also subsequently be attempted using a suitable equation of state. The equipment and procedures used in this work can

certainly be used for phase equilibria measurements of a large variety of systems, even beyond polymer mixtures.

In the end, there are few changes that can help the process in terms of measuring the cloud point values. First, manual hydraulic pump can be replaced. Size of the cylinder can be increased for more quantity of sample. This will make it easier to measure the accurate quantities of all the components. Temperature and pressure sensor can be connected with automated system to record the values after certain interval of time. All these suggestions can improve the efficiency of the process.

7. References

Blanks, R. F., & Prausnitz, J. M. (1964). Thermodynamics of Polymer Solubility in Polar and Nonpolar Systems. Industrial & Engineering Chemistry Fundamentals, 3(1), 1–8. https://doi.org/10.1021/i160009a001

Buckingham, A. D., & Longuet-Higgins, H. C. (1968). The quadrupole moments of dipolar molecules. Molecular Physics, 14(1), 63–72. https://doi.org/10.1080/00268976800100051

Cameron, M., T. (2016). M.Sc. Thesis; Phase equilibrium of polyethylene and n-hexane systems at different operating conditions, Aalto university school of chemical technology.

Cheremisinoff, N. P. (1989). Handbook of Polymer Science and Technology. Dekker.

Chen, shean jer and Radosz, maciej, Density-tuned polyolefin phase equilibria, Binary solutions of alternating poly(ethylene-propylene) in subcritical and supercritical propylene, 1-butene, and 1-hexene, Experiment and Flory-Patterson model, Macromolecules, 1992, 25 (12), pp 3089–3096.

Chen, shean jer, Economou, I.G. and Radosz, maciej, Density-tuned polyolefin phase equilibria, Multicomponent solutions of alternating poly(ethylene-propylene) in subcritical and supercritical olefins, Experiment and SAFT model, Macromolecules, 1992, 25 (12), pp 4987–4995.

Danner, R. P., & High, M. S. (1993). Handbook of Polymer Solution Thermodynamics. In Handbook of Polymer Solution Thermodynamics. Department of Chemical Engineering, the Pennsylvania State University, University Park, PA 16802: American Institute of Chemical Engineers.

De Loos, T. W., de Graaf, L. J., & de Swaan Arons, J. (1996). Liquid-Liquid Phase Separation in Linear Low-Density Polyethylene- Solvent Systems. Fluid Phase Equilibria. Fluid Phase Equilibria 117 (1996) 40-47.

De Loos, T. W., Lichtenthaler, R., & Diepen, G. (1983). Fluid phase equilibriums in the system polyethylene ethylene. 2. Calculation of cloud curves for systems of linear polyethylene ethylene. Macromolecules, 117-121.

Ehrlich, P., & Kurpen, J. J. (1963). Phase equilibria of polymer-solvent systems at high pressures near their critical loci: Polyethylene with n-alkanes. Journal of Polymer Science Part A: General Papers, 1(10), 3217–3229. https://doi.org/10.1002/pol.1963.100011016

Folie, B., & Radosz, M. (1996). Phase Equilibria in High-pressure Polyethylene Technology. Ind. Eng. Chem. Res. 1996, 34, 1501-1516.

Freeman, P. I., & Rowlinson, J. S. (1960). Lower critical points in polymer solutions. Polymer, 1, 20–26. https://doi.org/10.1016/0032-3861(60)90004-5

Hamada, F., Fujisawa, K., & Nakajima, A. (1973). Lower Critical Solution Temperature in Linear Polyethylene–n-Alkane Systems. Polymer Journal volume 4, pages 316–322.

J.-P. Hansen, C.I. Addison, A.A. Louis (2005). Polymer solutions from hard monomers to soft polymers. Journal of Physics: Condensed Matter, Volume 17, Number 45. S3185–S3193.

Irani, C. A., & Cozewith, C. (1986). Lower critical solution temperature behavior of ethylene propylene copolymers in multicomponent solvents. Journal of Applied Polymer Science, 31(6), 1879–1899. https://doi.org/10.1002/app.1986.070310630

Jog, P. K., Chapman, W. G., Gupta, S. K., & Swindoll, R. D. (2002). Modeling of Liquid−Liquid-Phase Separation in Linear Low-Density Polyethylene−Solvent Systems Using the Statistical Associating Fluid Theory Equation of State. Industrial & Engineering Chemistry Research, 41(5), 887–891. https://doi.org/10.1021/ie000604b

Kirby, C. F., & McHugh, M. A. (Eds.). (1999). Phase Behavior of Polymers in Supercritical Fluid Solvents. Chem. Rev. 1999, 99, 565−602.

Kirk-Othmer. (2006). Encyclopedia of Chemical. Technology, John Wiley and Sons, Inc., 6th edition.

Koningsveld, R., Stockmayer, WH. and Nies, E. Polymer Phase Diagrams: A Textbook. Oxford University Press, Oxford, 2001 841 pp (2001).

Lee, L. L. (1988). Molecular Thermodynamics of Non-ideal Fluids. (H. Brenner, Ed.). Butterworth: Butterworth Publishers.

Lee, S.-H., LoStracco, M. A., Hasch, B. M., & McHugh, M. A. (1994). Solubility of Poly(ethylene-co-acrylic acid) in Low Molecular Weight Hydrocarbons and Dimethyl Ether. Effect of Copolymer Concentration, Solvent Quality, and Copolymer Molecular Weight. The Journal of Physical Chemistry, 98(15), 4055–4060.

Lee, S.-H., & McHugh, M. A. (1997). Phase behaviour studies with poly(ethylene-co-methacrylic acid) at high pressures. Polymer, 38(6), 1317–1322.

Liu, D. D., & John M Prausnitz, (1980). Calculation of Phase Equilibria for Mixtures of Ethylene and Low-Density Polyethylene at High Pressures, Ind. Eng. Chem. Process Des. Dev. 1980, 19, 205-211

Luszczyk, M., Rebelo, L. P. N., & Van Hook, W. A. (1995). Isotope and pressure dependence of liquid-liquid equilibria in polymer solutions. 5. Measurements of solute and solvent isotope effects in polystyrene-acetone and polystyrene-methylcyclopentane. 6. A continuous polydisperse thermodynamic interpretation of demixing measurements in polystyrene-acetone and polystyrene-methylcyclopentane solutions. Macromolecules, 28(3), 745–767.

Lönnqvist, I. (2016). Master thesis; phase equilibria and modeling of polymer systems, Aalto university school of chemical technology.

Malpass, D. B. (2010). Introduction to Industrial Polyethylene Properties, Catalysts, Processes. In W. Scrivener (Ed.), Introduction to Industrial Polyethylene Properties, Catalysts, Processes. Scrivener Publishing.

McHugh, M. A., & Krukonis, V. J. (1994). Supercritical Fluid Extraction: Principles and Practice (2nd ed). Butterworth: Publishers, Stoneham,MA.

Nagy, I., Loos, T. W. de, Krenz, R. A., & Heidemann, R. A. (2006). High pressure phase equilibria in the systems linear low density polyethylene+n-hexane and linear low density polyethylene+n-hexane+ethylene: Experimental results and modelling with the Sanchez-Lacombe equation of state. The Journal of Supercritical Fluids, 37(1), 115–124. https://doi.org/10.1016/j.supflu.2005.08.004

Nagy, I., Krenz, R. A., Heidemannb, R. A., & Loos, T. W. de. (2007). High-pressure phase equilibria in the system linear low density polyethylene + isohexane: Experimental results and modelling, J. of Supercritical Fluids 40 (2007) 125–133.

Olabisi, O., Lloyd M. Robeson, & Montgomery T. Shaw. (1979). Polymer-Polymer Miscibility. 3, Fifth Avenue, New York10003: Academic press. Inc.

Pappa, G. D., Voutsas, E. C., & Tassios, D. P. (2001). Liquid−Liquid Phase Equilibrium in Polymer−Solvent Systems: Correlation and Prediction of the Polymer Molecular Weight and the Pressure Effect. Industrial & Engineering Chemistry Research, 40(21), 4654–4663. https://doi.org/10.1021/ie0103658

Patterson, D. (1969). Free Volume and Polymer Solubility. A Qualitative View. Macromolecules, 2(6), 672–677. https://doi.org/10.1021/ma60012a021

Patterson, Donald. (1982). Polymer compatibility with and without a solvent. Polymer Engineering & Science, 22(2), 64–73.

Prausnitz, J. M., Lichtenhaler, R. N., & Azevedo, E. G. (1999). Molecular Thermodynamics of Fluid-Phase Equilibria (3rd ed). Englewood Cliffs, NJ: Prentice Hall.

Prausnitz, J. M., Lichtenthaler, R. N., & Azevedo, E. G. (1986). Molecular Thermodynamics of Fluid Phase Equilibria (2nd ed). Englewood Cliff: Prentice Hall.

Rodriguez, F. (2003). Principles of Polymer Systems 5Th Ed. Taylor.

Rowlinson, John Shipley, F.L. Swinton (Editor), Fl Swinton (1982). Liquids and Liquid Mixtures (Monographs in Chemistry) (3rd Edition). 336 Pages, Butterworth & Co (Publishers) Ltd 1982. ISBN-10: 0-408-24192-6.

Siow, K.-S. (1972). Studies on phase behaviour and surface properties of polymer systems. Department of Chemistry McGill University Montreal, Canada.

Streett, W. B. (2009). Phase behavior in fluid and solid mixtures at high pressures. Pure and Applied Chemistry, 61(2), 143. https://doi.org/10.1351/pac198961020143

Utracki, L. A. (1994). Thermodynamics and Kinetics of Phase Separation. In L. H. S. D.Klempner & L.A.Utracki (Eds.), Interpenetrating Polymer Networks, 1994, Advances in Chemistry 239 (pp. 77–123).

Vasile, C., & Pascu, M. (2005). Practical Guide to Polyethylene. Rapra Technology.

Voorn, M. J. (1959). Phase separation in polymer solutions. In Fortschritte Der Hochpolymeren-Forschung (pp. 192–233). Berlin, Heidelberg: Springer Berlin Heidelberg.

Whaley, P. D., Winter, H. H., & Ehrlich, P. (1997). Phase Equilibria of Polypropylene with Compressed Propane and Related Systems. 1. Isotactic and Atactic Polypropylene with Propane and Propylene. Macromolecules, 30(17), 4882–4886.

WOHLFARTH, C. (2005). Handbook of Thermodynamic Data of Polymer Solutions at Elevated Pressures. CRC PRESS.

Xie, T., McAuley, K. B., Hsu, J. C. C., & Bacon, D. W. (1994). Gas Phase Ethylene Polymerization: Production Processes, Polymer Properties, and Reactor Modeling. Industrial & Engineering Chemistry Research, 33(3), 449–479.

Zeman, L., & Patterson, D. (1972). Pressure effects in polymer solution phase equilibriums. II. Systems showing upper and low critical solution temperatures. The Journal of Physical Chemistry, 76(8), 1214–1219.

Zhang, W. (2005, April 5). Phase Behavior and Phase Separation Kinetics in Polymer Solutions under High Pressure. Blacksburg, VA.

Appendix 1

Temperature Calibration:

M-17T047

Digital Thermometer F200

Model: CTR-2000-024

Calibration date: 02.06.2017

Calibration temperature ℃	Channel 1 Sensor T6172.1	Channel 1 Correction for a calibrated lamp meter ℃	Channel 2 Sensor T6172.2	Channel 2 Correction for a calibrated lamp meter ℃	Increased uncertainty of calibration ℃ (k=2)
50.00	50.01	-0.01	50.04	-0.04	0.02
100.02	100.03	-0.01	100.06	-0.05	0.03
150.01	150.03	-0.01	150.07	-0.05	0.03
200.09	200.12	-0.03	200.16	-0.07	0.03
250.06	250.13	-0.06	250.17	-0.11	0.03
299.10	299.22	-0.11	299.26	-0.15	0.10
350.15	350.37	-0.22	350.40	-0.25	0.10

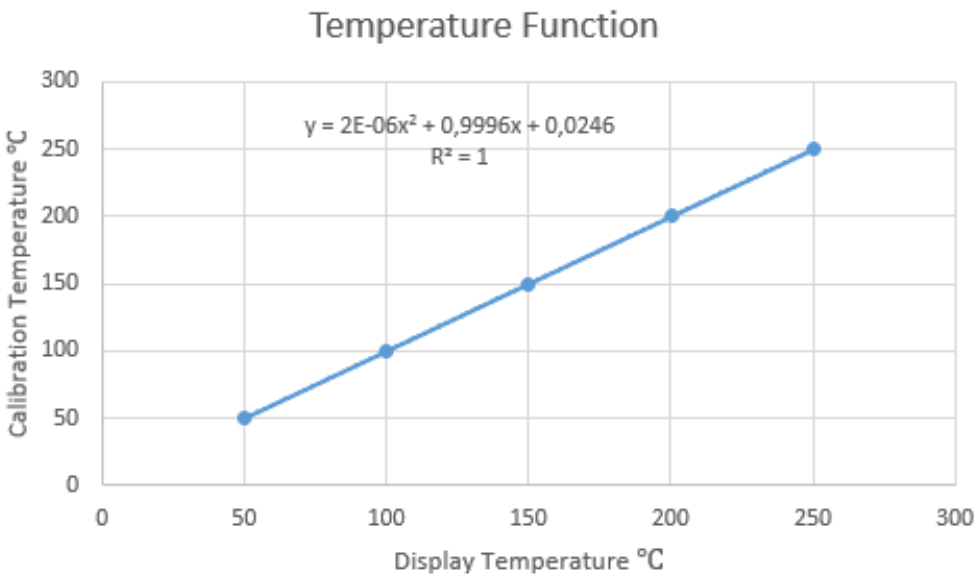

Pressure Calibrations:

First Set

Display Temperature ℃	Calibrated Temperature ℃
21.11	21.13

Display Pressure (bar)	Calibration meter Pressure (bar)	Calibrated Pressure (bar)	Difference between meter display & calibrated pressure (bar)
106.80	107.20	107.11	-0.31
91.30	91.10	90.94	0.36
81.10	80.30	80.30	0.80
71.40	70.24	70.18	1.22
61.50	59.90	59.85	1.65
52.50	50.46	50.46	2.04
42.20	39.69	39.71	2.49
31.10	28.15	28.13	2.97
21.90	18.52	18.53	3.37
13.90	10.20	10.18	3.72
5.10	0.96	1.00	4.10
Slope	Intercept		Average error
1.04	4.36		2.04

Display Temperature ℃	Calibrated Temperature ℃
50.94	50.95

Display Pressure (bar)	Calibration meter Pressure (bar)	Calibrated Pressure (bar)	Difference between meter display & calibrated pressure (bar)
103.40	102.14	101.76	1.64
93.30	91.62	91.35	1.95
82.60	80.60	80.32	2.28
72.50	70.10	69.91	2.59
62.70	60.00	59.81	2.89
52.30	49.30	49.10	3.20
43.50	40.21	40.03	3.47
33.40	29.80	29.62	3.78
23.60	19.62	19.52	4.08
14.50	10.28	10.14	4.36

5.50	0.96	0.86	4.64
Slope	Intercept		Average error
1.03	4.73		3.17

Display Temperature ℃	Calibrated Temperature ℃		
101.05	101.06		
Display Pressure (bar)	Calibration meter Pressure (bar)	Calibrated Pressure (bar)	Difference between meter display & calibrated pressure (bar)
105.00	101.87	100.92	4.08
91.30	87.81	87.04	4.26
81.40	77.70	77.01	4.39
69.70	65.79	65.16	4.54
59.50	55.38	54.82	4.68
49.90	44.54	45.10	4.80
39.80	35.22	34.86	4.94
31.40	26.73	26.35	5.05
23.00	18.09	17.84	5.16
14.00	8.93	8.72	5.28
6.20	0.96	0.82	5.38
Slope	Intercept		Average error
1.02	5.48		4.78

Display Temperature ℃	Calibrated Temperature ℃		
150.97	150.98		
Display Pressure (bar)	Calibration meter Pressure (bar)	Calibrated Pressure (bar)	Difference between meter display & calibrated pressure (bar)
106.30	102.34	100.47	1.87
95.90	91.61	90.06	1.55
88.30	83.86	82.45	1.41
76.40	71.78	70.54	1.24
65.00	60.26	59.13	1.13
56.10	51.21	50.23	0.98
44.30	39.16	38.42	0.74
35.10	29.83	29.21	0.62

24.40	18.93	18.50	0.43
14.40	8.77	8.49	0.28
6.70	0.96	0.79	0.17
Slope	Intercept		Average error
1.02	5.87		0.95

Display Temperature ℃	Calibrated Temperature ℃
200.63	200.66

Display Pressure (bar)	Calibration meter Pressure (bar)	Calibrated Pressure (bar)	Difference between meter display & calibrated pressure (bar)
104.60	100.50	97.74	2.76
94.90	90.57	88.10	2.47
84.00	79.47	77.28	2.19
75.70	70.99	69.03	1.96
64.90	59.99	58.30	1.69
56.00	50.89	49.46	1.43
44.80	39.56	38.33	1.23
35.60	30.18	29.19	0.99
26.20	20.60	19.85	0.75
16.30	10.55	10.02	0.53
6.90	0.96	0.68	0.28
Slope	Intercept		Average error
1.02	6.08		1.48

Calibrated Temperature ℃	Slope	Intercept
21.13	1.04	4.36
50.95	1.03	4.73
101.06	1.02	5.48
150.98	1.02	5.87
200.66	1.02	6.08

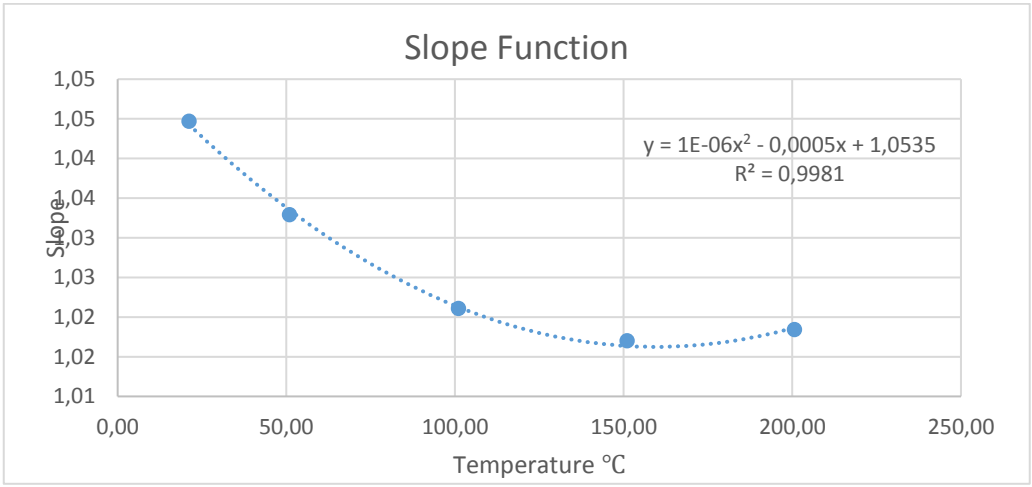

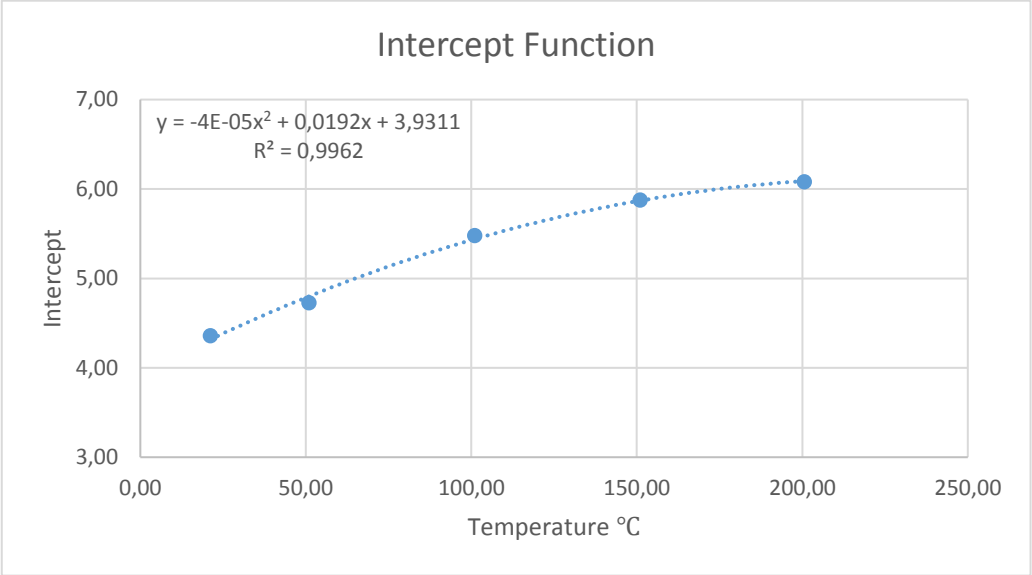

Second set

Display Temperature ℃	Calibrated Temperature ℃		
25.50	25.49		
Display Pressure (bar)	Calibration meter Pressure (bar)	Calibrated Pressure (bar)	Difference between meter display & calibrated pressure (bar)
104.3	105.05	105.27	-0.97
93.8	94.32	94.44	-0.64
82	82.12	82.27	-0.27
70.6	70.41	70.52	0.08
61	60.53	60.62	0.38

50	49.21	49.28	0.72
40.3	39.21	39.27	1.03
31.3	29.91	29.99	1.31
20.6	18.91	18.96	1.64
11.2	9.23	9.27	1.93
3.2	0.98	1.02	2.18
Slope	Intercept		Average error
1.03	2.30		0.67

Display Temperature ℃	Calibrated Temperature ℃
51.11	51.10

Display Pressure (bar)	Calibration meter Pressure (bar)	Calibrated Pressure (bar)	Difference between meter display & calibrated pressure (bar)
103.9	103.89	103.97	-0.07
90.1	89.74	89.83	0.27
80.8	80.19	80.30	0.50
71.4	70.56	70.66	0.74
60.5	59.43	59.49	1.01
51.8	50.54	50.58	1.22
42	40.5	40.53	1.47
34.8	33.13	33.15	1.65
21.7	19.71	19.73	1.97
11.4	9.25	9.17	2.23
3.4	0.98	0.97	2.43
Slope	Intercept		Average error
1.02	2.48		1.22

Display Temperature ℃	Calibrated Temperature ℃
101.28	101.28

Display Pressure (bar)	Calibration meter Pressure (bar)	Calibrated Pressure (bar)	Difference between meter display & calibrated pressure (bar)
102.9	101.39	102.09	0.81
91.9	90.22	90.87	1.03
80.9	79.1	79.65	1.25

72	70.06	70.57	1.43
62.2	60.15	60.57	1.63
52.5	50.31	50.67	1.83
42.5	40.19	40.47	2.03
32.8	30.34	30.58	2.22
22.5	19.93	20.07	2.43
12.6	9.94	9.97	2.63
3.7	0.98	0.89	2.81
Slope	Intercept		Average error
1.01	2.83		1.83

Display Temperature ℃	Calibrated Temperature ℃
151.41	151.40

Display Pressure (bar)	Calibration meter Pressure (bar)	Calibrated Pressure (bar)	Difference between meter display & calibrated pressure (bar)
102.6	100.6	102.06	0.54
92.4	90.25	91.60	0.80
82	79.7	80.93	1.07
71.7	69.28	70.37	1.33
62.7	60.2	61.14	1.56
52.3	49.73	50.48	1.82
41.9	39.22	39.82	2.08
33	30.25	30.69	2.31
22.7	19.87	20.13	2.57
12.4	9.39	9.57	2.83
4	0.98	0.95	3.05
Slope	Intercept		Average error
1.01	3.10		1.82

Display Temperature ℃	Calibrated Temperature ℃
201.43	201.40

Display Pressure (bar)	Calibration meter Pressure (bar)	Calibrated Pressure (bar)	Difference between meter display & calibrated pressure (bar)
102.5	100.97	103.35	-0.85

92.1	90.38	92.53	-0.43
81.6	79.78	81.60	0.00
72.5	70.53	72.13	0.37
62.2	60.04	61.41	0.79
52.7	50.35	51.53	1.17
43	40.51	41.43	1.57
32.8	30.22	30.82	1.98
23.2	20.46	20.83	2.37
14.8	11.85	12.09	2.71
4.1	0.98	0.95	3.15
Slope	Intercept		Average error
1.02	3.16		1.17

Calibrated Temperature ℃	Slope	Intercept
201.40	1.02	2.30
151.40	1.01	2.48
101.28	1.01	2.83
51.10	1.02	3.10
25.49	1.03	3.16

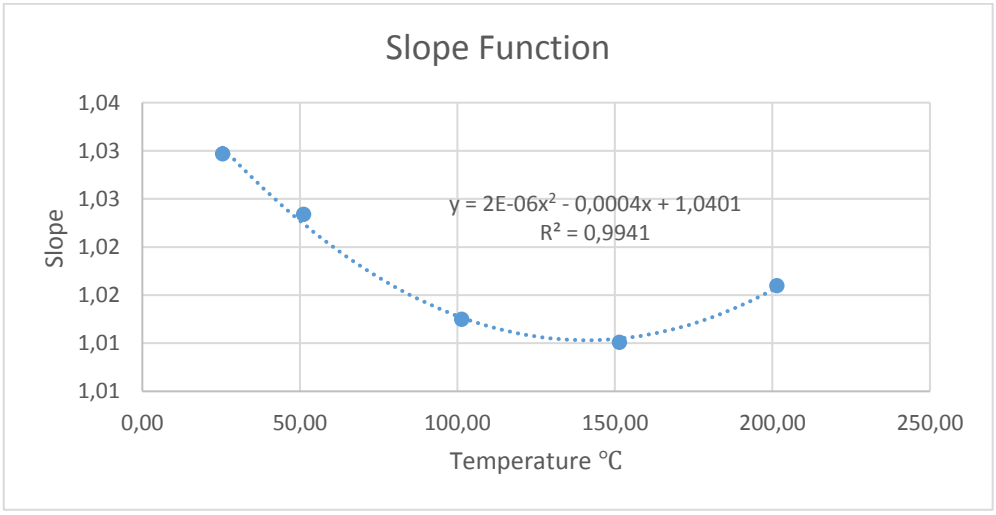

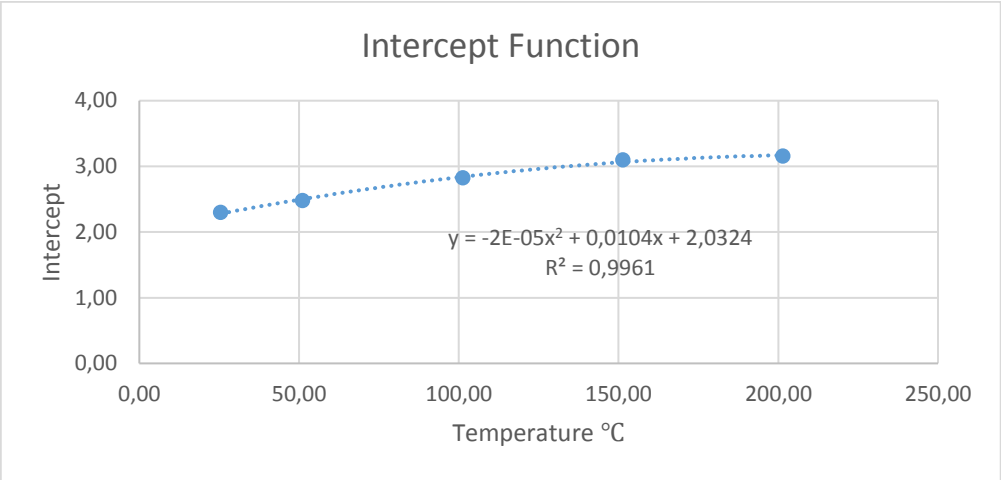

Third set

Display Temperature ℃	Calibrated Temperature ℃		
24.56	24.55		
Display Pressure (bar)	Calibration meter Pressure (bar)	Calibrated Pressure (bar)	Difference between meter display & calibrated pressure (bar)
86.3	100.97	100.80	0.17
79.6	90.48	90.34	0.14
73	80.05	80.04	0.01
67	70.74	70.68	0.06
60.2	60.06	60.07	-0.01
54.2	50.72	50.71	0.01
47.7	40.58	40.57	0.01
41	30.19	30.11	0.08
34.9	20.72	20.60	0.12
28.3	10.36	10.30	0.06
22.3	0.98	0.94	0.04
Slope	Intercept		Average error
1.56	33.84		0.06

Display Temperature ℃	Calibrated Temperature ℃
50.41	50.40

Display Pressure (bar)	Calibration meter Pressure (bar)	Calibrated Pressure (bar)	Difference between meter display & calibrated pressure (bar)
86.8	100.22	100.02	0.20
80.3	90.15	89.97	0.18
74.4	80.89	80.85	0.04
68	70.99	70.95	0.04
61.2	60.47	60.44	0.03
54.9	50.69	50.70	-0.01
48.2	40.42	40.34	0.08
41.6	30.21	30.14	0.07
35.5	20.73	20.71	0.02
28.7	10.18	10.19	-0.01
22.7	0.98	0.91	0.07
Slope	Intercept		Average error
1.55	34.22		0.06

Display Temperature ℃	Calibrated Temperature ℃
99.77	99.76

Display Pressure (bar)	Calibration meter Pressure (bar)	Calibrated Pressure (bar)	Difference between meter display & calibrated pressure (bar)
89.1	101.73	101.23	0.50
81.5	89.99	89.63	0.36
75.2	80.32	80.01	0.31
68.7	70.37	70.09	0.28
62.2	60.53	60.17	0.36
55.7	50.55	50.25	0.30
49.2	40.54	40.33	0.21
42.7	30.67	30.40	0.27
35.7	19.86	19.72	0.14
29.6	10.57	10.41	0.16
23.3	0.98	0.79	0.19
Slope	Intercept		Average error
1.53	34.73		0.28

Display Temperature ℃	Calibrated Temperature ℃		
148.90	148.89		
Display Pressure (bar)	Calibration meter Pressure (bar)	Calibrated Pressure (bar)	Difference between meter display & calibrated pressure (bar)
89.1	100.53	99.79	0.74
82.1	89.97	89.17	0.80
75.9	80.45	79.77	0.68
69.4	70.54	69.91	0.63
63.2	61.09	60.51	0.58
56.4	50.76	50.20	0.56
49.6	40.4	39.89	0.51
43.2	30.51	30.18	0.33
36.6	20.56	20.18	0.38
30.1	10.52	10.32	0.20
23.8	0.98	0.77	0.21
Slope	Intercept		Average error
1.53	35.33		0.51

Display Temperature ℃	Calibrated Temperature ℃		
197.84	197.82		
Display Pressure (bar)	Calibration meter Pressure (bar)	Calibrated Pressure (bar)	Difference between meter display & calibrated pressure (bar)
88.9	100.16	98.94	1.22
82.7	90.63	89.54	1.09
76	80.45	79.38	1.07
69.1	69.93	68.92	1.01
63.1	60.7	59.82	0.88
56.3	50.35	49.51	0.84
50.3	41.13	40.42	0.71
43.1	30.14	29.50	0.64
36.7	20.33	19.80	0.53
30.2	10.39	9.94	0.45
24.1	0.98	0.70	0.28
Slope	Intercept		Average error
1.53	35.82		0.79

Calibrated Temperature ℃	Slope	Intercept
24.55	1.56	33.84
50.40	1.55	34.22
99.76	1.53	34.73
148.89	1.53	35.33
197.82	1.53	35.82

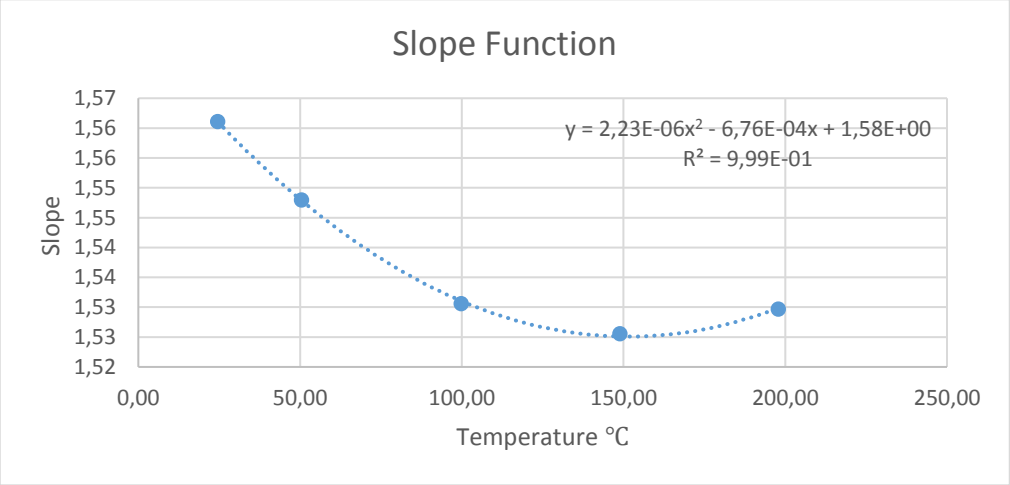

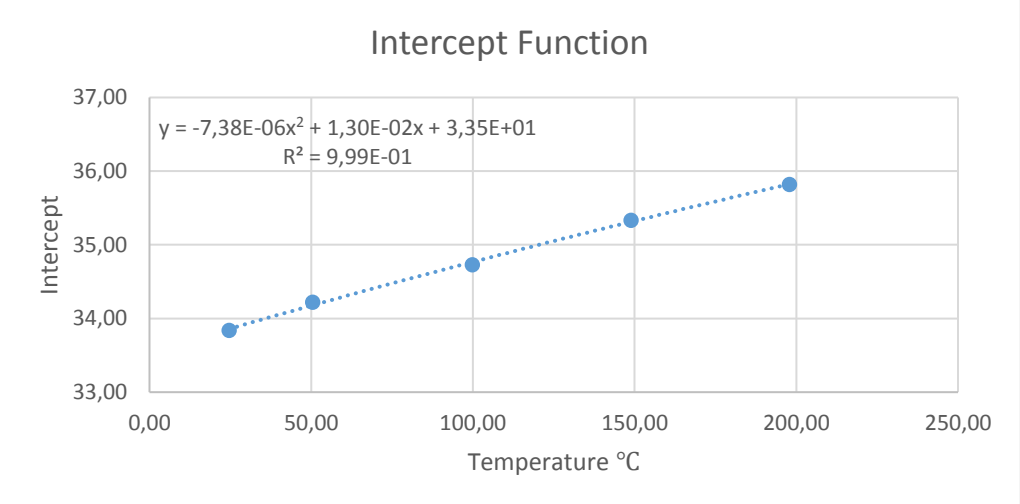

Forth Set

Display Temperature ℃	Calibrated Temperature ℃
99.91	99.91

Display Pressure (bar)	Calibration meter Pressure (bar)	Calibrated Pressure (bar)	Difference between meter display & calibrated pressure (bar)
102.3	102.2	102.49	-0.29
93.8	91.78	92.02	-0.24
85.7	81.76	82.05	-0.29
77.5	71.64	71.95	-0.31
69.4	61.65	61.97	-0.32
61.2	51.58	51.87	-0.29
53.2	41.76	42.02	-0.26
44.7	31.31	31.56	-0.25
36.4	21.19	21.33	-0.14
27.4	10.23	10.25	-0.02
19.9	1	1.02	-0.02
Slope	Intercept		Average error
1.23	23.52		-0.22

Display Temperature ℃	Calibrated Temperature ℃
149.10	149.09

Display Pressure (bar)	Calibration meter Pressure (bar)	Calibrated Pressure (bar)	Difference between meter display & calibrated pressure (bar)
103	102.16	102.50	-0.34
92.9	89.78	90.11	-0.33
85.9	81.18	81.53	-0.35
77.1	70.42	70.74	-0.32
69.1	60.66	60.92	-0.26
61.4	51.26	51.48	-0.22
52.5	40.32	40.57	-0.25
44.2	30.26	30.39	-0.13
36.7	21.03	21.19	-0.16
27.9	10.25	10.39	-0.14
20.3	1	1.07	-0.07
Slope	Intercept		Average error
1.22	23.85		-0.23

Display Temperature ℃	Calibrated Temperature ℃

197.93	197.91		
Display Pressure (bar)	Calibration meter Pressure (bar)	Calibrated Pressure (bar)	Difference between meter display & calibrated pressure (bar)
102	100.95	101.33	-0.38
93.1	89.98	90.36	-0.38
85.1	80.2	80.51	-0.31
77.1	70.35	70.65	-0.30
68.8	60.17	60.43	-0.26
61.9	51.7	51.93	-0.23
52.5	40.16	40.35	-0.19
44.6	30.42	30.62	-0.20
36	19.91	20.02	-0.11
28.5	10.57	10.78	-0.21
20.6	1	1.05	-0.05
Slope	Intercept		Average error
1.23	24.35		-0.24

Calibrated Temperature °C	a_slope	b_Intercept
99.91	1.231	23.57
149.09	1.226	23.96
197.91	1.231	24.54

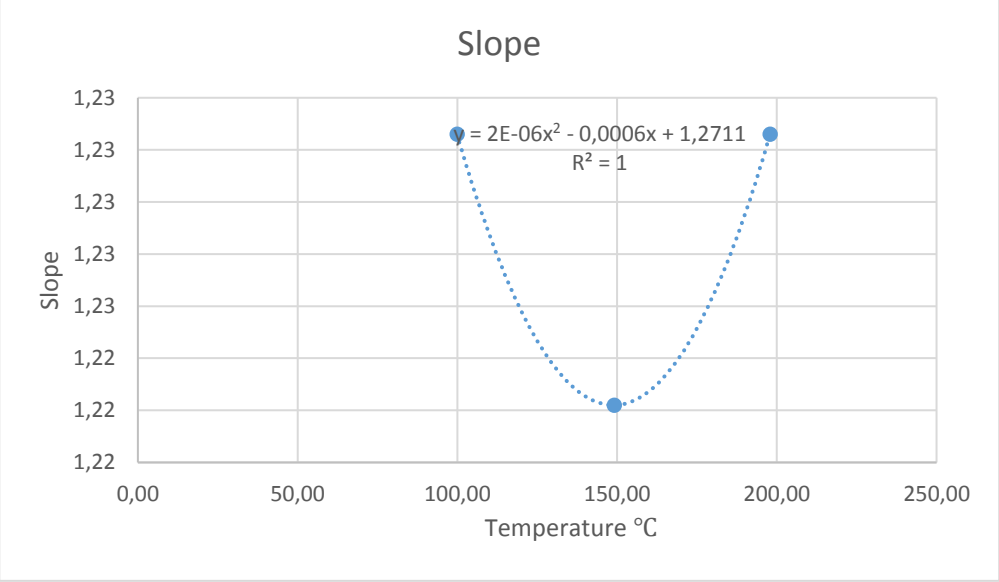

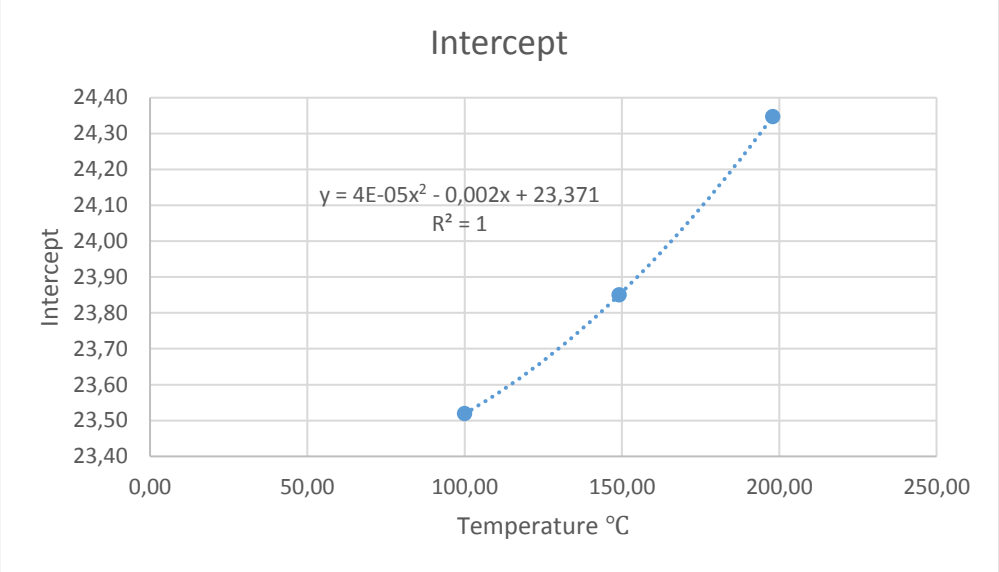

Fifth Set

Display Temperature °C	Calibrated Temperature °C		
21.96	21.95		
Display Pressure (bar)	Calibration meter Pressure (bar)	Calibrated Pressure (bar)	Difference between meter display & calibrated pressure (bar)
78.8	99.16	98.98	0.18
70.5	88.64	88.54	0.10
63.1	79.34	79.24	0.10
54.4	68.42	68.30	0.12
44.3	55.73	55.60	0.13
36.1	45.4	45.29	0.11
27.8	35.06	34.85	0.21
15.1	19.1	18.88	0.22
7.8	9.89	9.70	0.19
0.7	1.01	0.77	0.24
Slope	Intercept		Average error
1.26	0.11		0.16

Display Temperature ℃	Calibrated Temperature ℃		
100.87	100.87		
Display Pressure (bar)	Calibration meter Pressure (bar)	Calibrated Pressure (bar)	Difference between meter display & calibrated pressure (bar)
82.9	100.64	100.78	-0.14
73.2	88.71	88.88	-0.17
64.3	77.83	77.95	-0.12
54.6	65.96	66.05	-0.09
45.6	54.88	55.01	-0.13
37.3	44.73	44.82	-0.09
29.2	34.76	34.88	-0.12
20.2	23.83	23.84	-0.01
13.2	15.23	15.25	-0.02
1.6	1.02	1.02	0.00
Slope	Intercept		Average error
1.23	0.96		-0.09

Display Temperature ℃	Calibrated Temperature ℃		
201.44	201.41		
Display Pressure (bar)	Calibration meter Pressure (bar)	Calibrated Pressure (bar)	Difference between meter display & calibrated pressure (bar)
83.2	99.63	99.75	-0.12
73.8	88.2	88.27	-0.07
65.3	77.77	77.88	-0.11
57.7	68.6	68.60	0.00
49.1	58.04	58.09	-0.05
41	48.18	48.20	-0.02
31.8	36.93	36.96	-0.03
22.4	25.44	25.48	-0.04
14	15.2	15.22	-0.02
2.4	1.02	1.05	-0.03
Slope	Intercept		Average error
1.22	1.89		-0.05

Display Temperature ℃	Calibrated Temperature ℃		
201.44	201.41		
Display Pressure (bar)	Calibration meter Pressure (bar)	Calibrated Pressure (bar)	Difference between meter display & calibrated pressure (bar)
83.2	99.63	99.75	-0.12
73.8	88.2	88.27	-0.07
65.3	77.77	77.88	-0.11
57.7	68.6	68.60	0.00
49.1	58.04	58.09	-0.05
41	48.18	48.20	-0.02
31.8	36.93	36.96	-0.03
22.4	25.44	25.48	-0.04
14	15.2	15.22	-0.02
2.4	1.02	1.05	-0.03
Slope	Intercept		Average error
1.22	1.89		-0.05

Calibrated Temperature ℃	a_slope	b_Intercept
21.95	1.26	0.11
100.87	1.23	0.95
201.41	1.22	1.89
251.43	1.23	2.30

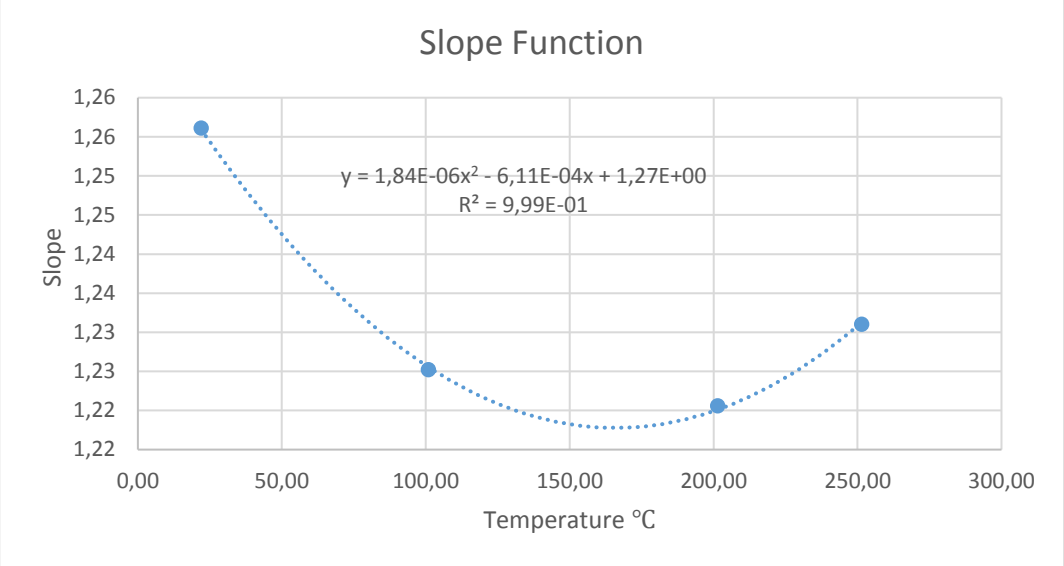
Slope Function
y = 1,84E-06x² - 6,11E-04x + 1,27E+00
R² = 9,99E-01
Slope
1,26
1,26
1,25
1,25
1,24
1,24
1,23
1,23
1,22
1,22
0,00
50,00
100,00
150,00
200,00
250,00
300,00
Temperature °C

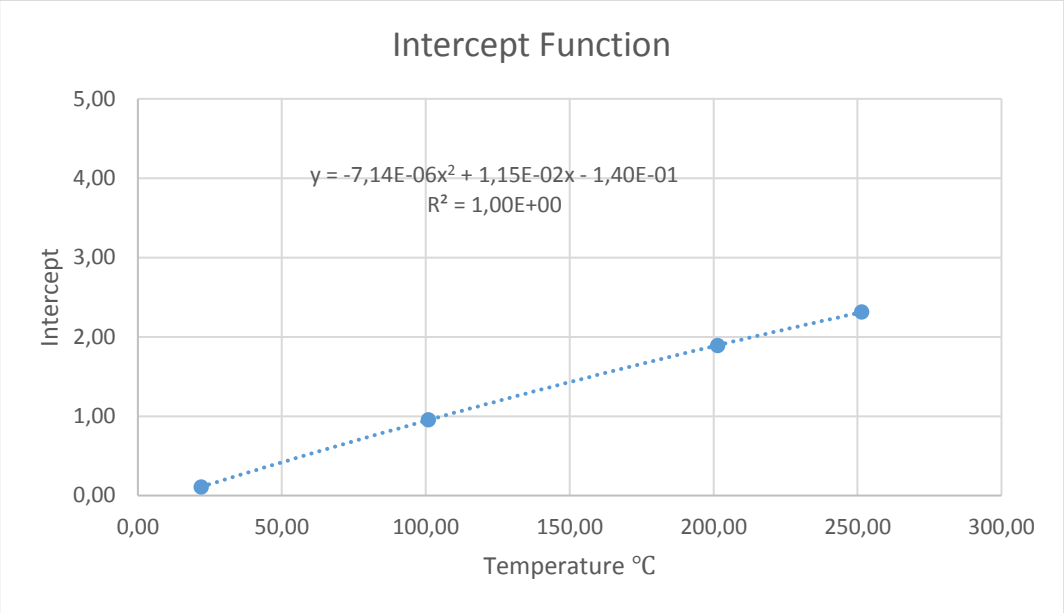
Intercept Function
y = -7,14E-06x² + 1,15E-02x - 1,40E-01
R² = 1,00E+00
Intercept
5,00
4,00
3,00
2,00
1,00
0,00
0,00
50,00
100,00
150,00
200,00
250,00
300,00
Temperature °C

Appendix 2

Measurement data from all successful bubble point and cloud point measurements are available in a supplementary file.